UNIVERSITÀ DEGLI STUDI DI NAPOLI FEDERICO II

FACOLTÀ DI INGEGNERIA

DIPARTIMENTO DI INGEGNERIA AEROSPAZIALE

DOTTORATO DI RICERCA IN
INGEGNERIA AEROSPAZIALE, NAVALE, E DELLA QUALITA'
INDIRIZZO AEROSPAZIALE, XXI CICLO

CREATION AND VALIDATION OF A FEM STRUCTURAL CALCULATION PROCEDURE FOR GAS TURBINE DESIGN, PROVIDING AN ELASTO-VISCO-PLASTIC MATERIAL MODEL IMPLEMENTING NON-LINEAR INTERACTION BETWEEN FATIGUE AND CREEP.

TUTORES:
CH.MO PROF. ING. SERGIO DE ROSA
ING. FRANCESCO FRANCO

CANDIDATO:
SALVATORE COSTAGLIOLA

COORDINATORE CORSO DI DOTTORATO:
CH.MO PROF. ING. ANTONIO MOCCIA

NOVEMBER 2008

My education was the liberty I had to read indiscriminately and all the time, with my eyes hanging out.

Dylan Thomas

The pure and simple truth is rarely pure and never simple.

Oscar Wilde

TABLE OF CONTENTS

Acknowledgements

The completion of this work has been a monumental accomplishment in my professional career. I am grateful for this opportunity to acknowledge and thank those that have helped me throughout this process. If it were not for my girlfriend, my parents, my sister, colleagues and friends, who have supported me throughout all of my different interests, I would not have finished or either started such activities.

I would like to express my sincere gratitude to my tutors: Professor Sergio De Rosa and Engineer Francesco Franco for having accepted me as their student in this department and for their guidance. Without their support this work would never have been.

I would like also to thank my company General Electric Oil&Gas, and my ex-manager in GE Gas Turbines Machine Design: Engineer Luca Aurelio which allowed me to use, within all the allowed GE policies, materials and resources to bring this work at the end. A special thank goes to all the people in GE (in Florence, in Bangalore and in Munich), that greatly supported me in this activity.

I would like to thank my first sponsor for this activity Ing.Vincenzo Cirillo from AVIO Aerospace Propulsion S.p.A. - Research and Development Department. Without his precious support during our first activities, this work would neither have started.

I would like to express my appreciation to my ex-colleague Engineer Daniela Capasso, which proposed me to join to PhD, and started my first year working on the main subject of this study. I also would like to thank people from *Ecole de Mines* – Paris and ANSYS Inc. corporation for providing me valuable helps in using respectively the software Z-Mat and the user subroutine USERMAT in the finite Element code ANSYS.

List of Tables

List of Figures

Summary

The request to obtain refined simulations of a real behaviour, in structural analysis, is one of the most important goals that actually researchers are attempting to reach. Actually, the automated calculation procedures that structural analysts use through Finite Element Modelling (FEM), allow reaching a very high level of refinement if we refer to the prediction of the structural behaviour of a component/machine under a very complex load system. In this field, the capability to be able to reproduce material behaviours is one of the most intriguing points because the ability to manage the material matrix in FEM software is the necessary starting point to have a satisfying result. Traditionally the possibility to not implement such a complex model has been faced through the use of factors of safety, which are developed and refined on the basis of experience and historical evidence. For systems where efficient design is of the utmost importance (for example the minimum weight design of an aircraft structure) it is possible that the traditional factors of safety may be overly conservative, so that optimal efficiency cannot be achieved. Furthermore, historical factors of safety are unlikely to be appropriate for new design concepts or new complex metal super-alloys. These materials, for instance, have very different behaviours if we consider that depending mainly on the type of load and the temperature. They can present hardening, softening, cyclic stabilization, stress relaxation, creep, etc. The main scope of this work is to provide a procedure for the implementation of an elasto-visco-plastic material model that is able to take in account of non-linear interaction of creep and fatigue for structural analysis and life prediction. This is done creating and validating a procedure that, using dedicated software, provides to the FEM software a “real time” updated material model, providing significant improvements in industrial software for life predictions and fracture mechanics. Significant sponsorship and support of this work have been provided to the author by Department of Aerospace Engineering of the University of Naples “Federico II”, Avio Areospace Propulsion S.p.A. and General Electric – Oil&Gas.

Introduction

The development of power systems with greater thermodynamic efficiency makes the need for accurate analytical representations of inelastic deformation a necessity. More complex material models have been developed to support this emerging need. These mathematical models must be capable of accurately predicting short-term plastic strain, long-term creep strain, and the interactions between them. Multiaxial, cyclic, and non-isothermal conditions are becoming the norm, not the exception, and the capability to implement these features became an issue in the three past decades. This is the reason why, such a formidable task has received considerable attention, resulting in an emerging field of continuum mechanics called elasto-visco-plasticity.

In Chapter 1 are treated the fundamentals of material behaviours, models and characterization. Basic assumptions and definition of the quantities used in this branch are defined and briefly accounted.

Chapter 2 discusses on the methodologies that actually are used to evaluate fatigue, creep and fracture mechanics. For each methodology have been exposed advantages, limitations and field of interest.

Chapter 3 deals with the description of the material models available in modern FEM software. At the end of this chapter, all these models are treated and compared in order to define their capabilities and limitations. The chapter ends describing non-linear methodologies that are used in stress analysis. Starting from a brief description of the state of the art, this part goes through the different non-linear theories and analysis methods.

Chapter 4 examines the theories and the methods that can allow implementing a user-defined material model in FEM software. These theories have been here deepened and treated grouping them in two categories.

Chapter 5 covers the description of some of the tools that are used to help implementation of external material models in FEM software. Here is described the chosen one, Z-Mat, and the software procedures used to link the FEM software to the over mentioned external tool.

Chapter 6 includes a detailed description of the theories and the methodologies at the basis of the elasto-visco-plastic material model. More in detail, the chapter describes the Chaboche theory that is the one that is implemented in this work.

Chapter 7 discusses the characterization of Inconel 7xx, a nickel super alloy used in gas turbine components subjected to high temperatures and cyclic mechanical loads. In this chapter the tests campaign is described too.

Chapter 8 describes the methodology used to build the elasto-visco-plastic material model coefficients, and the steps arranged to verify the correctness of each coefficient, passing through the comparison with the elastic and the plastic models already present in the software FEM.

Chapter 9 deals with the application of the elasto-visco-plastic model to a real industrial issue. A stator component of a gas turbine, subjected to creep and fatigue has been taken into account to evaluate if the FEM analysis was able to accurately simulate cone's status at the foreseen maintenance interval. Crystallographic analyses, measurements and data acquisition from field, have been correlated with the analysis results.

Chapter 10 is finally reserved to a brief description of all the activities and the actions that are directly linked to the results of this work. More in detail are considered the implementation of the elasto-visco-plastic coefficient into the tools that General Electric uses to evaluate creep, low cycle fatigue and fracture mechanics.

The conclusions drawn from this research are given in the devoted section.

1 Definitions and base assumptions

The main requirement of large deformation problems such as structural components design, life prediction, high-speed machining, impact, and various primarily metal forming, is to develop constitutive relations which are widely applicable and capable of accounting for complex paths of deformation. Achieving such desirable goals for material like metals and steel alloys involves a comprehensive study of their microstructures and experimental observations under different loading conditions. In general, metal structures display a strong rate- and temperature-dependence when deformed non-uniformly into the inelastic range.

This effect has important implications for an increasing number of applications in structural and engineering mechanics. The mechanical behavior of these applications cannot be characterized by classical (rate-independent) continuum theories because they incorporate no ‘material length scales’. It is therefore necessary to develop a rate-dependent (visco-plasticity) continuum theory bridging the gap between the classical continuum theories and the microstructure simulations.

One of the most challenging engineering research fields, is to be able to simulate the material behaviour not only in ordinary conditions, but especially when it is subjected to large deformations. To reach this goal is of primary importance to exactly define its elastic field in order to build the most solid bases to schematize it’s plastic behaviour.

1.1 Elasticity

A material is said to be elastic if it deforms under stress (e.g., external forces), but then returns to its original shape when the stress is removed. The amount of deformation is the strain. The elastic regime is characterized by a linear relationship between stress and strain, denoted linear elasticity. This idea was first stated by Robert Hooke in 1675 as a Latin anagram whose solution he published in 1678 as *"Ut tension, sic vis"*.

This linear relationship is called Hooke's law that states that the amount by which a material body is deformed (the strain) is linearly related to the force causing the deformation (the stress). Materials for which Hooke's law is a useful

approximation are known as linear-elastic or *"Hookean"* materials. The classic model of linear elasticity is the perfect spring.

Its extension, strain, is linearly proportional to its tensile stress, σ by a constant factor, the inverse of its modulus of elasticity, E

$$\sigma = E\varepsilon \tag{1.1}$$

Or

$$\Delta L = \frac{F}{EA}L = \frac{\sigma}{E}L. \tag{1.2}$$

Steel exhibits linear-elastic behaviour in most engineering applications. Hooke's law is valid for it throughout its elastic range (i.e., for stresses below the yield strength). For some other materials, such as aluminium, Hooke's law is only valid for a portion of the elastic range. For these materials a proportional limit stress is defined, below which the errors associated with the linear approximation are negligible.

1.2 Tensor Expression of Hooke's Law

When working with a three-dimensional stress state, a 4th order tensor (c_{ijkl}) must be defined. Containing 81 elastic coefficients to link the stress tensor (σ_{ij}) and the strain tensor (or Green tensor) (ε_{kl}).

$$\sigma_{ij} = \sum_{kl} c_{ijkl} \cdot \varepsilon_{kl}. \tag{1.3}$$

Due to the symmetry of the stress tensor, strain tensor, and stiffness tensor, only 21 elastic coefficients are independent. As stress is measured in units of pressure and strain is dimensionless, the entries of c_{ijkl} are also in units of pressure.

1.3 Linear Elasticity

Linear elasticity is the mathematical study of how solid objects deform and become internally stressed due to prescribed loading conditions. Linear elasticity

relies upon the continuum hypothesis and is applicable at macroscopic (and sometimes microscopic) length scales. Linear elasticity is a simplification of the more general nonlinear theory of elasticity and is a branch of continuum mechanics.

The fundamental *"linearizing"* assumptions of linear elasticity are: "small" deformations (or strains) and linear relationships between the components of stress and strain. In addition linear elasticity is only valid for stress states that do not produce yielding. These assumptions are reasonable for many engineering materials and engineering design scenarios. Linear elasticity is therefore used extensively in structural analysis and engineering design, often through the aid of finite element analysis.

1.4 Isotropic Material

Isotropic materials are characterized by properties which are independent of direction in space. Physical equations involving isotropic materials must therefore be independent of the coordinate system chosen to represent them. The strain tensor is a symmetric tensor. Since the trace of any tensor is independent of coordinate system, the most complete coordinate-free decomposition of a symmetric tensor is to represent it as the sum of a constant tensor and a traceless symmetric tensor. Thus:

$$\varepsilon_{ij} = \left(\frac{1}{3}\varepsilon_{kk}\delta_{ij}\right) + \left(\varepsilon_{ij} - \frac{1}{3}\varepsilon_{kk}\delta_{ij}\right) \tag{1.4}$$

Where δ_{ij} is the Kronecker delta. The first term on the right is the constant tensor, also known as the pressure, and the second term is the traceless symmetric tensor, also known as the shear tensor.

The most general form of Hooke's law for isotropic materials may now be written as a linear combination of these two tensors:

$$\sigma_{ij} = 3K\left(\frac{1}{3}\varepsilon_{kk}\delta_{ij}\right) + 2G\left(\varepsilon_{ij} - \frac{1}{3}\varepsilon_{kk}\delta_{ij}\right) \tag{1.5}$$

Where K is the bulk modulus and G is the shear modulus.

Using the relationships between the elastic moduli, these equations may also be expressed in various other ways. For example, the strain may be expressed in terms of the stress tensor as:

$$\begin{aligned}
\varepsilon_{11} &= \frac{1}{E}\left(\sigma_{11} - \nu(\sigma_{22} + \sigma_{33})\right) \\
\varepsilon_{22} &= \frac{1}{E}\left(\sigma_{22} - \nu(\sigma_{11} + \sigma_{33})\right) \\
\varepsilon_{33} &= \frac{1}{E}\left(\sigma_{33} - \nu(\sigma_{11} + \sigma_{22})\right) \\
\varepsilon_{13} &= \frac{\sigma_{13}}{2G} \\
\varepsilon_{13} &= \frac{\sigma_{13}}{2G} \\
\varepsilon_{23} &= \frac{\sigma_{23}}{2G}
\end{aligned} \tag{1.6}$$

Where E is the modulus of elasticity and ν is Poisson's ratio.

In isotropic media, the elasticity tensor gives the relationship between the stresses (resulting internal stresses) and the strains (resulting deformations). For an isotropic medium, the elasticity tensor has no preferred direction: an applied force will give the same displacements (relative to the direction of the force) no matter the direction in which the force is applied. In the isotropic case, the elasticity tensor may be written:

$$C_{ijkl} = K\,\delta_{ij}\,\delta_{kl} + \mu\left(\delta_{ik}\delta_{jl} + \delta_{il}\delta_{jk} - \tfrac{2}{3}\,\delta_{ij}\,\delta_{kl}\right) \tag{1.7}$$

Where K is the bulk modulus (or incompressibility), and μ is the shear modulus (or rigidity), two elastic moduli. If the medium is homogeneous as well, then the elastic moduli will not be a function of position in the medium. The constitutive equation may now be written as:

$$\sigma_{ij} = K\delta_{ij}\varepsilon_{kk} + 2\mu(\varepsilon_{ij} - \tfrac{1}{3}\delta_{ij}\varepsilon_{kk}) \tag{1.8}$$

This expression separates the stress into a scalar part on the left which may be associated with a scalar pressure, and a traceless part on the right which may be associated with shear forces. A simpler expression is:

$$\sigma_{ij} = \lambda\delta_{ij}\varepsilon_{kk} + 2\mu\varepsilon_{ij} \tag{0.2}$$

Where λ is Lamé's first parameter.

Since the constitutive equation is simply a set of linear equations, the strain may be expressed as a function of the stresses as: (Sommerfeld 1964)

$$\varepsilon_{ij} = \frac{1}{9K}\delta_{ij}\sigma_{kk} + \frac{1}{2\mu}\left(\sigma_{ij} - \tfrac{1}{3}\delta_{ij}\sigma_{kk}\right) \tag{0.3}$$

Which is again, a scalar part on the left and a traceless shear part on the right. More simply:

$$\varepsilon_{ij} = \frac{1}{2\mu}\sigma_{ij} - \frac{\nu}{E}\delta_{ij}\sigma_{kk} \tag{0.4}$$

Where ν is Poisson's ratio and E is Young's modulus.

1.5 Yield

The yield strength or yield point of a material is defined in engineering and materials science as the stress at which a material begins to deform plastically. Prior to the yield point the material will deform elastically and will return to its original shape when the applied stress is removed. Once the yield point is passed some fraction of the deformation will be permanent and non-reversible. In the three-dimensional space of the principal stresses (σ_1,σ_2,σ_3), an infinite number of yield points form together a yield surface.

Knowledge of the yield point is vital when designing a component since it generally represents an upper limit to the load that can be applied. It is also important for the control of many materials production techniques such as forging,

rolling, or pressing. In structural engineering, this is a soft failure mode which does not normally cause catastrophic failure or ultimate failure unless it accelerates buckling.

It is often difficult to precisely define yielding due to the wide variety of stress–strain curves exhibited by real materials. In addition, there are several possible ways to define yielding:

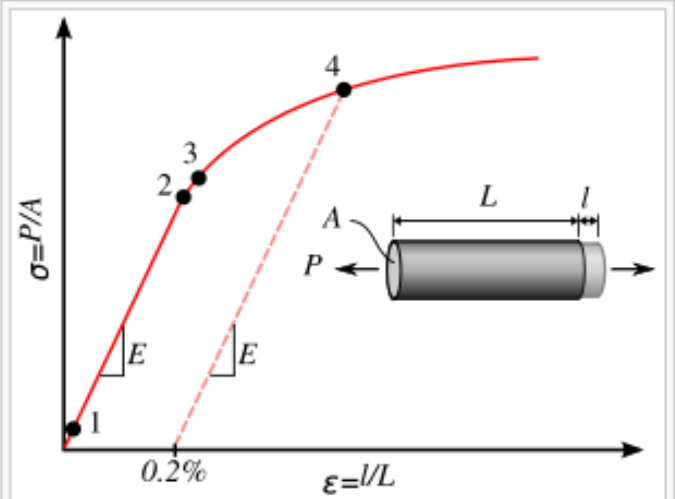

Typical yield behavior for non-ferrous alloys.
1: True elastic limit
2: Proportionality limit
3: Elastic limit
4: Offset yield strength

Figure 1.1- Stress vs Strain Curve – Definitions of Yield Points

1.5.1 True elastic limit

It is the lowest stress at which dislocations move. This definition is rarely used, since dislocations move at very low stresses, and detecting such movement is very difficult.

1.5.2 Proportionality limit

Up to this amount of stress, stress is proportional to strain (Hooke's law), so the stress-strain graph is a straight line, and the gradient will be equal to the elastic modulus of the material.

1.5.3 Elastic limit (yield strength)

Beyond the elastic limit, permanent deformation will occur. It is the lowest stress at which permanent deformation can be measured. This requires a manual load-unload procedure, and the accuracy is critically dependent on equipment and operator skill. For elastomers, such as rubber, the elastic limit is much larger than the proportionality limit. Also, precise strain measurements have shown that plastic strain begins at low stresses.

1.5.4 Offset yield point (proof stress)

This is the most widely used strength measure of metals, and is found from the stress-strain curve as shown in the figure to the right. A plastic strain of 0.2% is usually used to define the offset yield stress, although other values may be used depending on the material and the application. The offset value is given as a subscript, e.g. $R_p0.2$ = 310 MPa. In some materials there is essentially no linear region and so a certain value of strain is defined instead. Although somewhat arbitrary, this method does allow for a consistent comparison of materials.

1.5.5 Upper yield point and lower yield point

Some metals, such as mild steel, reach an upper yield point before dropping rapidly to a lower yield point. The material response is linear up until the upper yield point, but the lower yield point is used in structural engineering as a conservative value.

1.6 Yield Criterion

A yield criterion, often expressed as yield surface, or yield locus, is an hypothesis concerning the limit of elasticity under any combination of stresses. There are two interpretations of yield criterion: one is purely mathematical in taking a statistical approach while other models attempt to provide a justification

based on established physical principles. Since stress and strain are tensor qualities they can be described on the basis of three principal directions, in the case of stress these are denoted by σ_1, σ_2 and σ_3.

The following represent the most common yield criterion as applied to an isotropic material (uniform properties in all directions). Other equations have been proposed or are used in specialist situations.

1.6.1 Isotropic yield criteria

Maximum Principal Stress Theory - Yield occurs when the largest principal stress exceeds the uniaxial tensile yield strength. Although this criterion allows for a quick and easy comparison with experimental data it is rarely suitable for design purposes.

$$\sigma_1 \leq \sigma_y \tag{0.5}$$

Maximum Principal Strain Theory - Yield occurs when the maximum principal strain reaches the strain corresponding to the yield point during a simple tensile test. In terms of the principal stresses this is determined by the equation:

$$\sigma_1 - \nu(\sigma_2 + \sigma_3) \leq \sigma_y. \tag{0.6}$$

Maximum Shear Stress Theory - Known as the Tresca yield criterion, after the French scientist Henri Tresca. This assumes that yield occurs when the shear stress exceeds the shear yield strength τ_y:

$$\tau = \frac{\sigma_1 - \sigma_3}{2} \leq \tau_{ys}. \tag{0.7}$$

Total Strain Energy Theory - This theory assumes that the stored energy associated with elastic deformation at the point of yield is independent of the specific stress tensor. Thus yield occurs when the strain energy per unit volume is greater than the strain energy at the elastic limit in simple tension. For a 3-dimensional stress state this is given by:

$$\sigma_1^2 + \sigma_2^2 + \sigma_3^2 - 2\nu(\sigma_1\sigma_2 + \sigma_2\sigma_3 + \sigma_1\sigma_3) \leq \sigma_y^2 \tag{0.8}$$

Distortion Energy Theory - This theory proposes that the total strain energy can be separated into two components: the volumetric (hydrostatic) strain energy and the shape (distortion or shear) strain energy. It is proposed that yield occurs when the distortion component exceeds that at the yield point for a simple tensile test. This is generally referred to as the *Von Mises* yield criterion and is expressed as:

$$\frac{1}{2}\left[(\sigma_1 - \sigma_2)^2 + (\sigma_2 - \sigma_3)^2 + (\sigma_3 - \sigma_1)^2\right] \leq \sigma_y^2 \quad (0.9)$$

Based on a different theoretical underpinning this expression is also referred to as octahedral shear stress theory.

Most commonly used isotropic yield criteria is the ***von Mises* yield criterion**.

1.6.2 von Mises Yield Criterion

The *von Mises* yield criterion suggests that the yielding of materials begins when the second deviatoric stress invariant J_2 reaches a critical value k^2. For this reason, it is sometimes called the J_2- plasticity or J_2 flow theory. It is part of a plasticity theory that applies best to ductile materials, such as metals. Prior to yield, material response is assumed to be elastic.

In material science and engineering the *von Mises* yield criterion can be also formulated in terms of the *von Mises* stress or equivalent tensile stress, σ_v, a scalar stress value that can be computed from the stress tensor. In this case, a material is said to start yielding when its *von Mises* stress reaches a critical value known as the yield strength, σ_y. The *von Mises* stress is used to predict yielding of materials under any loading condition from results of simple uniaxial tensile tests. The *von Mises* stress satisfies the property that two stress states with equal distortion energy have equal *von Mises* stress.

Because the von Mises yield criterion is independent of the first stress invariant, I_1, it is applicable for the analysis of plastic deformation for ductile materials such as metals, as the onset of yield for these materials does not depend on the hydrostatic component of the stress tensor.

Although formulated by Maxwell in 1865, it is generally attributed to *von Mises* (1913). Huber (1904), in a paper in Polish, anticipated to some extent this criterion. This criterion is referred also as the **Maxwell–Huber–Hencky–von Mises theory**.

1.6.2.1 Mathematical Formulation

Mathematically the yield function for the *von Mises* condition is expressed as:

$$f(J_2) = \sqrt{J_2} - k = 0 \tag{0.10}$$

An alternative form is:

$$f(J_2) = J_2 - k^2 = 0 \tag{0.11}$$

Where k can be shown to be the yield stress of the material in pure shear. As it will become evident later in the article, at the onset of yielding, the magnitude of the shear stress in pure shear is $\sqrt{3}$ times lower than the tensile stress in the case of simple tension. Thus, we have

$$k = \frac{\sigma_y}{\sqrt{3}} \tag{0.12}$$

Furthermore, if we define the *von Mises* stress as $\sigma_v = \sqrt{3J_2}$, the von Mises yield criterion can be expressed as:

$$\begin{aligned} f(J_2) &= \sqrt{3J_2} - \sigma_y \\ &= \sigma_v - \sigma_y = 0 \end{aligned} \tag{0.13}$$

Substituting J_2 in terms of the principal stresses into the von Mises criterion equation we have:

$$(\sigma_1 - \sigma_2)^2 + (\sigma_2 - \sigma_3)^2 + (\sigma_1 - \sigma_3)^2 = 6k^2 = 2\sigma_y^2 \tag{0.14}$$

Or

$$(\sigma_1^2 + \sigma_2^2 + \sigma_3^2) - \sigma_1\sigma_2 - \sigma_2\sigma_3 - \sigma_1\sigma_3 = 3k^2 = \sigma_y^2$$

(0.15)

or as a function of the stress tensor components

$$(\sigma_{11} - \sigma_{22})^2 + (\sigma_{22} - \sigma_{33})^2 + (\sigma_{11} - \sigma_{33})^2 + 6(\sigma_{23}^2 + \sigma_{31}^2 + \sigma_{12}^2) = 6k^2$$

(0.16)

This equation defines the yield surface as a circular cylinder (See Figure) whose yield curve, or intersection with the deviatoric plane, is a circle with radius $\sqrt{2}k$, or $\sqrt{3/2}\sigma_y$

This implies that the yield condition is independent of hydrostatic stresses.

In the case of uniaxial stress or simple tension, $\sigma_1 \neq 0$, $\sigma_3 = \sigma_2 = 0$, the *von Mises* criterion reduces to $\sigma_1 = \sigma_y$.

Therefore, the material starts to yield, when σ_1 reaches the yield strength of the material σ_y, which is a characteristic material property. In practice, this parameter is, indeed, determined in a tensile test satisfying the uniaxial stress condition.

It is also convenient to define an Equivalent tensile stress or *von Mises* stress, σ_v, which is used to predict yielding of materials under multiaxial loading conditions using results from simple uniaxial tensile tests. Thus, we define

$$\begin{aligned}\sigma_v &= \sqrt{3J_2} \\ &= \sqrt{\frac{(\sigma_{11} - \sigma_{22})^2 + (\sigma_{22} - \sigma_{33})^2 + (\sigma_{33} - \sigma_{11})^2 + 6(\sigma_{12}^2 + \sigma_{23}^2 + \sigma_{31}^2)}{2}} \\ &= \sqrt{\frac{(\sigma_1 - \sigma_2)^2 + (\sigma_2 - \sigma_3)^2 + (\sigma_3 - \sigma_1)^2}{2}} \\ &= \sqrt{\tfrac{3}{2}\, s_{ij}s_{ij}}\end{aligned}$$

(0.17)

Where s_{ij} are the components of the stress deviator tensor σ^{dev}:

$$\boldsymbol{\sigma}^{dev} = \boldsymbol{\sigma} - \frac{1}{3}(\boldsymbol{\sigma} \cdot \mathbf{I})\,\mathbf{I} \tag{0.18}$$

1.6.2.2 Von Mises criterion for different stress conditions

In this case, yielding occurs when the equivalent stress, σ_t, reaches the yield strength of the material in simple tension, σ_y.

As an example, the stress state of a steel beam in compression differs from the stress state of a steel axle under torsion, even if both specimens are of the same material. In view of the stress tensor, which fully describes the stress state, this difference manifests in six degrees of freedom, because the stress tensor has six independent components. Therefore, it is difficult to tell which of the two specimens is closer to the yield point or has even reached it. However, by means of the *von Mises* yield criterion, which depends solely on the value of the scalar *von Mises* stress, i.e., one degree of freedom, this comparison is straightforward: A larger *von Mises* value implies that the material is closer to the yield point.

In the case of pure shear stress, $\sigma_{12} = \sigma_{21} \neq 0$, while all other $\sigma_{ij} = 0$, *von Mises* criterion becomes:

$$\sigma_{12} = k = \frac{\sigma_y}{\sqrt{3}} \tag{0.19}$$

This means that, at the onset of yielding, the magnitude of the shear stress in pure shear is $\sqrt{3}$times lower than the tensile stress in the case of simple tension. The *von Mises* yield criterion for pure shear stress, expressed in principal stresses, is:

$$(\sigma_1 - \sigma_2)^2 + (\sigma_2 - \sigma_3)^2 + (\sigma_1 - \sigma_3)^2 = 6\sigma_{12}^2 \tag{0.20}$$

In the case of plane stress, $\sigma_3 = 0$, the *von Mises* criterion becomes:

$$\sigma_1^2 - \sigma_1\sigma_2 + \sigma_2^2 = 3k^2 = \sigma_y^2 \tag{0.21}$$

This equation represents an ellipse in the plane $\sigma 1 - \sigma 2$, as shown in the Figure above.

1.6.2.3 Physical interpretation of the von Mises yield criterion

Hencky (1924) offered a physical interpretation of *von Mises* criterion suggesting that yielding begins when the elastic energy of distortion reaches a critical value. For this, the *von Mises* criterion is also known as the maximum distortion strain energy criterion. This comes from the relation between J_2 and the elastic strain energy of distortion W_D:

$$W_D = \frac{J_2}{2G}$$

with the elastic shear modulus (0.22)

$$G = \frac{E}{2(1+\nu)}$$

In 1937 Arpad L. Nadai suggested that yielding begins when the octahedral shear stress reaches a critical value, i.e. the octahedral shear stress of the material at yield in simple tension. In this case, the von Mises yield criterion is also known as the maximum octahedral shear stress criterion in view of the direct proportionality that exist between J_2 and the octahedral shear stress, τ_{oc}, which by definition is

$$\tau_{oct} = \sqrt{\tfrac{2}{3} J_2} \qquad (0.23)$$

Thus we have

$$\tau_{oct} = \tfrac{\sqrt{2}}{3}\sigma_y \qquad (0.24)$$

1.6.3 Mohr-Coulomb yield criterion

Mohr-Coulomb theory is a mathematical model (see yield surface) describing the response of a material such as rubble piles or concrete to shear stress as well as normal stress. Most of the classical engineering materials somehow follow this rule in at least a portion of their shear failure envelope.

In structural engineering it is used to determine failure load as well as the angle of fracture of a displacement fracture in concrete and similar materials. Coulomb's friction hypothesis is used to determine the combination of shear and normal stress that will cause a fracture of the material. Mohr's circle is used to determine which principal stresses that will produce this combination of shear and normal stress, and the angle of the plane in which this will occur. According to the principle of normality the stress introduced at failure will be perpendicular to the line describing the fracture condition.

It can be shown that a material failing according to Coulomb's friction hypothesis will show the displacement introduced at failure forming an angle to the line of fracture equal to the angle of friction. This makes the strength of the material determinable by comparing the external mechanical work introduced by the displacement and the external load with the internal mechanical work introduced by the strain and stress at the line of failure. By conservation of energy the sum of these must be zero and this will make it possible to calculate the failure load of the construction.

A common improvement of this model is to combine Coulomb's friction hypothesis with Rankine's principal stress hypothesis to describe a separation fracture.

The Mohr-Coulomb yield surface is often used to model the plastic flow of geomaterials (and other cohesive-frictional materials). Many such materials show dilatational behaviour under triaxial states of stress, which the Mohr-Coulomb model does not include. Also, since the yield surface has corners, it may be inconvenient to use the original Mohr-Coulomb model to determine the direction of plastic flow (in the flow theory of plasticity).

A common approach that is used is to use a non-associated plastic flow potential that is smooth. An example of such a potential is the function

$$g := \sqrt{(\alpha\ c_y\ \tan\psi)^2 + G^2(\phi,\theta)\ q^2}\ - p\ \tan\phi$$

(0.25)

where α is a parameter, c_y is the value of c when the plastic strain is zero (also called the initial cohesion yield stress), ψ is the angle made by the yield surface in the Rendulic plane at high values of p (this angle is also called the dilation angle), and G(φ,θ) is an appropriate function that is also smooth in the deviatoric stress plane.

1.6.4 Drucker-Prager yield criterion

The Drucker-Prager yield criterion is a pressure-dependent model for determining whether a material has failed or undergone plastic yielding. The criterion was introduced to deal with the plastic deformation of soils. It and its many variants have been applied to rock, concrete, polymers, foams, and other pressure-dependent materials.

The Drucker-Prager yield criterion has the form

$$\sqrt{J_2} = A + B\ I_1 \tag{0.26}$$

where I_1 is the first invariant of the Cauchy stress and J_2 is the second invariant of the deviatoric part of the Cauchy stress. The constants A, B are determined from experiments.

In terms of the equivalent stress (or *Von Mises* stress) and the hydrostatic (or mean) stress, the Drucker-Prager criterion can be expressed as

$$\sigma_e = a + b\ \sigma_m \tag{0.27}$$

Where σ_e is the equivalent stress, σ_m is the hydrostatic stress, and a,b are material constants. The Drucker-Prager yield criterion expressed in Haigh-Westergaard coordinates is

$$\frac{1}{\sqrt{2}}\rho - \sqrt{3}\ B\xi = A \tag{0.28}$$

The Drucker-Prager yield surface is a smooth version of the Mohr-Coulomb yield surface.

1.6.4.1 Expressions for A and B

The Drucker-Prager model can be written in terms of the principal stresses as

$$\sqrt{\frac{1}{6}[(\sigma_1-\sigma_2)^2+(\sigma_2-\sigma_3)^2+(\sigma_3-\sigma_1)^2]} = A + B\ (\sigma_1+\sigma_2+\sigma_3)\ . \tag{0.29}$$

If σ_t is the yield stress in uniaxial tension, the Drucker-Prager criterion implies

$$\frac{1}{\sqrt{3}}\,\sigma_t = A + B\ \sigma_t\ . \tag{0.30}$$

If σ_c is the yield stress in uniaxial compression, the Drucker-Prager criterion implies

$$\frac{1}{\sqrt{3}}\,\sigma_c = A - B\ \sigma_c\ . \tag{0.31}$$

Solving these two equations gives

$$A = \frac{2}{\sqrt{3}}\left(\frac{\sigma_c\ \sigma_t}{\sigma_c+\sigma_t}\right)\ ;\quad B = \frac{1}{\sqrt{3}}\left(\frac{\sigma_t-\sigma_c}{\sigma_c+\sigma_t}\right)\ . \tag{0.32}$$

1.6.4.2 Uniaxial asymmetry ratio

The Drucker-Prager model predicts different uniaxial yield stresses in tension and in compression. The uniaxial asymmetry ratio for the Drucker-Prager model is

$$\beta = \frac{\sigma_c}{\sigma_t} = \frac{1-\sqrt{3}\ B}{1+\sqrt{3}\ B}\ . \tag{0.33}$$

1.6.4.3 Expressions in terms of cohesion and friction angle

Since the Drucker-Prager yield surface is a smooth version of the Mohr-Coulomb yield surface, it is often expressed in terms of the cohesion (c) and the angle of internal friction (φ) that are used to describe the Mohr-Coulomb yield surface. If we assume that the Drucker-Prager yield surface circumscribes the Mohr-Coulomb yield surface then the expressions for A and B are

$$A = \frac{6\ c\ \cos\phi}{\sqrt{3}(3+\sin\phi)}\ ;\quad B = \frac{2\ \sin\phi}{\sqrt{3}(3+\sin\phi)} \tag{0.34}$$

If the Drucker-Prager yield surface inscribes the Mohr-Coulomb yield surface then

$$A = \frac{6\ c\ \cos\phi}{\sqrt{3}(3-\sin\phi)}\ ;\quad B = \frac{2\ \sin\phi}{\sqrt{3}(3-\sin\phi)} \tag{0.35}$$

1.6.4.4 Extensions of the isotropic Drucker-Prager model

The Drucker-Prager criterion can also be expressed in the alternative form

$$J_2 = (A + B\ I_1)^2 = a + b\ I_1 + c\ I_1^2\ . \tag{0.36}$$

1.6.5 Bresler-Pister yield criterion

The Bresler-Pister yield criterion is a function that was originally devised to predict the strength of concrete under multiaxial stress states. This yield criterion is an extension of the Drucker-Prager yield criterion and can be expressed on terms of the stress invariants as

$$\sqrt{J_2} = A + B\ I_1 + C\ I_1^2 \tag{0.37}$$

where I_1 is the first invariant of the Cauchy stress, J_2 is the second invariant of the deviatoric part of the Cauchy stress, and A,B,C are material constants.

Yield criteria of this form have also been used for polypropylene and polymeric foams.

The parameters A,B,C have to be chosen with care for reasonably shaped yield surfaces. If σ_c is the yield stress in uniaxial compression, σ_t is the yield stress in uniaxial tension, and σ_b is the yield stress in biaxial compression, the parameters can be expressed as

$$B = \left(\frac{\sigma_t - \sigma_c}{\sqrt{3}(\sigma_t + \sigma_c)}\right)\left(\frac{4\sigma_b^2 - \sigma_b(\sigma_c + \sigma_t) + \sigma_c\sigma_t}{4\sigma_b^2 + 2\sigma_b(\sigma_t - \sigma_c) - \sigma_c\sigma_t}\right)$$

$$C = \left(\frac{1}{\sqrt{3}(\sigma_t + \sigma_c)}\right)\left(\frac{\sigma_b(3\sigma_t - \sigma_c) - 2\sigma_c\sigma_t}{4\sigma_b^2 + 2\sigma_b(\sigma_t - \sigma_c) - \sigma_c\sigma_t}\right)$$

$$A = \frac{\sigma_c}{\sqrt{3}} + c_1\sigma_c - c_2\sigma_c^2 \qquad (0.38)$$

1.6.5.1 Alternative forms of the Bresler-Pister yield criterion

In terms of the equivalent stress (σe) and the mean stress (σm), the Bresler-Pister yield criterion can be written as

$$\sigma_e = a + b\ \sigma_m + c\ \sigma_m^2\ ;\quad \sigma_e = \sqrt{3J_2}\ ,\quad \sigma_m = I_1/3 \qquad (0.39)$$

The Etse-Willam form of the Bresler-Pister yield criterion for concrete can be expressed as

$$\sqrt{J_2} = \frac{1}{\sqrt{3}}\,I_1 - \frac{1}{2\sqrt{3}}\left(\frac{\sigma_t}{\sigma_c^2 - \sigma_t^2}\right)\ I_1^2 \qquad (0.40)$$

where σc is the yield stress in uniaxial compression and σ_t is the yield stress in uniaxial tension.

The GAZT yield criterion for plastic collapse of foams also has a form similar to the Bresler-Pister yield criterion and can be expressed as

$$\sqrt{J_2} = \begin{cases} \frac{1}{\sqrt{3}}\sigma_t - 0.03\sqrt{3}\frac{\rho}{\rho_m\ \sigma_t}\ I_1^2 \\ -\frac{1}{\sqrt{3}}\sigma_c + 0.03\sqrt{3}\frac{\rho}{\rho_m\ \sigma_c}\ I_1^2 \end{cases} \quad (0.41)$$

Where ρ is the density of the foam and ρ_m is the density of the matrix material.

2 Deformation, Fatigue and Creep – Theories and Models

The inelastic material behaviour of metals is often involved in technical processes like metal forming. The material properties of metals are well investigated (see e.g. Benallal et al., 1989; Bruhns et al., 1992; Chaboche and Lemaitre, 1990; Haupt and Lion, 1995; Khan and Jackson, 1999; Krempl, 1979; Krempl and Khan, 2003; Lion, 1994) and the origin of the visco-plastic behaviour is well understood. Basically, the distortion of the metallic lattice as well as the production and motion of dislocations leads to a static hysteresis and non-linear rate dependence. It is worthy to be mentioned that the rate-dependent behaviour of metals is already observable at moderate strain rates (cf. Haupt and Lion, 1995; Krempl, 1979; Lion, 1994).

In order to represent the inelastic behaviour of metals a lot of constitutive theories were developed: see e.g. Bertram (2003), Bucher et al. (2004), Bruhns et al. (1992), Green and Naghdi (1965), Haupt and Kamlah (1995), Miehe and Stein (1992), Lehmann (1983), Rajagopal and Srinivasa (1998a), Scheidler and Wright (2001), Simo and Miehe (1992), Tsakmakis (1996), and Tsakmakis (2004) for a common overview see the textbooks Haupt (2002) and Lubliner (1990). Furthermore, the visco-plastic behaviour of metals is discussed in Chaboche (1977), Haupt and Lion (1995), Krempl (1987), Lion (2000), and Perzyna (1963).

It is known that because of the different crystallographic orientation of the grains in polycrystalline metal materials, micro stresses in such materials differ considerably (also because of the anisotropy of the coefficient of elasticity) from the average stresses both by the value and by the direction of the deviator vector.

For this reason, the micro plastic deformations differ considerably in terms of value from the average deformation and this induces residual stresses usually referred to as residual stresses of type II, which cause the Bauschinger effect and plastic hysteresis. It is evident that the time-independent micro plastic deformations and micro creep deformations may take place both when deforming with stresses higher and lower than the elastic limit and may produce the relaxation of internal stresses of type II. B. I. Rovinsky and V. G. Liuttsau have linked the processes of micro- and macro creep and have shown that the character of the process of micro stress relaxation was similar to that of macro stress relaxation.

Which deformations, micro plastic or micro creep, are larger in magnitude in conditions of stresses under the elastic limit (σ_y), including cyclic stresses, is the question that can only be answered on the basis of experimental results. It is known, as proved by the analysis of data on the micro deformations of different materials under single loading, that at low temperatures the micro plastic deformations are considerably larger. However, in the case of cyclic deformation the process of development of micro plastic deformations in many materials is slowed as the number of cycles increases, whereas the rate of accumulation of micro creep deformations under cyclic alternating loading increases with the number of cycles.

At high temperatures the micro creep deformations are considerably larger than the micro plastic deformations.

2.1 Time independent Models

Some of the current models of plasticity consider time-dependent irreversible deformations separately from time-independent deformations. At the same time,

the parameters of a number of other models for plasticity are time-dependent components of the tensor of plastic deformation.

In a number of cases it is not correct to use the second approach and it is more appropriate to use the models of thermo-elasto-visco-plasticity (and thermo-visco-elasto-plasticity, according to the classification of Perzyna) and the division of irreversible deformations into time-dependent and time-independent components. It should be noted that the question about such divisibility (on the basis of the notion of momentary deformation curves introduced by Yu. N. Rabotnov) was resolved positively in experimental studies of different alloys based on iron and nickel. The results of an experimental study pertaining the conditions of a uniaxial stress state were observed mainly for heat-resistant steels and alloys.

2.2 Time dependent models

In all cases it was assumed that the deformation of the trusses was very small and (as a consequence) their behaviour was linearly elastic. In this chapter we will again focus the attention on (simple) truss structures. Now, however, we will allow deformations to become large. Also the material behaviour is not longer linearly elastic. For example we can consider elastomeric, elasto-plastic and visco-elastic

material behaviour. Large deformations and nonlinear material behaviour will render the problem strongly non-linear such as the equations which must be solved using nonlinear solvers.

2.3 Deformation Models

For all these reasons is evident how deformation models play a significant role into material description abilities. The main role is played by the ability and capability to describe deformation models.

2.3.1 Mechanisms

The active deformation mechanism in a material depends on the homologous temperature, confining pressure, strain rate, stress, grain size, presence or absence of a pore fluid, presence or absence of impurities in the material. Note these variables are not fully independent e.g. for a pure material of a fixed grain size, at a given pressure, temperature and stress, the strain-rate is given by the flow-law associated with the particular mechanism(s). More than one mechanism may be active under a given set of conditions and some mechanisms cannot operate independently but must act in conjunction with another in order that significant permanent strain can develop. In a single deformation episode, the dominant mechanism may change with time e.g. recrystallization to a fine grain size at an early stage may allow diffusive mass transfer processes to become dominant.

The recognition of the active mechanism(s) in a material almost always requires the use of microscopic techniques, in most cases using a combination of optical microscopy, SEM and TEM.

Using a combination of experimental deformation to find the flow-laws under particular conditions and from microscopic examination of the samples afterwards it has been possible to represent the conditions under which individual deformation mechanisms dominate for some materials in the form of deformation mechanism maps.

Five main mechanisms are recognized; cataclasis, dislocation creep, recrystallization, diffusive mass transfer and grain-boundary sliding.

2.3.2 Cataclasis

This is a mechanism that operates under low to moderate homologous temperature, low confining pressure and relatively high strain rates.

2.3.3 Dislocation creep

Dislocation glide is the main process but cannot act on its own to produce large strains due to the effects of strain hardening. Some form of recovery process, such as dislocation climb or grain-boundary migration must also be active.

2.3.4 Dynamic recrystallization

Two main mechanisms of recrystallization are known, sub-grain rotation and grain boundary migration, and only the former involves actual deformation. Grain boundary migration involves no strain in itself, but is one of the recovery mechanisms that can allow dislocation processes to proceed to large strains.

2.3.5 Diffusive mass transfer

In this group of mechanisms, strain is accommodated by a change in shape involving the transfer of mass by diffusion; through the lattice (Nabarro-Herring creep), the grain boundaries (Coble creep) and via a pore fluid (Pressure solution).

- *Nabarro-Herring creep* acts at high homologous temperatures and is grain size dependent with the strain-rate inversely proportional to the square of the grain size.

- *Coble-creep* acts at high homologous temperatures and is strongly grain-size dependent, with a flow-law where strain-rate is inversely proportional to the cube of the grain size .

- *Pressure solution* operates at moderate homologous temperatures and relatively low strain-rates and requires the presence of a pore fluid.

2.3.6 Grain-boundary sliding

This mechanism must act with another to change the shapes of the grains so that they can slide past each other without creating significant voids. This mechanism,

acting with diffusive mass transfer has been linked with the development of super-plasticity.

2.4 Creep Models

Creep is the tendency of a solid material to slowly move or deform permanently under the influence of stresses. It occurs as a result of long term exposure to levels of stress that are below the yield strength or ultimate strength of the material. Creep is more severe in materials that are subjected to heat for long periods, and near the melting point. It is often observed in glasses.[citation needed] Creep always increases with temperature.

The rate of this deformation is a function of the material properties, exposure time, exposure temperature and the applied load (stress). Depending on the magnitude of the applied stress and its duration, the deformation may become so large that a component can no longer perform its function — for example creep of a turbine blade will cause the blade to contact the casing, resulting in the failure of the blade. Creep is usually of concern to engineers and metallurgists when evaluating components that operate under high stresses or high temperatures. Creep is not necessarily a failure mode, but is instead a deformation mechanism. Moderate creep in concrete is sometimes welcomed because it relieves tensile stresses that otherwise may have led to cracking.

Unlike brittle fracture, creep deformation does not occur suddenly upon the application of stress. Instead, strain accumulates as a result of long-term stress. Creep deformation is "time-dependent" deformation.

The temperature range in which creep deformation may occur differs in various materials. For example, Tungsten requires a temperature in the thousands of degrees before creep deformation can occur while ice formations such as the Antarctic ice cap will creep in freezing temperatures. Generally, the minimum temperature required for creep deformation to occur is 30% of the melting point for metals and 40–50% of melting point for ceramics. Virtually any material will creep upon approaching its melting temperature. Since the minimum temperature is relative to melting point, creep can be seen at relatively low temperatures for some materials. Plastics and low-melting-temperature metals, including many solders, creep at room temperature as can be seen markedly in old lead hot-water pipes. Planetary ice is often at a high temperature relative to its melting point, and creeps.

Creep deformation is important not only in systems where high temperatures are endured such as nuclear power plants, jet engines and heat exchangers, but also in the design of many everyday objects. For example, metal paper clips are stronger than plastic ones because plastics creep at room temperatures. Aging glass windows are often erroneously used as an example of this phenomenon: measurable creep would only occur at temperatures above the glass transition temperature around 900°F/500°C.

An example of an application involving creep deformation is the design of tungsten light bulb filaments. Sagging of filament coil between its supports increases with time due to creep deformation caused by the weight of the filament itself. If too much deformation occurs, the adjacent turns of the coil touch one another, causing an electrical short and local overheating, which quickly lead to failure of the filament. The coil geometry and supports are therefore designed to limit the stresses caused by the weight of the filament, and a special tungsten alloy with small amounts of oxygen trapped in the crystallite grain boundaries is used to slow the rate of coble creep.

In steam turbine power plants, steam pipes carry superheated vapour at high temperatures (1050°F/566°C) and high pressures of 3500 psi (24.1 MPa) or greater. In modern jet engines, temperatures can reach up to 1400°C (2550°F) and initiate creep deformation in even advanced-coated turbine blades. Hence, it is crucial for safety's sake to understand creep deformation behaviour of materials.

2.4.1 Stages of creep

In the initial stage, or primary creep, the strain rate is relatively high, but slows with increasing strain. The strain rate eventually reaches a minimum and becomes near constant. This is known as secondary or steady state creep. This stage is the most understood. The characterized "creep strain rate" typically refers to the rate in this secondary stage. Stress dependence of this rate depends on the creep mechanism. In tertiary creep, the strain rate exponentially increases with strain.

2.4.2 Implemented creep model

The process allowing the calculation of the creep damage is called **process creep. In this process the equation that regulated the increment of creep damage is the following:

$$dD = \left(\frac{|\sigma|}{A}\right)^{r} (1-D)^{-k} dt$$

Obtained implementing Rabotnov-Kachanov creep model.

A, r and k coefficients are typical for each material and are determined throug a serie of uniaxial creep experimental tests. For each test condition, must be calculated the creep time to rupture tR.

Extracting *dt* from the previous formula and integrating with fitted boundary conditions, user gets:

$$t_R = \frac{1}{k+1}\left(\frac{|\sigma|}{A}\right)^{-r}$$

Once known the cycle duration, user can determine the time number of cycles to creep rupture.

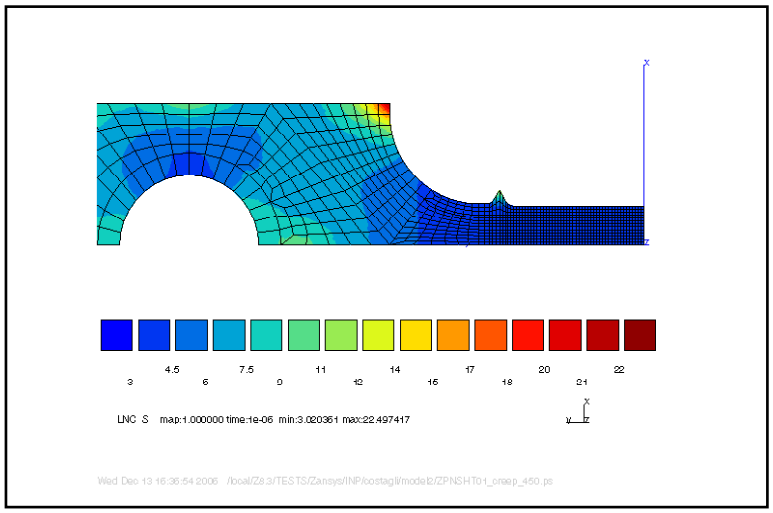

Figure 2.1- Creep life – contour plot.

2.5 Fatigue Models

In materials science, fatigue is the progressive and localized structural damage that occurs when a material is subjected to cyclic loading. The maximum stress values are less than the ultimate tensile stress limit, and may be below the yield stress limit of the material.

2.5.1 Fatigue life

ASTM defines fatigue life, N_f, as the number of stress cycles of a specified character that a specimen sustains before failure of a specified nature occurs.

2.5.2 Characteristics of fatigue

The process starts with dislocation movements, eventually forming persistent slip bands that nucleate short cracks. Fatigue is a stochastic process, often showing considerable scatter even in controlled environments. The greater the applied stress, the shorter the life.

Figure 2.2- Fracture of Inconel Crank Arm. Dark area: slow crack growth. Bright area: sudden fracture.

Fatigue life scatter tends to increase for longer fatigue lives. Damage is cumulative. Materials do not recover when rested. Fatigue life is influenced by a variety of factors, such as temperature, surface finish, presence of oxidizing or inert chemicals, residual stresses, contact (fretting), etc.

Some materials (e.g., some steel and titanium alloys) exhibit a theoretical fatigue limit below which continued loading does not lead to failure. In recent years, researchers (see, for example, the work of Bathias, Murakami, and Stanzl-Tschegg) have found that failures occur below the theoretical fatigue limit at very high fatigue lives (109 to 1010 cycles). An ultrasonic resonance technique is used in these experiments with frequencies around 10–20 kHz.

High cycle fatigue strength (about 103 to 108 cycles) can be described by stress-based parameters. A load-controlled servo-hydraulic test rig is commonly used in these tests, with frequencies of around 20–50 Hz. Other sorts of machines, like resonant magnetic machines, can also be used, achieving frequencies up to 250 Hz.

Low cycle fatigue (typically less than 103 cycles) is associated with widespread plasticity; thus, a strain-based parameter should be used for fatigue life prediction. Testing is conducted with constant strain amplitudes at 1–5 Hz.

2.5.3 Probabilistic nature of fatigue

As coupons sampled from a homogeneous frame will manifest variation in their number of cycles to failure, the S-N curve should more properly be an S-N-P curve capturing the probability of failure after a given number of cycles of a certain stress. Probability distributions that are common in data analysis and in design against fatigue include the lognormal distribution, extreme value distribution, Birnbaum-Saunders distribution, and Weibull distribution.

2.5.4 Complex loadings

In practice, a mechanical part is exposed to a complex, often random, sequence of loads, large and small. In order to assess the safe life of such a part is necessary to reduce the complex loading to a series of simple cyclic loadings using a technique such as Rainflow analysis.

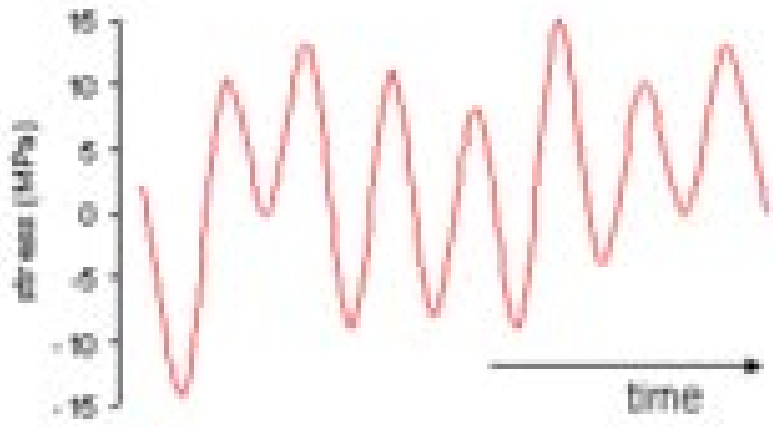

Figure 2.3- Spectrum loading

For this type of technique is necessary to create a histogram of cyclic stress vs time. For each stress level, is necessary to calculate the degree of cumulative

damage incurred from the S-N curve; and combine the individual contributions using an algorithm such as Miner's rule.

2.5.4.1 Miner's rule

In 1945, M. A. Miner popularised a rule that had first been proposed by A. Palmgren in 1924. The rule, variously called Miner's rule or the Palmgren-Miner linear damage hypothesis, states that where there are k different stress magnitudes in a spectrum, Si ($1 \leq i \leq k$), each contributing $n_i(S_i)$ cycles, then if $N_i(S_i)$ is the number of cycles to failure of a constant stress reversal Si, failure occurs when:

$$\sum_{i=1}^{k} \frac{n_i}{N_i} = C \tag{0.42}$$

C is experimentally found to be between 0.7 and 2.2. Usually for design purposes, C is assumed to be 1. This can be thought of as assessing what proportion of life is consumed by stress reversal at each magnitude then forming a linear combination of their aggregate.

Though Miner's rule is a useful approximation in many circumstances, it has two major limitations: It fails to recognise the probabilistic nature of fatigue and there is no simple way to relate life predicted by the rule with the characteristics of a probability distribution.

There is sometimes an effect in the order in which the reversals occur. In some circumstances, cycles of low stress followed by high stress cause more damage than would be predicted by the rule. It does not consider the effect of overload or high stress, which may result in a compressive residual stress. High stress followed by low stress may have less damage due to the presence of compressive residual stress.

2.5.4.2 Paris' Relationship

Anderson, Gomez and Paris derived relationships for the stage II crack growth with cycles N, in terms of the cyclical component ΔK of the Stress Intensity Factor K:

$$\frac{da}{dN} = C(\Delta K)^m \tag{0.43}$$

where a is the crack length and m is typically in the range 3 to 5 (for metals).

This relationship was later modified (by Forman, 1967) to make better allowance for the mean stress, by introducing a factor depending on (1-R) where R = min. stress/max stress, in the denominator.

2.5.5 Low-cycle fatigue

Where the stress is high enough for plastic deformation to occur, the account in terms of stress is less useful and the strain in the material offers a simpler description. Low-cycle fatigue is usually characterised by the Coffin-Manson relation (published independently by L. F. Coffin in 1954 and S. S. Manson 1953):

$$\frac{\Delta\epsilon_p}{2} = \epsilon'_f(2N)^c \tag{0.44}$$

Where:

- $\Delta\varepsilon_p /2$ is the plastic strain amplitude
- ε_f' is an empirical constant known as the fatigue ductility coefficient, the failure strain for a single reversal
- 2N is the number of reversals to failure (N cycles)
- c is an empirical constant known as the fatigue ductility exponent, commonly ranging from -0.5 to -0.7 for metals.

A similar relationship for materials such as Zirconium, used in the nuclear industry, is due to W.J. O'Donnell and B. F. Langer.

2.5.6 Fatigue and fracture mechanics

The account above is purely phenomenological and, though it allows life prediction and design assurance, it does not enable life improvement or design

optimisation. For the latter purposes, an exposition of the causes and processes of fatigue is necessary. Such an explanation is given by fracture mechanics in four stages.

- Crack nucleation
- Stage I crack-growth
- Stage II crack-growth
- Ultimate ductile failure

2.5.7 Implemented Fatigue model

The implemented fatigue model is recalled through the procedure **process fatigue_S in which the number of cycles to rupture is calculated with the following relation:

$$N_F = \frac{\langle \sigma_u - \sigma_{Max} \rangle}{a(\beta+1)\langle \sigma_{Max} - \sigma_l(\bar{\sigma}) \rangle} \left(\frac{\sigma_{Max} - \bar{\sigma}}{M(\bar{\sigma})} \right)^{-\beta} \tag{0.45}$$

Obtained through the integration of the damage growth rate law:

$$\frac{dD}{dN} = \left[1 - (1-D)^{\beta+1} \right]^{\alpha(\sigma_{Max}, \bar{\sigma})} \left(\frac{\sigma_{Max} - \bar{\sigma}}{M(\bar{\sigma})} \right)^{\beta}$$

Where:

σ_{Max} = Maximum stress of the cycle
$\bar{\sigma}$ = Average stress of the cycle
σ_u = Ultimate tensile stress
α = Material coefficient

$\sigma_l(\overline{\sigma})$= Fatigue limit for cycle with mean stress value $\neq 0$ expressed in terms of maximum stress.

$$\sigma_l(\overline{\sigma}) = \overline{\sigma} + \sigma_{l_0}(1 - b_1\overline{\sigma}) \tag{0.46}$$

with:

σ_{l_0} = Fatigue limit for cycle with mean stress value = 0 expressed in terms of maximum stress.

b_1, b_2 , M = Material coefficients

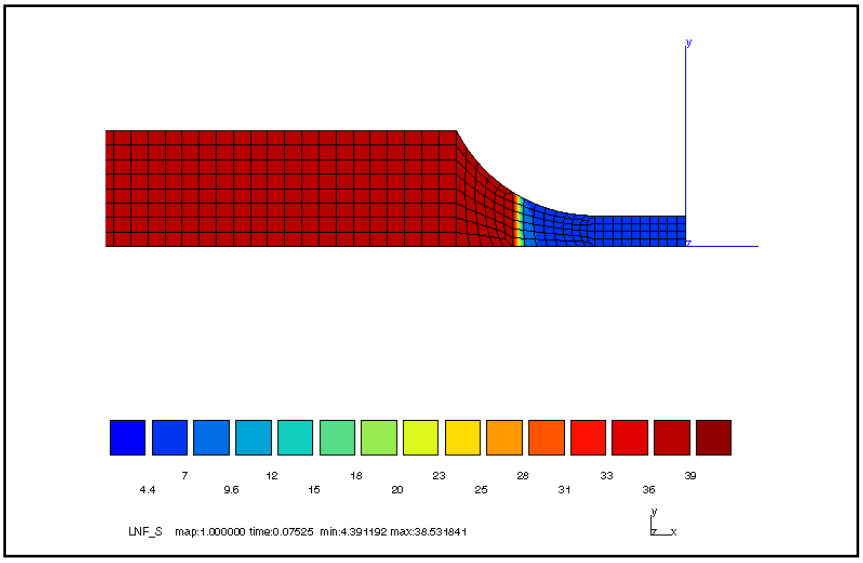

Figure 2.4- Fatigue Life - Contour plot

2.6 Non Linear damage accumulation theory

Non-Linear damage accumulation theory is here utilized to apply a damage accumulation model able to predict life of a structural component considering a non-linear interaction mechanism between creep and fatigue.

The number of cycles to rupture N_F, obtained considering only fatigue contribution, has been calculated using the following formulas:

$$N_F = \frac{\langle \sigma_u - \sigma_{Max} \rangle}{a(\beta+1)\langle \sigma_{Max} - \sigma_1(\overline{\sigma}) \rangle} \left(\frac{\sigma_{Max} - \overline{\sigma}}{M(\overline{\sigma})} \right)^{-\beta} \tag{0.47}$$

And

$$t_R = \frac{1}{k+1}\left(\frac{|\sigma|}{A}\right)^{-r} \tag{0.48}$$

Obtained from the Chaboche and Rabotnov-Kachanov theories, herein explained.

According to these formulations, user can calculate damage evolution (from D_i to D_f), inside each cycle, according to the following formulas:

$$1/N_c = (1-D_i)^{k+1} - (1-D)^{k+1} \tag{0.49}$$

And

$$1/N_f = \left[1-(1-D_f)^{\beta+1}\right]^{(1-\alpha)} - \left[1-(1-D)^{\beta+1}\right]^{(1-\alpha)} \tag{0.50}$$

Where

$$\alpha = 1 - a \cdot \left(\frac{\sigma_{\max} - \sigma_l}{\sigma_u - \sigma_{\max}}\right) \tag{0.51}$$

$$\sigma_1(\bar{\sigma}) = \bar{\sigma} + \sigma_{1_0}(1 - b_1\bar{\sigma})$$

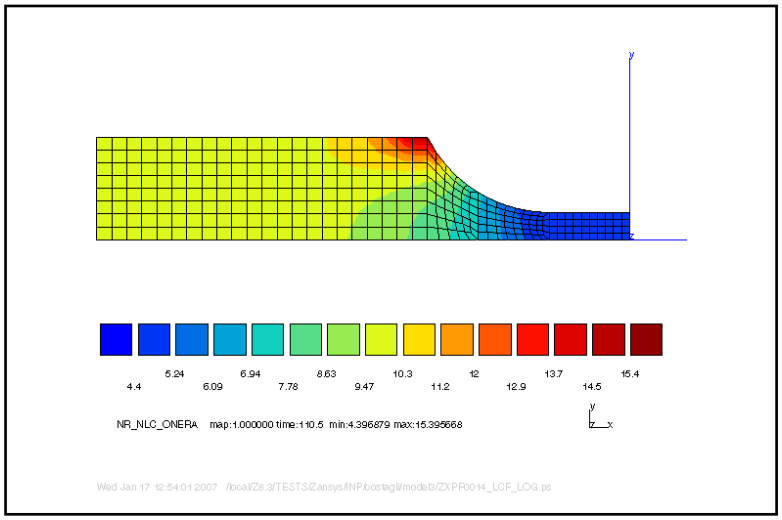

Figure 2.5- Fatigue Life - Contour plot

The results of these creep and fatigue models implementation, are that considering non-linear damage accumulation, evolution of creep-fatigue life calculation is significantly different.

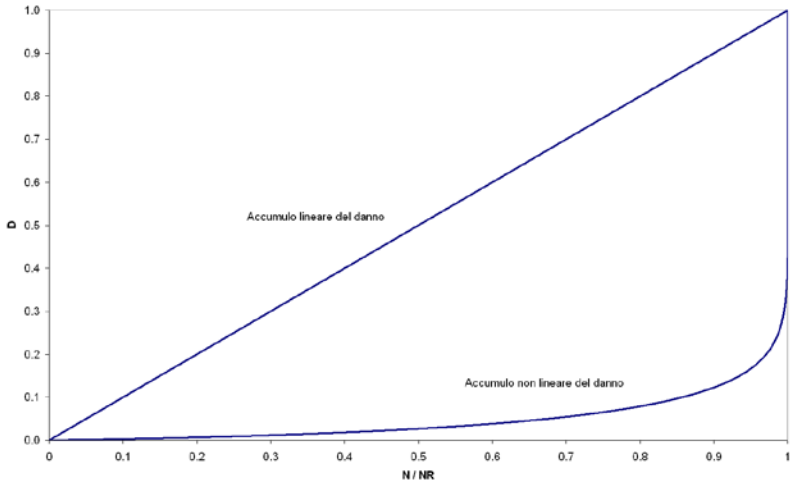

Figure 2.6- Damage cumulation – Linear vs non-linear cumulation

In this way, is clear that life calculation of a component can give significantly different results if compared to linear superimposing of effects principle.

3 Material models for FEM software

The finite element method (FEM) (sometimes referred to as finite element analysis) is a numerical technique for finding approximate solutions of partial differential equations (PDE) as well as of integral equations. The solution approach is based either on eliminating the differential equation completely (steady state problems), or rendering the PDE into an approximating system of ordinary differential equations, which are then solved using standard techniques such as Euler's method, Runge-Kutta, etc.

In solving partial differential equations, the primary challenge is to create an equation that approximates the equation to be studied, but is numerically stable, meaning that errors in the input data and intermediate calculations do not accumulate and cause the resulting output to be meaningless. There are many ways of doing this, all with advantages and disadvantages. The Finite Element Method is a good choice for solving partial differential equations over complex domains (like cars and oil pipelines), when the domain changes (as during a solid state reaction with a moving boundary), when the desired precision varies over the entire domain, or when the solution lacks smoothness.

3.1 Theories Overview

FEM software became a valid design tool as soon as visco-plasticity theories arose and were implemented in automatic calculation software.

The theoretical development of visco-plasticity has its origin with the works of Stowell [1957], Prager [1961], and Perzyna [1963], whose theories did not contain evolving internal state variables. The field blossomed in the 1970's when rapid advances in computing technology enabled accurate solutions to be obtained readily. Internal state variable theories began to appear in the models of Geary & Onat [1974], Bodner & Partom [1975], Hart [1976] and Miller [1976], Ponter & Lechie [1976], Chaboche [1977], Krieg et al. [1978], and Robinson [1978].

Theoretical refinements have continued to occur throughout the 1980's in the models of Stouffer & Bodner [1979], Valanis [1980], Walker [1981], Schmidt & Miller [1981], Chaboche & Rousselier [1983], Estrin & Mecking[1984], Krempl et al. [1986], Lone & Miller [1986], and Anand & Brown [1987].

Reviews on various aspects of visco-plasticity have been written by Perzyna [1966], Walker [1981], Chan et al. [1984], Lemaitre & Chaboche [1985], and Swearengen & Holbrook [1985]. Although this listing is by no means complete, it is representative of the work that has been done in visco-plasticity and of the attention that it has received.

3.2 Elasticity

Elastic material model is the one based on the hook's law previously introduced. It is based on the linear proportionality between stress and strain. Do not allow permanent deformation and is valid only under yield point of the material. In any case, as evaluation of the stress results, it is always more conservative than the other analyses.

The elastic regime is characterized by a linear relationship between stress and strain, denoted linear elasticity. Good examples are a rubber band and a bouncing ball. This idea was first stated by Robert Hooke in 1675 as a Latin anagram whose solution he published in 1678 as "Ut tensio, sic vis" which means "As the extension, so the force."

This linear relationship is called Hooke's law. The classic model of linear elasticity is the perfect spring. Although the general proportionality constant between stress and strain in three dimensions is a 4th order tensor, when considering simple situations of higher symmetry such as a rod in one dimensional loading, the relationship may often be reduced to applications of Hooke's law.

Because most materials are elastic only under relatively small deformations, several assumptions are used to linearize the theory. Most importantly, higher order terms are generally discarded based on the small deformation assumption. In certain special cases, such as when considering a rubbery material, these assumptions may not be permissible. However, in general, elasticity refers to the linearized theory of the continuum stresses and strains.

3.3 Elasto-plasticity

Above a certain stress known as the elastic limit or the yield strength of an elastic material, the relationship between stress and strain becomes nonlinear. Beyond this limit, the solid may deform irreversibly, exhibiting plasticity.

3.4 Visco-Elasticity

Unlike purely elastic substances, a viscoelastic substance has an elastic component and a viscous component. The viscosity of a viscoelastic substance gives the substance a strain rate dependent on time. Purely elastic materials do not dissipate energy (heat) when a load is applied, then removed. However, a viscoelastic substance loses energy when a load is applied, then removed. Hysteresis is observed in the stress-strain curve, with the area of the loop being equal to the energy lost during the loading cycle. Since viscosity is the resistance to thermally activated plastic deformation, a viscous material will lose energy through a loading cycle. Plastic deformation results in lost energy, which is uncharacteristic of a purely elastic material's reaction to a loading cycle.

Specifically, viscoelasticity is a molecular rearrangement. When a stress is applied to a viscoelastic material such as a polymer, parts of the long polymer chain change position. This movement or rearrangement is called Creep. Polymers remain a solid material even when these parts of their chains are rearranging in order to accompany the stress, and as this occurs, it creates a back stress in the material. When the back stress is the same magnitude as the applied stress, the material no longer creeps. When the original stress is taken away, the accumulated back stresses will cause the polymer to return to its original form. The material creeps, which gives the prefix visco-, and the material fully recovers, which gives the suffix -elasticity.

3.4.1 Visco-Elastic Creep

When subjected to a step constant stress, visco-elastic materials experience a time-dependent increase in strain. This phenomenon is known as visco-elastic creep.

At a time t_0, a visco-elastic material is loaded with a constant stress that is maintained for a sufficiently long time period. The material responds to the stress

with a strain that increases until the material ultimately fails. When the stress is maintained for a shorter time period, the material undergoes an initial strain until a time t1, after which the strain immediately decreases (discontinuity) then gradually decreases at times t > t1 to a residual strain.

Visco-elastic creep data can be presented by plotting the creep modulus (constant applied stress divided by total strain at a particular time) as a function of time [6]. Below its critical stress, the visco-elastic creep modulus is independent of stress applied. A family of curves describing strain versus time response to various applied stress may be represented by a single visco-elastic creep modulus versus time curve if the applied stresses are below the material's critical stress value.

Visco-elastic creep is important when considering long-term structural design. Given loading and temperature conditions, designers can choose materials that best suit component lifetimes.

3.5 Visco-Plasticity

The general structure of a visco-plastic theory is developed from physical and thermo dynamical considerations. The flow equation is of classical form. The dynamic recovery approach is shown to be superior to the hardening function approach for incorporating nonlinear strain hardening into the material response through the evolutionary equation for back stress. Attention has been paid mainly to gradient plasticity, visco-plasticity, and Cosserat-type plasticity. It seems that formulations based on non-local averaging, widely used in continuum damage mechanics, have not been fully explored in the context of the theory of plasticity.

3.5.1 Hardening test

The hardening curves of a visco-plastic material are not significantly different from those of plastic material. Nevertheless, three essential differences are apparent: at the same strain, the higher the rate of strain (or stress) is, the higher will be the stress. A change in the rate of strain during the test results in an immediate change in the stress – strain curve. Also, the concept of a plastic yield limit is no longer strictly applicable.

The hypothesis of portioning the partitioning the strains by decoupling is still applicable in most cases (where the strains are small):

$$\varepsilon = \varepsilon_e + \varepsilon_p$$

Where:

ε_e is the linear elastic strain and
ε_p is the visco-plastic strain.

3.5.2 Creep test

The classical creep curve represents the evolution of strain as a function of time in a material subjected to uniaxial stress at a constant temperature.

This curve shows three phases or periods of behaviour: a 'primary' creep phase $0 \leq \varepsilon \leq \varepsilon_1$ during which hardening of the material leads to a decrease in the rate of flow which is initially very high. A 'secondary' creep phase $\varepsilon_1 \leq \varepsilon \leq \varepsilon_2$ during which the rate of flow is almost constant. Finally a 'tertiary' creep phase $\varepsilon_2 \leq \varepsilon \leq \varepsilon_R$ in which the usual increase in the strain rate up to the fracture strain.

3.5.3 Relaxation test

Relaxation tests demonstrate the decrease in the stress which results from maintaining a volume element in uniaxial loading at constant strain. In fact these tests characterize the viscosity and can be used to determine the relation which exists between the stress and the rate of visco-plasticity strain. In terms of rates:

$$\dot{\varepsilon} = \dot{\varepsilon_e} + \dot{\varepsilon_p}$$

Where, with the linear elasticity $\dot{\varepsilon_e} = -\dot{\sigma}/E$. Thus, each point on the relaxation curve $\sigma(t)$ gives the stress and rate of visco-plastic strain $\dot{\varepsilon_p} = -\dot{\sigma}/E$

3.6 Non Linear FEM Analyses

Each method can be applied for powerful analysis. But has noteworthy limitations. The method of mechanics of materials is limited to very simple structural elements under relatively simple loading conditions. The structural elements and loading conditions allowed, however, are sufficient to solve many useful engineering problems. The theory of elasticity allows the solution of structural elements of general geometry under general loading conditions, in principle. Analytical solution, however, is limited to relatively simple cases.

The solution of elasticity problems also requires the solution of a system of partial differential equations, which is considerably more mathematically demanding than the solution of mechanics of materials problems, which require at most the solution of an ordinary differential equation. The finite element method is perhaps the most restrictive and most useful at the same time. This method itself relies upon other structural theories (such as the other two discussed here) for equations to solve. It does, however, make it generally possible to solve these equations, even with highly complex geometry and loading conditions, with the restriction that there is always some numerical error. Effective and reliable use of this method requires a solid understanding of its limitations.

3.6.1 State of the art Description

Several methods of solving the system of simultaneous equations are available in the FEM programs: sparse direct solution, Preconditioned Conjugate Gradient (PCG) solution, Jacobi Conjugate Gradient (JCG) solution, Incomplete Cholesky Conjugate Gradient (ICCG) solution, frontal direct solution, and an automatic iterative solver option (ITER).

Regarding the ANSYS product, the sparse direct solver is the default solver for all analyses that include both p-elements and constraint equations, and sub structuring analyses (which each use the frontal direct solver by default). In addition to these solvers, the Parallel Performance for ANSYS add-on product includes the Algebraic Multigrid (AMG) solver as well as distributed versions of the PCG, JCG, and Sparse solvers for use in Distributed ANSYS.

The sparse direct solver (including the Block Lanczos method for modal analyses) is based on a direct elimination of equations, as opposed to iterative

solvers, where the solution is obtained through an iterative process that successively refines an initial guess to a solution that is within an acceptable tolerance of the exact solution. Direct elimination requires the factorization of an initial very sparse linear system of equations into a lower triangular matrix followed by forward and backward substitution using these triangular systems. The lower triangular matrix factors are typically much larger than the initial assembled sparse matrix; hence the large disk or in-core memory requirements for direct methods.

Sparse direct solvers seek to minimize the cost of factorizing the matrix as well as the size of the factor using sophisticated equation reordering strategies. Iterative solvers do not require a matrix factorization and typically iterate towards the solution using a series of very sparse matrix-vector multiplications along with a preconditioning step, both of which require less memory and time per iteration than direct factorization. However, convergence of iterative methods is not guaranteed and the number of iterations required to reach an acceptable solution may be so large that direct methods are faster in some cases.

Because the sparse direct solver is based on direct elimination, poorly conditioned matrices do not pose any difficulty in producing a solution. Direct factorization methods will always give an answer if the equation system is not singular. When the system is close to singular, the solver can usually give a solution (although you will need to verify the accuracy).

The ANSYS sparse solver can run completely in memory if sufficient memory is available. Although the sparse solver can run efficiently in optimal out-of-core mode (default), requiring about the same memory usage as the PCG solver (1 GB per million DOFs), it will require a large disk file to store the factorized matrix, usually 10 GB per million DOFs. The amount of I/O required for a typical static analysis is three times the size of the matrix factorization. Running the factorization in-core (completely in memory) for modal runs can save significant amounts of wall (elapsed) time because modal analyses require repeated factorization and forward/backward substitution. For nonlinear runs with repeated factor/solve steps, running in-core can save hours of elapsed time.

Use

the BCSOPTION command to set the memory usage for optimal out-of-core (default), in-core, or minimum out-of-core operation, depending on the availability of memory on the system. Usually, you can just increase the total job memory to

increase available memory to the sparse solver (using the -m command option). The ANSYS sparse solver uses sophisticated memory usage heuristics to balance available memory with the specific memory requirements of the sparse solver for each job. Many jobs will automatically run in-core, but larger jobs will most often run in optimal out-of-core mode unless you increase the default memory settings. In some cases, you may want to explicitly set the sparse solver memory mode or size using the BCSOPTION command.

If the available memory on your system is less than that required for in-core, the sparse solver will automatically be run in optimal out-of-core mode. If the available memory is less than that required for optimal out-of-core, the sparse solver will be run in minimum out-of-core mode, which could be two to four times slower than optimal out-of-core mode. It is rare for the sparse solver to run in minimum out-of-core mode; you can usually tune the sparse solver memory to avoid this mode by using the BCSOPTION command, or by just increasing the initial ANSYS memory setting (using the -m command option).

3.6.2 Elastic Analysis

All solvers can easily manage this kind of analysis, simple but effective in most of engineering fields. Elastic analysis is based on Hooke's law previously detailed and is reliable only to describe just the sress-strain field under yielding.

3.6.3 Elasto-Plastic and Visco-Elastic Analyses - PCG

The PCG solver starts with element matrix formulation. Instead of factoring the global matrix, the PCG solver assembles the full global stiffness matrix and calculates the DOF solution by iterating to convergence (starting with an initial guess solution for all DOFs). The PCG solver uses a proprietary preconditioner algorithm that is material property and element-dependent.

The PCG solver is usually about 4 to 10 times faster than the JCG solver for structural solid elements and about 10 times faster than JCG for shell elements. Savings increase with the problem size. The PCG solver usually requires approximately twice as much memory as the JCG solver because it retains two matrices in memory:

- The preconditioner, which is almost the same size as the stiffness matrix

- The symmetric, nonzero part of the stiffness matrix

You can use the /RUNST command to determine the memory needed, or use Table 3.1: "Solver Selection Guidelines" as a general memory guideline.

This solver is available only for static or steady-state analyses and transient analyses, or for subspace eigenvalue analyses (PowerDynamics). The PCG solver performs well on most static analyses and certain nonlinear analyses. It is valid for elements with symmetric, sparse, definite or indefinite matrices. Contact analyses that use penalty-based or penalty and augmented Lagrangian-based methods work well with the PCG solver as long as contact does not generate rigid body motions throughout the nonlinear iterations. However, Lagrange-formulation contact methods and incompressible u-P formulations cannot be used by the PCG solver and require the sparse solver.

Because they take less iteration to converge, well-conditioned models perform better than ill-conditioned models when using the PCG solver. Ill-conditioning often occurs in models containing elongated elements (i.e., elements with high aspect ratios) or contact elements. To determine if your model is ill-conditioned, view the Jobname.PCS file to see the number of PCG iterations needed to reach a converged solution. Generally, solutions that require more than 1500 PCG iterations are considered to be ill-conditioned for the PCG solver. When the model is very ill-conditioned (e.g., over 3000 iterations are needed for convergence) a direct solver may be the best choice unless you need to use an iterative solver due to memory or disk space limitations.

For ill-conditioned models, the PCGOPT command can sometimes reduce solution times. You can adjust the level of difficulty (PCGOPT,Lev_Diff) depending on the amount of ill-conditioning in the model. By default, ANSYS automatically adjusts the level of difficulty for the PCG solver based on the model. However, sometimes forcing a higher level of difficulty value for ill-conditioned models can reduce the overall solution time.

The PCG solver primarily solves for displacements/rotations (in structural analysis), temperatures (in thermal analysis), etc. The accuracy of other derived variables (such as strains, stresses, flux, etc.) is dependent upon accurate prediction of primary variables. Therefore, ANSYS uses a very conservative setting for PCG tolerance (defaults to 1.0E-8) The primary solution accuracy is controlled by the PCG. For most applications, setting the PCG tolerance to 1.0E-6 provides a very accurate displacement solution and may save considerable CPU time compared with the default setting. Use the EQSLV command to change the PCG solver tolerance.

Direct solvers (such as the sparse direct solver) produce very accurate solutions. Iterative solvers, such as the PCG solver, require that a PCG convergence tolerance be specified. Therefore, a large relaxation of the default tolerance may significantly affect the accuracy, especially of derived quantities.

The PCG solver is not recommended for models with SHELL150 elements. For these types of problems, use the sparse solver. Also, the PCG solver does not support SOLID62 or MATRIX50 elements.

User can use the command MSAVE, ON for memory savings of up to 70%. The MSAVE command will cause an element-by-element approach (rather than globally assembling the stiffness matrix) for the parts of the structure using SOLID45, SOLID92, SOLID95, SOLID185, SOLID186, and/or SOLID187 elements that have linear material properties. This feature applies only to static analyses or modal analyses using the Power Dynamics method. (You specify these analysis types using the commands ANTYPE,STATIC, or ANTYPE,MODAL; EQSLV,PCG respectively.) When using SOLID186 and/or SOLID187, only small strain (NLGEOM,OFF) analyses are allowed. NLGEOM, ON is valid for SOLID45, SOLID92, and SOLID95. The solution time may be affected depending on the processor speed and manufacturer of your computer, as well as the chosen element options (for example, 2 x 2 x 2 integration for SOLID95) .

4 User-Defined Models Implementation in FEM Software

Plastic/Visco-plastic deformation in metals is a very complex phenomenon originating from highly nonlinear dynamical processes associated with microscopic defects, such as dislocations which tend to self-organize in the form of patterns, resulting into a heterogeneous field of deformation at the micro-scale although the overall macroscopic field is thought to be homogeneous.

Although there has been a tremendous effort to understand work hardening/strain softening and associated material instability phenomena, this research area is still in a parlous state, and rife with controversy. This is due to the difficulty of carrying out truly definitive experiments on critical aspects of the evolution of the dislocation structure. But more important have been the immense theoretical difficulties of dealing with large numbers of dislocations and defects. Nevertheless, it is well understood that plastic deformation and strengthening in metals can be related to a number of heterogeneous patterns, such as dislocation cells, slip bands, micro-shear bands, persistent slip bands and dislocation tangles, which are critical for material properties.

The understanding of high-strain-rate behaviour of metals is essential for the modelling and analysis of numerous processes including high-speed machining, impact, penetration and shear localization. Thus, a desirable goal in constitutive modelling is to develop models which are widely applicable and capable of accounting for complex paths of deformation, temperature and strain rate which represent the main requirements of large deformation problems. The intended applications of the model as well as the availability and ease in obtaining experimental data specify the degree of complexity of the constitutive model.

Moreover, the degree of success of the model mainly depends on the flexibility and simplicity of determining material constants from a limited set of experimental data and capturing the important aspects of static and/or dynamic behaviour besides being mathematically and computationally accurate.

4.1 Stress-rate based theories

As macroscopic plasticity theories are usually based on a yield condition, we have to identify this feature within the microscopic theory. This dissertation address the need of consistent physically based definitions for the yield surface that is required for dynamic localizations.

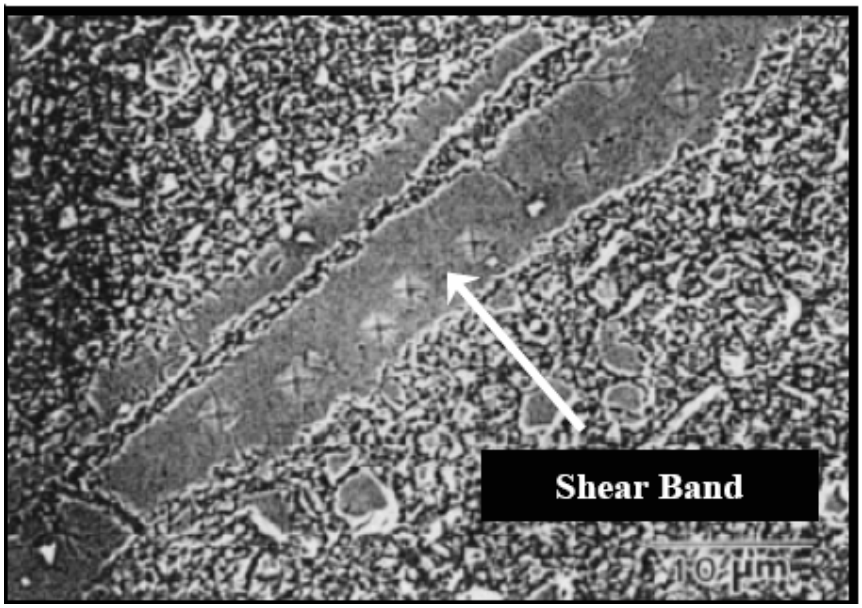

Figure 4.1- Shear bands a material micro structure

In inelastic deformation, the localization of deformation into narrow bands of intense straining is considered one of the characteristic features in metals and steel alloys. Localization for the case of rate-independent formulation is associated with a change in the character of the governing equations. That is, under quasi-static loading conditions the equations governing incremental equilibrium lose ellipticity, while under dynamic loading conditions wave speeds become imaginary.

Standard boundary value problems are then ill posed; one manifestation of this is that the width of the band of localized deformation is arbitrary narrow. As a consequence numerical solutions to localization problems for rate-independent solids exhibit inherent mesh dependence. The minimum width of the band of localized deformation is set by the mesh spacing. Furthermore, global quantities such as the overall stiffness characteristics of the body depend on the mesh size used to resolve the band of localized deformations.

Under both quasi static and dynamic loading conditions, the solutions to localization problems for rate-independent solids permit arbitrary narrow bands of intense deformation. There is nothing in the formulation to set a minimum width to such bands. On the other hand, in numerical solutions the minimum width is set by

the mesh spacing and key features of the solutions can be a consequence of the discretization. This is clearly an undesirable state of affairs and stems from the character of the continuum problem.

4.1.1 Stress evolution representative functional

The development of stress integration algorithms with improved performance has received considerable attention in the recent literature on computational plasticity and visco-plasticity.

The very efficient implementations of the implicit integration using the radial return schemes for metals corresponding to the special case of full isotropy (both elastic and inelastic responses), enabled by the complete reductions of the rate tensor equations to a final single/scalar nonlinear equation; e.g. in terms of the effective stress, or equivalently the plastic multiplier or the "magnitude" of the inelastic strain vector. In order to achieve a strong algorithmic treatment for any complex visco-plasticity constitutive models used for large-scale deformation, the following three tasks are required (Saleeb et al., 2000); (1) detailed study of the mathematical structure of the Visco-plastic equations, and the corresponding integrated field of stress and internal state variables, (2) development and implementation of the implicit backward-Euler stress-updating algorithm, and the associated nonlinear iteration equation solver (e.g, Newton Raphson technique), (3) testing the convergence, stability, and accuracy properties of the algorithms.

On the theoretical side, the general framework is developed in the specific context of the fully implicit (backward Euler) difference scheme which is known to exhibit excellent convergence and accuracy characteristics in large scale computations that involve large time steps, particularly with complex anisotropic inelastic models (Ortiz and Popov, 1985). Radial return algorithm which is a special case of the backward-Euler method is used to introduce a nonlinear scalar equation in terms of the Visco-plastic multiplier for the case of the Consistency Visco-plastic model and in terms of the equivalent stress for the case of Perzyna Visco-plastic model. Consistent algorithmic tangent stiffness matrices are derived for both small and finite strain Visco-plastic models

4.1.2 Plasticity constitutive equations

Nemat-Nasser and his co-workers (e.g., Nemat-Nasser and Isaacs, 1997, Nemat-Nasser & Li, 1998, Nemat-Nasser et al., 1999, and Nemat-Nasser & Guo, 2000) developed an experimental technique measuring the flow stress of different (bcc), (fcc) and hcp metals and alloys over a broad range of strains, strain rate, and temperatures in uniaxial compression.

Some of their experimental results are, actually, used in this work for models evaluation and comparisons. They also presented a constitutive model that characterizes the plastic deformation of different metals and alloys using the thermal activation concept and assuming constant dislocation density throughout the deformation process. That is neither the plastic strain evolution of dislocation density nor the rate multiplication of the dislocation density evolution is considered.

There has been a significant progress made over the years in the development theories of plasticity and visco-plasticity for the phenomenological representation of inelastic constitutive properties. In particular, mathematical modelling of metal visco-plasticity developed based on the so-called internal state variable formalism in the thermodynamics of irreversible processes.

A large number of specialized forms of theses modern unified Visco-plastic models (e.g. isotropic or anisotropic, fully associative or non-associative, isothermal or non-isothermal, etc.) have been successfully applied to different metals with different crystal structures (Coleman and Gurtin, 1967; Lublinear, 1973; Germain et al., 1983; Lemaitre and Chaboche, 1990; Chaboche, 1989; Arnold and Saleeb, 1994; Robinson and Duffy, 1990; Arnold et al.,1995, 1996; Robinson et al., 1987; Freed and Walker, 1993; Simo and Taylor, 1985, 1986).

4.1.3 Equilibrium surfaces evolution

Zerilli and Armstrong (1987) used equilibrium equations to describe the dislocation mechanics concept to develop a constitutive model that accounts for strain, strain rate and temperature dependence in a coupled manner, which can be incorporated in high rates of loading related computer codes. Their model considers two different forms for the two different classes of metals; body centred cubic (bcc) and face centred cubic (fcc). The rational for the differences in the two

forms mainly depends on the dislocation characteristics for each this particular structure. Bcc metals show stronger dependence of the yield stress on temperature and strain rate while in the case of (fcc) metals the yield stress is mainly affected by strain hardening. In other words, the cutting of dislocation forests is the principal mechanism in (fcc) metals, while in bcc metals; the overcoming of Peierls-Nabarro barriers is the principal mechanism.

These two different dislocation mechanisms of the two different metal classes will be further investigated in the following sections. The Zerilli-Armstrong model has been derived based on the concept of thermal activation analysis for overcoming local obstacles to dislocation motion. This model has been widely used in many computer codes from which its material parameters are physically interpreted. In fact, this physical interpretation of material constants becomes meaningless if one tries to identify them from the experimental data by using a very small reference strain rate rather than using the one corresponding to the reference dislocation velocity as been derived in the their model. Moreover, their material parameters lose their physical meaning when they are used for high temperature and strain rate applications which will be discussed in the following sections. It has been shown that the Zerilli-Armstrong model as compared to the Johnson-Cook model gives slightly better correlation with experimental results; however, none of these two models is very accurate in describing the behaviour of metals at very large strains (Johnson and Holmquist, 1988).

4.2 Strain-rate based theories

In dynamic problems that introduce high strain rates, the dynamic yield stress is considered the most important expression needed to characterize the material behaviour and is also used in finite element codes. Although we are concerned with the macroscopic response of the plastic flow, investigating the grain and atomic level of the material deformation will help us understand the failure mechanisms for different material structures.

Accordingly, the definition of dynamic yield (flow) stress differs from metal to metal depending on their internal crystal structure; body centred cubic (bbc), face centred cubic (fcc), hexagonal close packing (hcp), and others. These crystal structure differences affect differently the dislocations movement during the plastic deformation process under high strain rates loading. Each of these three crystal

structures exhibits a characteristic thermo mechanical behaviour which is associated with the available slip systems and symmetries as well as the nature of dislocation cores. The Visco-plastic deformation of steel alloys is generally controlled by the dislocation mechanisms attributed to the content of their compositions. The percentage of carbon in steel plays a crucial role in determining the phase behaviour (Ferrite and Austenite) of the material over a wide range of temperatures.

Generally, the plastic flow is characterized macroscopically as a visible distortion, microscopically as the appearance of slip systems, and atomically as a movement of dislocations. Microscopic plasticity in metals is primarily the result of dislocation moving through the crystal lattice. The interaction of these dislocations with the lattice and the various obstacles encountered through the lattice determine the flow strength of the material. The motion of a dislocation through the lattice or past an obstacle requires the surmounting of an energy barrier by a combination of applied stress and thermal activation.

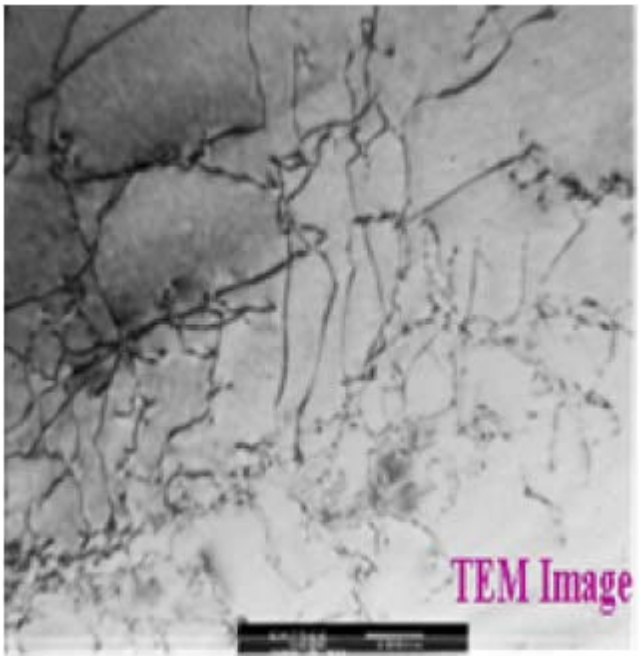

Figure 4.2- Dislocation in a material micro structure

The result is that the effective shear stress required to generate an overall plastic strain rate is intimately tied to the temperature at which the deformation occurs. Competing thermal activation effects will influence deformations that occur at both high temperature and high strain rates. The coupling of rate and temperature through dislocation kinematics indicates that the rate of thermal softening of metals should be related to the rate of deformation. These considerations are particularly important in the development of material models for use within simulation of high-rate phenomena, which generally involve high temperatures because of adiabatic heating.

4.2.1 Residual strain evolution functions

Many researchers extensively investigated the subject of modelling the dynamic flow stress of the material plastic flow at high strain rates and elevated temperatures. Studies were made in characterizing material behaviour through both phenomenological and physically based models. Empirical equations were initially developed with simple uniaxial stress-strain models (Campbell et al., 1977; Nicholas, 1982) and one-dimensional stress wave propagation models (Nicholas, 1982b) by describing the effect of temperature and strain hardening as well as strain rate on the flow stress. However, for the *von Mises* type material, the one-dimensional models that express flow stress as a function of strain and strain rate can be converted into the equivalent three-dimensional material models by replacing stresses, strains, and strain rates by their equivalent invariant three-dimensional forms (Zukas, 1990). Johnson and Cock (1983) proposed a phenomenological model that is widely used in most computer codes for static and dynamic analyses in order to predict the behaviour of the material flow stress at different strain rates ($10^{-4}s^{-1}$-$10^{5}s^{-1}$) and temperatures. The main advantage of this model is that it is relatively easy to calibrate with a minimum of experimental data in the form of stress-strain curves at different strain rates and temperatures.

Moreover, the strain rate and temperature effects on the flow stress are uncoupled which implies that the strain rate sensitivity is independent of temperature. This is not the case as observed in most metals. It is rather found that the rate sensitivity increases with increasing temperature while the flow stress decreases. For this reason was born a new branch of theories able to keep into account of these effects.

4.2.2 Strain potentials based methods

The understanding of high-strain-rate behaviour of metals is essential for the modelling and analysis of numerous processes including high-speed machining, impact, penetration and shear localization. Recently, considerable progress has been made in understanding the role of rate controlling dislocation mechanisms on the temperature and strain rate dependence of the flow stress for metals and alloys. Hoge and Murkherjee (1977) studied the effect of both temperature and strain rates on the lower yield stress of Tantalum and proposed a model incorporating the combined operation of the Peierls' mechanism and dislocation drag process.

They concluded from the stress-temperature relationship and the variation of the activation volume with stress and strain that the rate controlling mechanism for deformation could be rationalized in terms of Peierls mechanism. This behaviour is mainly attributed to the specific crystal structure of body cubic centred metals. Steinberg and co-workers (see for example, Steinberg et al., 1980; Steinberg and Sharp, 1981; Steinberg and Lund, 1989) described a constitutive model for use with hydrodynamic codes to account for the dependence of shear modulus and yield strength on high strain rates, temperature, and pressure-dependent melting. Although their model is intended to be used at high strain rates, their formulation did not specifically include strain rate effects.

This model has been widely used in many computer codes from which its material parameters are physically interpreted. In fact, this physical interpretation of material constants becomes meaningless if one tries to identify them from the experimental data by using a very small reference strain rate rather than using the one corresponding to the reference dislocation velocity as been derived in the model. It has been shown that the Zerilli-Armstrong model as compared to the Johnson-Cook model gives slightly better correlation with experimental results; however, none of these two models is very accurate in describing the behaviour of metals at elevated temperatures (Johnson and Holmquist, 1988; Abed and Voyiadjis, 2005).

5 Implementation of an external Material Model in ANSYS

Large-scale finite element numerical simulations provide a feasible approach for assessing the performance of inelastic structural components operating under complex thermo-mechanical and multiaxial loading conditions. The global solutions for any discretized finite element model are typically achieved, from the computational point of view, by an increment iterative procedure (e.g., Newton-Raphson technique). The mathematical forms, accuracy and stability properties of a selected integration procedure will directly affect the accuracy and efficiency of the overall finite element solution. The development of stress integration algorithms with improved performance has received considerable attention in the recent literature on computational plasticity and visco-plasticity. In this regard, due to their stability and wide range of applicability, a number of well-established implicit schemes of time integration have been attracted the attention of many authors for plasticity and visco-plasticity (Simo and Taylor, 1985, 1986; Simo, 1991; Ju, 1990; Loret et al, 1992; Lush et al., 1987; Caddemi and Martin, 1991; Hornberger and Stamm, 1989; Auricchio and Taylor,1994; Freed and Walker, 1992; Saleeb, 1993; Kojic and Bathe, 1987; Bathe, 1996).

5.1 Parallel Software

Parallelism is generally desirable, especially in large, complicated programs. Inputs are usually specified syntactically in the form of arguments and the outputs delivered as return values. Parallel software uses scoping that is another technique that helps keep procedures strongly modular. It prevents the procedure from accessing the variables of other procedures (and vice-versa), including previous instances of itself, without explicit authorization.

Less modular procedures, often used in small or quickly written programs, tend to interact with a large number of variables in the execution environment, which other procedures might also modify. Because of the ability to specify a simple interface, to be self-contained, and to be reused, procedures are a convenient vehicle for making pieces of code written by different people or different groups, including through programming libraries.

Another noticeable feature of parallel software is modular programming, a software design technique that increases the extent to which software is composed from separate parts, called modules. Conceptually, modules represent a separation

of concerns, and improve maintainability by enforcing logical boundaries between components. Modules are typically incorporated into the program through interfaces. A module interface expresses the elements that are provided and required by the module. The elements defined in the interface are visible to other modules. The implementation contains the working code that corresponds to the elements declared in the interface. One of the most important and famous software that are able to use parallelism and modularity is FORTRAN.

5.2 FORTRAN

FORTRAN is a general-purpose, procedural, imperative programming language that is especially suited to numeric computation and scientific computing. Originally developed by IBM in the 1950s for scientific and engineering applications, Fortran came to dominate this area of programming early on and has been in continual use for over half a century in computationally intensive areas such as numerical weather prediction, finite element analysis, computational fluid dynamics (CFD), computational physics, and computational chemistry. It is one of the most popular languages in the area of High-performance computing and programs to benchmark and rank the world's fastest supercomputers are written in FORTRAN.

FORTRAN (a blend word derived from The IBM Mathematical Formula Translating System) encompasses a lineage of versions, each of which evolved to add extensions to the language while usually retaining compatibility with previous versions. Successive versions have added support for processing of character-based data (FORTRAN 77), array programming, module-based programming and object-based programming (Fortran 90/95), and object-oriented and generic programming (Fortran 2003).

The main body of all Ansys procedures and commands are written in this language, included external interfaces, whose parts are compiled in C++ too.

5.2.1 APDL (ANSYS Parametric Design Language)

Set of commands (FORTRAN based) useful to automate common tasks and to implement parametric modelling.

APDL stands for ANSYS Parametric Design Language, a scripting language that you can use to automate common tasks or even build your model in terms of parameters (variables). While all ANSYS commands can be used as part of the scripting language, the APDL commands discussed here are the true scripting commands and encompass a wide range of other features such as repeating a command, macros, if-then-else branching, do-loops, and scalar, vector and matrix operations.

While APDL is the foundation for sophisticated features such as design optimization and adaptive meshing, it also offers many conveniences that can be used in day-to-day analyses. In this brief description, will be introduced the basic features, parameters, macros, branching, looping, and repeating. A mention will be done on array parameters too.

A frequently used sequence of ANSYS commands can be recorded in a macro file (these are sometimes called command files). Creating a macro enables user to, in effect, create your own custom ANSYS command. For example, calculating power loss due to eddy currents in a magnetic analysis would require a series of ANSYS commands in the postprocessor. By recording this set of commands in a macro, user will have a new, single command that executes all of the commands required for that calculation. In addition to executing a series of ANSYS commands, a macro can call GUI functions or pass values into arguments.

Macros can also be nested. That is, one macro can call a second macro; the second macro can call a third macro, and so on. Macros can be used on up to 20 nesting levels, including any file switches caused by the ANSYS /INPUT command. After each nested macro executes, the ANSYS program returns control to the previous macro level.

Within an ANSYS macro, you have several ways to access components of the ANSYS graphical user interface (GUI):

You can modify and update the ANSYS toolbar (this is discussed in detail in Adding Commands to the Toolbar)

- The *ASK command can be issued to prompt a user to enter a single parameter value.

- A dialog box can be created to prompt a user to enter multiple parameter values.
- The *MSG command can be issued to have the macro write an output message.
- The user can be allowed to select entities through graphical picking from within a macro.
- Any dialog box can be recalled.

5.2.1.1 Branching (IF-THEN-ELSE)

A branch (or jump on some computer architectures, such as the PDP-8 and Intel x86) is a point in a computer program where the flow of control is altered. The term branch is usually used when referring to a program written in machine code or assembly language; in a high-level programming language, branches usually take the form of conditional statements, subroutine calls or GOTO statements.

An instruction that causes a branch, a branch instruction, can be taken or not taken: if a branch is not taken, the flow of control is unchanged and the next instruction to be executed is the instruction immediately following the current instruction in memory; if taken, the next instruction to be executed is an instruction at some other place in memory. There are two usual forms of branch instruction: a conditional branch that can be either taken or not taken, depending on a condition such as a CPU flag, and an unconditional branch which is always taken.

5.2.1.2 Looping (FOR, DO, REPEAT, etc .)

A loop is a sequence of statements which is specified once but which may be carried out several times in succession. The code "inside" the loop is obeyed a specified number of times, or once for each of a collection of items, or until some condition is met.

In some languages, such as Scheme, loops are often expressed using tail recursion rather than explicit looping constructs. Most programming languages

have constructions for repeating a loop a certain number of times. These commands are named Count-controlled loops (FOR).

Again, most programming languages have constructions for repeating a loop until some condition changes. These commands are called Condition controlled loops. Note that some variations place the test at the start of the loop, while others have the test at the end of the loop. In the former case the body may be skipped completely, while in the latter case the body is always obeyed at least once (WHILE – DO).

5.2.1.3 Macro

A macro (from the Greek 'μάκρο' for long or far) in computer science is a rule or pattern that specifies how a certain input sequence (often a sequence of characters) should be mapped to an output sequence (also often a sequence of characters) according to a defined procedure. The mapping process which instantiates a macro into a specific output sequence is known as macro expansion.

The term originated with macro-assemblers, where the idea is to make available to the programmer a sequence of computing instructions as a single program statement, making the programming task less tedious and less error-prone.

Keyboard macros and mouse macros allow short sequences of keystrokes and mouse actions to be transformed into other, usually more time-consuming, sequences of keystrokes and mouse actions. In this way, frequently-used or repetitive sequences of keystrokes and mouse movements can be automated. Separate programs for creating these macros are called macro recorders.

During the 1980s, macro programs -- originally SmartKey, then SuperKey, KeyWorks, Prokey -- were very popular, first as a means to automatically format screenplays, then for a variety of user input tasks. These programs were based on the TSR (Terminate and stay resident) mode of operation and applied to all keyboard input, no matter in which context it occurred. They have to some extent fallen into obsolescence following the advent of mouse-driven user interface and the availability of keyboard and mouse macros in applications, such as word processors and spreadsheets, which makes it possible to create application-sensitive keyboard macros.

Keyboard macros have in more recent times come to life as a method of exploiting the economy of massively multiplayer online role-playing game (MMORPG)s. By tirelessly performing a boring, repetitive, but low risk action, a player running a macro can earn a large amount of the game's currency. This effect is even larger when a macro-using player operates multiple accounts simultaneously, or operates the accounts for a large amount of time each day. As this money is generated without human intervention, it can dramatically upset the economy of the game by causing runaway inflation. For this reason, use of macros is a violation of the TOS or EULA of most MMORPGs, and administrators of MMORPGs fight a continual war to identify and punish macro users.

Keyboard and mouse macros that are created using an application's built-in macro features are sometimes called application macros. They are created by carrying out the sequence once and letting the application record the actions. An underlying macro programming language, most commonly a Scripting language, with direct access to the features of the application may also exist.

The programmers' text editor Emacs (short for "editing macros") follows this idea to a conclusion. In effect, most of the editor is made of macros. Emacs was originally devised as a set of macros in the editing language TECO; it was later ported to dialects of Lisp.

Visual Basic for Applications (VBA) is a programming language included in Microsoft Office and some other applications. However, its function has evolved from and replaced the macro languages which were originally included in some of these applications.

5.3 User Programmable Features - UPF

User-programmable features (UPFs) are ANSYS capabilities for which you can write your own FORTRAN routines. UPFs allow you to customize the ANSYS program to your needs, which may be a user-defined material-behaviour option, element, failure criterion (for composites), and so on. You can even write your own design-optimization algorithm that calls the entire ANSYS program as a subroutine. UPFs are available in the ANSYS Multiphysics, ANSYS Mechanical, ANSYS Structural, ANSYS PrepPost, and ANSYS University (Advanced and

Research versions) products. For detailed information, see the Guide to ANSYS User Programmable Features

UPFs can range from a simple element output routine for custom output to a much more complex user element or user-optimization algorithm; therefore, it is difficult to present the process without describing specific programming details. This section presents a general sequence of steps to follow. The Guide to ANSYS User Programmable Features contains more detail on UPFs.

A typical UPF involves the following steps:

1. Design and program the desired user routine in FORTRAN 90. The source codes for all user routines are available on your ANSYS distribution medium. Most of them demonstrate at least simple functionality.

2. Compile and link your user routine into the ANSYS program. The Guide to ANSYS User Programmable Features describes how to do this on your system.

3. Verify that the changes you have made do not affect other, standard ANSYS features. (One way to do so is by running a set of ANSYS Verification Manual problems.)

4. Verify the user routine using whatever procedures you feel are adequate

The ANSYS program activates some UPFs (such as user elements) automatically when you use them. For example, to activate a user element, all you need to do is specify it as one of the element types in the model (via the ET command), set the element type attribute pointer (via the TYPE command)), and define elements using the solid modelling (AMESH, VMESH, etc.) or direct generation (ET, etc.) method.

In this work, UPF are used to recall an external material, to use Ansys as a subroutine and to allow a user plasticity, stress and creep laws.

5.4 Ansys User Subroutines - USERMAT

A data table is a series of constants that are interpreted when they are used. Data tables are always associated with a material number and are most often used to define nonlinear material data (stress-strain curves, creep constants, swelling constants, and magnetization curves)

For some element types, the data table is used for special element input data other than material properties. The form of the data table (referred to as the TB table) depends upon the data being defined. Sometimes the form is peculiar to only one element type. If the form applies to more than one element, it is described below and referenced in the element description.

The User Defined (USER) material option describes input parameters for defining a material model based on either of two subroutines, which are ANSYS user-programmable features (see the Guide to ANSYS User Programmable Features). The choice of which subroutine to use is based on which element you are using.

The USER option works with the USERMAT subroutine in defining any material model (except incompressible materials), when you use any of the following elements: LINK180, SHELL181, PLANE182, PLANE183, SOLID185, SOLID186, SOLID187, SOLSH190, BEAM188, BEAM189, SHELL208, and SHELL209.

The USER option works with the USERPL subroutine in defining plasticity or visco-plasticity material models, when you use any of the following elements: LINK1, PLANE2, LINK8, PIPE20, BEAM23, BEAM24, PLANE42, SHELL43, SOLID45, SHELL51, PIPE60, SOLID62, SOLID65, PLANE82, SHELL91, SOLID92, SHELL93, SOLID95.

The USER option's input is determined by user-defined constants. The number of constants can be any combination of the number of temperatures (NTEMP) and the number of data points per temperature (NPTS), to a maximum limit of NTEMP x NPTS = 1000. Initialize the constant table with TB, USER. The constants are defined with TBDATA commands (6 per command).

State variables can also be used in the USERMAT subroutine (not in USERPL). To use state variables, initialize the constant table with TB, STATE then define the constants with the TBDATA command. You can define a maximum of 1000 state variables (NPTS = 1000). See User Defined Material in the ANSYS Structural Analysis Guide for more information on this material option.

In this work, USERMAT subroutine is recalled at each integration point (SOLVE) and for each equilibrium iteration (Newton-Raphson). Inputs for each cycle are state variables, stresses, strains, strain increments and time variable. Output of each cycle is the Jacobian Material Matrix (stress, strain) at the end of each time increment.

5.5 User Material Model Creation Methods and Software

A number of material-related factors can cause structure's stiffness to change during the course of an analysis. Nonlinear stress-strain relationships of plastic, multilinear elastic, and hyperelastic materials will cause a structure's stiffness to change at different load levels (and, typically, at different temperatures). Creep, visco-plasticity, and viscoelasticity will give rise to nonlinearities that can be time-, rate-, temperature-, and stress-related. Swelling will induce strains that can be a function of temperature, time, neutron flux level (or some analogous quantity), and stress.

Any of these kinds of material properties can be incorporated into an ANSYS analysis if you use appropriate element types or a special material model. Nonlinear constitutive models (TB command, except for TB, FAIL) are not applicable for the ANSYS Professional program.

5.5.1 Nonlinear Materials

If a material displays nonlinear or rate-dependent stress-strain behaviour, then you must use the TB family of commands [TB, TBTEMP, TBDATA, TBPT, TBCOPY, TBLIST, TBPLOT, TBDELE] to define the nonlinear material property relationships in terms of a data table. The exact form of these commands varies depending on the type of nonlinear material behaviour being defined. The different material behaviour options are described briefly below. See Data Tables - Implicit

Analysis in the ANSYS Elements Reference for specific details for each material behaviour type.

5.5.2 Plasticity

Most common engineering materials exhibit a linear stress-strain relationship up to a stress level known as the proportional limit. Beyond this limit, the stress-strain relationship will become nonlinear, but will not necessarily become inelastic. Plastic behaviour, characterized by non-recoverable strain, begins when stresses exceed the material's yield point. Because there is usually little difference between the yield point and the proportional limit, the ANSYS program assumes that these two points are coincident in plasticity analyses.

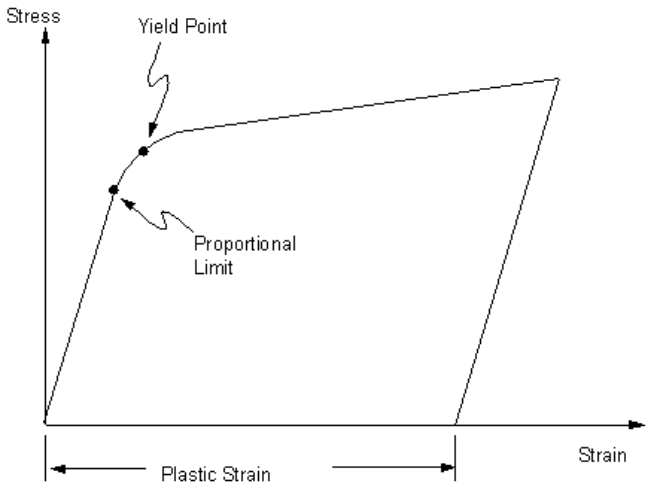

Figure 5.1- Elasto-plastic Stress-Strain Curve

Plasticity is a non-conservative, path-dependent phenomenon. In other words, the sequence in which loads are applied and in which plastic responses occur affects the final solution results. If you anticipate plastic response in your analysis, you should apply loads as a series of small incremental load steps or time steps, so that your model will follow the load-response path as closely as possible. The maximum plastic strain is printed with the sub-step summary information in your output (Jobname.OUT).

The automatic time stepping feature [AUTOTS] will respond to plasticity after the fact, by reducing the load step size after a load step in which a large number of equilibrium iterations was performed or in which a plastic strain increment greater than 15% was encountered. If too large a step was taken, the program will bisect and resolve using a smaller step size.

Other kinds of nonlinear behaviour might also occur along with plasticity. In particular, large deflection and large strain geometric nonlinearities will often be associated with plastic material response. If you expect large deformations in your structure, you must activate these effects in your analysis with the NLGEOM command. For large strain analyses, material stress-strain properties must be input in terms of true stress and logarithmic strain.

5.5.3 FEM Software

A variety of specializations under the umbrella of the mechanical engineering discipline (such as aeronautical, biomechanical, and automotive industries) commonly use integrated FEM in design and development of their products. Several modern FEM packages include specific components such as thermal, electromagnetic, fluid, and structural working environments. In a structural simulation, FEM helps tremendously in producing stiffness and strength visualizations and also in minimizing weight, materials, and costs. FEM allows detailed visualization of where structures bend or twist, and indicates the distribution of stresses and displacements. FEM software provides a wide range of simulation options for controlling the complexity of both modeling and analysis of a system.

Similarly, the desired level of accuracy required and associated computational time requirements can be managed simultaneously to address most engineering applications. FEM allows entire designs to be constructed, refined, and optimized before the design is manufactured. This powerful design tool has significantly improved both the standard of engineering designs and the methodology of the design process in many industrial applications. The introduction of FEM has substantially decreased the time to take products from concept to the production line. It is primarily through improved initial prototype designs using FEM that testing and development have been accelerated. In summary, benefits of FEM include increased accuracy, enhanced design and better insight into critical design

parameters, virtual prototyping, fewer hardware prototypes, a faster and less expensive design cycle, increased productivity, and increased revenue.

From the application point of view, it is important to model the system such that:

- Symmetry or anti-symmetry conditions are exploited in order to reduce the size of the domain.

- Displacement compatibility, including any required discontinuity, is ensured at the nodes, and preferably, along the element edges as well, particularly when adjacent elements are of different types, material or thickness. Compatibility of displacements of many nodes can usually be imposed via constraint relations--When such a feature is not available in the software package, a physical model that imposes the constraints may be used instead.

- Elements' behaviours capture the dominant actions of the actual system, both locally and globally.

- The element mesh is sufficiently fine in order to have acceptable accuracy. To assess accuracy, the mesh is refined until the important results show little change. For higher accuracy, the aspect ratio of the elements should be as close to unity as possible and smaller elements are used over the parts of higher stress gradient.

- Proper support constraints are imposed with special attention paid to nodes on symmetry axes.

Large scale commercial software packages often provide facilities for generating the mesh, graphical display of input and output, which greatly facilitate the verification of both input data and interpretation of the results

5.5.4 Object Oriented Programming (C++, Fortran 90)

Object-oriented programming (OOP) is a programming paradigm that uses "objects" and their interactions to design applications and computer programs. Programming techniques may include features such as encapsulation, modularity, polymorphism, and inheritance. It was not commonly used in mainstream software

application development until the early 1990s. Many modern programming languages now support OOP.

Through all computing literature, user can easily identify a number of ‘quarks’, or fundamental concepts, found in the strong majority of definitions of OOP. They are the following.

- **Class**

Defines the abstract characteristics of a thing (object), including the thing's characteristics (its attributes, fields or properties) and the thing's behaviors (the things it can do, or methods, operations or features). One might say that a class is a blueprint or factory that describes the nature of something. For example, the class Dog would consist of traits shared by all dogs, such as breed and fur color (characteristics), and the ability to bark and sit (behaviors). Classes provide modularity and structure in an object-oriented computer program. A class should typically be recognizable to a non-programmer familiar with the problem domain, meaning that the characteristics of the class should make sense in context. Also, the code for a class should be relatively self-contained (generally using encapsulation). Collectively, the properties and methods defined by a class are called members.

- **Object**

Object can be considered a pattern (exemplar) of a class. The class of Dog defines all possible dogs by listing the characteristics and behaviors they can have; the object Lassie is one particular dog, with particular versions of the characteristics. A Dog has fur; Lassie has brown-and-white fur.

- **Instance**

One can have an instance of a class or a particular object. The instance is the actual object created at runtime. In programmer jargon, the Lassie object is an instance of the Dog class. The set of values of the attributes of a particular object is called its state. The object consists of state and the behaviour that's defined in the object's class.

- **Method**

Method is an object's abilities. In language, methods are verbs. Lassie, being a Dog, has the ability to bark. So bark() is one of Lassie's methods. She may have other methods as well, for example sit() or eat() or walk() or save_timmy(). Within

the program, using a method usually affects only one particular object; all Dogs can bark, but you need only one particular dog to do the barking.

- **Message passing**

"The process by which an object sends data to another object or asks the other object to invoke a method." Also known to some programming languages as interfacing. E.g. the object called Breeder may tell the Lassie object to sit by passing a 'sit' message which invokes Lassie's 'sit' method. The syntax varies between languages, for example: [Lassie sit] in Objective-C. In Java code-level message passing corresponds to "method calling". Some dynamic languages use double-dispatch or multi-dispatch to find and pass messages.

- **Inheritance**

'Subclasses' are more specialized versions of a class, which inherit attributes and behaviors from their parent classes, and can introduce their own.

For example, the class Dog might have sub-classes called Collie, Chihuahua, and Golden Retriever. In this case, Lassie would be an instance of the Collie subclass. Suppose the Dog class defines a method called bark() and a property called fur Color. Each of its sub-classes (Collie, Chihuahua, and Golden Retriever) will inherit these members, meaning that the programmer only needs to write the code for them once. Each subclass can alter its inherited traits.

- **Abstraction**

Abstraction is simplifying complex reality by modeling classes appropriate to the problem, and working at the most appropriate level of inheritance for a given aspect of the problem.

For example, Lassie the Dog may be treated as a Dog much of the time, a Collie when necessary to access Collie-specific attributes or behaviors, and as an Animal (perhaps the parent class of Dog) when counting Timmy's pets. Abstraction is also achieved through Composition. For example, a class Car would be made up of an Engine, Gearbox, Steering objects, and many more components. To build the Car class, one does not need to know how the different components work internally, but only how to interface with them, i.e., send messages to them, receive messages from them, and perhaps make the different objects composing the class interact with each other.

- **Encapsulation**

Encapsulation conceals the functional details of a class from objects that send messages to it.

For example, the Dog class has a bark() method. The code for the bark() method defines exactly how a bark happens (e.g., by inhale() and then exhale(), at a particular pitch and volume). Timmy, Lassie's friend, however, does not need to know exactly how she barks. Encapsulation is achieved by specifying which classes may use the members of an object. The result is that each object exposes to any class a certain interface — those members accessible to that class. The reason for encapsulation is to prevent clients of an interface from depending on those parts of the implementation that are likely to change in future, thereby allowing those changes to be made more easily, that is, without changes to clients.

- **Polymorphism**

Polymorphism allows the programmer to treat derived class members just like their parent class' members. More precisely, Polymorphism in object-oriented programming is the ability of objects belonging to different data types to respond to method calls of methods of the same name, each one according to an appropriate type-specific behavior. One method, or an operator such as +, -, or *, can be abstractly applied in many different situations. If a Dog is commanded to speak(), this may elicit a bark(). However, if a Pig is commanded to speak(), this may elicit an oink(). They both inherit speak() from Animal, but their derived class methods override the methods of the parent class; this is Overriding Polymorphism. Overloading Polymorphism is the use of one method signature, or one operator such as '+', to perform several different functions depending on the implementation. The '+' operator, for example, may be used to perform integer addition, float addition, list concatenation, or string concatenation. Any two subclasses of Number, such as Integer and Double, are expected to add together properly in an OOP language. The language must therefore overload the addition operator, '+', to work this way. This helps improve code readability. How this is implemented varies from language to language, but most OOP languages support at least some level of overloading polymorphism. Many OOP languages also support Parametric Polymorphism, where code is written without mention of any specific type and thus can be used transparently with any number of new types. Pointers are an example of a simple polymorphic routine that can be used with many different types of objects.

- **Decoupling**

Decoupling allows for the separation of object interactions from classes and inheritance into distinct layers of abstraction. A common use of decoupling is to polymorphically decouple the encapsulation, which is the practice of using reusable code to prevent discrete code modules from interacting with each other.

Not all of the above concepts are to be found in all object-oriented programming languages, and so object-oriented programming that uses classes is called sometimes class-based programming. In particular, prototype-based programming does not typically use classes. As a result, a significantly different yet analogous terminology is used to define the concepts of object and instance.

5.5.5 Application Programming Interfaces - API

An application programming interface (API) is a set of functions, procedures, methods, classes or protocols that an operating system, library or service provides to support requests made by computer programs.

- Language-dependent APIs are available only in a particular programming language. They utilize the syntax and elements of the programming language to make the API convenient to use in this particular context.

- Language-independent APIs are written in a way that means they can be called from several programming languages. This is a desired feature for a service-style API which is not bound to a particular process or system and is available as a remote procedure call.

The software that provides the functionality described by an API is said to be an implementation of the API. The API itself is abstract, in that it specifies an interface and the behavior of the identifiers specified in that interface; it does not specify how the behavior may be implemented.

The F2PY project is created to unify the efforts of supporting easy connection between FORTRAN and Python languages. The project will provide software, documentation, and support to solve a difficult task of automatically generating Python wrappers to FORTRAN libraries. It will also coordinate the further development of the F2PY tool and related software. Our ultimate aim is to have a tool that can automatically generate Python wrappers to any FORTRAN program,

be it written in Fortran 66/77 or in Fortran 90/95/2003. This is the tool used to create interfaces between Z-Mat and ANSYS

5.5.6 Object oriented software, modules and classes

The most advanced software, nowadays, are programmed and compiled using tools that can be assimilated with boxes. In each box, user can find useful tools (in our case constitutive equations of material behaviours. These boxes, to be versatile and usable for many purposes, have to be provided with user programmable features that, on one side, have to be able to interface the program with the outer world, while on the other one should be able to provide user friendly commands and scheme to allow user building his functions.

This is the reason why modular software can allow creating modules and classes to associate each one. This is almost the same structure for all modular software that are used for material model simulations.

5.5.7 Z-Mat

The Z-Mat product is thus mainly a library of material behaviour routines (constitutive equations), which can be interfaced with FEA software, and its supporting utilities. In contrast with other FEA software products however, Z-set and Z-mat are built on C++ with a strong object-oriented design, and many utility programming classes for advanced tensorial mathematics. Such advanced program design techniques have enabled the software to be enormously extensible, on many different levels of sophistication. In developing extensions to Z-mat, a user can make new behaviours using the many abstract “building bricks" to create a modular, flexible model based on fundamentals.

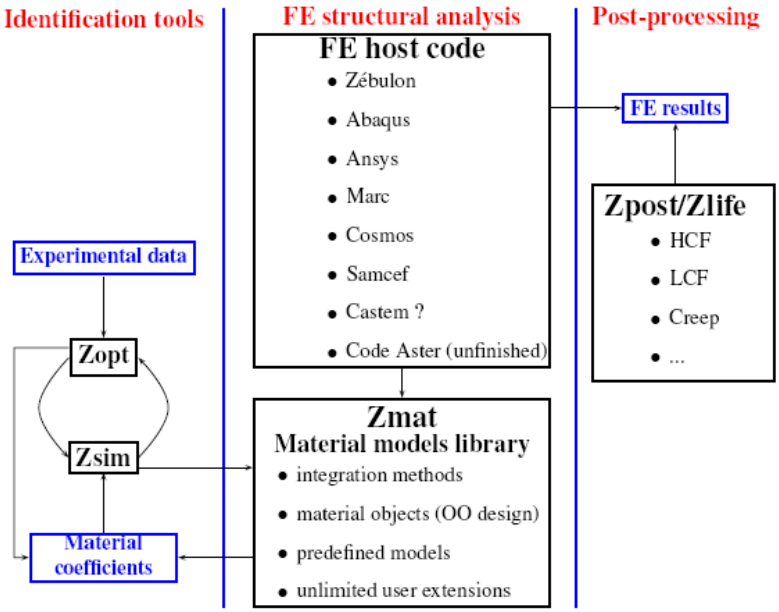

Figure 5.2- Z-Mat modules

For final use, we then let the different implemented “bricks" define the specifics. That is to say, the user always chooses the final model form (e.g specific evolution or state equations) in the input file, after development is finished. In that way, each model is really a “model class" or framework within which a user has a high degree of flexibility. One can also add to the “types" available for these building bricks. This not only lets one work on a smaller specific aspect, but allows extending the capabilities of every model using that particular \abstract" type.

5.5.7.1 Modular analysis

The program itself is organized in different modules:

Z-set is a FEA solver, generally used for non-linear analyses, whose main feature is flexibility and capability to model innovative material models. Z-set has been designed to support the complete characterization process of materials including the capability to perform structural analysis, allowing the creation and utilization of robust and reliable material models.

Here is reported a brief description of the modules used within the scopes of this activity:

- **Z-Mat** is a dynamic library which extends the material modelling capabilities of ABAQUS and provides a more flexible, object-oriented interface for developing user models. There are a large number of proven constitutive equations built into the library, including sophisticated models for plasticity, visco-plasticity, coupled plasticity-visco-plasticity, crystallographic plasticity, and creep, brittle and ductile damage. The nature of the library also allows all these models to be simultaneously available from a centralized location, so the user is not obliged to copy a large umat.f file to each calculation directory. Due to the modular design, the user can also build new user models from the input file, simply by combining several types of yield functions, flow rules and hardening rules. For example, plasticity-visco-plasticity does not exist as a predefined model; In this case, user can fabricate in the input file a material model to combine simultaneously time-independent and visco-plastic strain components.

- **Z-Sim** is a small simulator, allowing the user to load any representative volume element (RVE) in terms of mixed stresses and strains instead of forces and displacements, which allows fast simulation of material tests without FEA. Note that the material model code is shared 100% between the simulation and FEA. Functionality is also available to plot yield or damage (actually any potential) n stress space, at different points in the loading history. This tool is used to simulate material conditions under cyclic thermo-mechanical loads in order to understand and compare its behaviour. For example, a simulation can be performed in order to simulate material's stress relaxation under creep-like conditions.

- **Z-Optim** Optimization including several classical methods such as SQP, simplex or Levenberg-Marquardt, and also genetic algorithms. In connection with Z-Sim this is a powerful tool for the identification of material parameters, while keeping exactly the same user interface as Z-Mat and Z-Sim. The optimal parameters can be determined through a

process of least square minimization process using a set of experimental curves for reference and the simulated ones

- Z-Post is a module to manage FEM results data post-processing execution and operations. It can be used to evaluate damage from fatigue and creep with the aim of calculating life of a structural component. It has got interfaces and subroutines to be able to read results file from many FEM software.

- Z-Ansys is a bounch of tools that allow executing advanced and complex FE analyses, oriented to manage much material behaviour, utilizing ANSYS. This module uses a dynamic library of materials in order to extend ANSYS capabilities to model different material behaviours. It has got a simple and powerful interface to develop new material models. It is linked directly to Z-Mat, Z-Sim and Z-Opt.

In the following periods, there will be described briefly how constitutive equations can be arranged in order to obtain the material card useful for an evp analysis.

5.5.7.2 Z-Mat Material Behaviours

Material behaviours in Z-mat use by far the most dynamic and object oriented input of all the Z-set modules. This is because behaviours are a set of constitutive equations which get built from fundamental \building bricks" of sub-models. There is widespread re-use of all these “bricks" between different behaviour models. It is therefore necessary to adjust our input syntax (or at least documentation of it) to allow for more flexibility.

5.5.7.2.1 Classes and Objects

The most important concept for this chapter is the notion of a class of permissible options, of which the user will choose one or more objects from that class in the material definition.

A class is an abstract notion of basic functionality.

An example is the ELASTICITY class which handles the calculation of stress from a strain, usually employing a 4th order tensor of various modulus coefficients.

Because of this very general function, many behaviour models allow for an ELASTICITY instance.

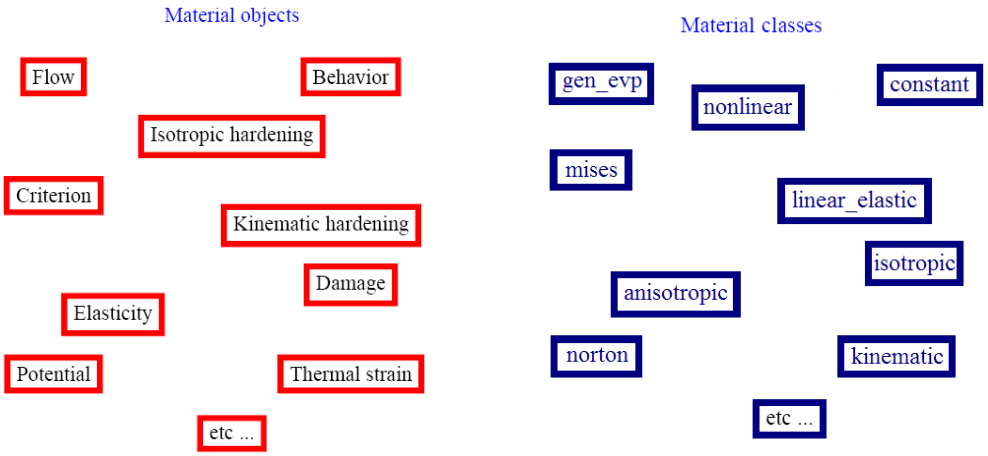

Figure 5.3- Z-Mat Objects and Classes

In turn, the elasticity class has many possible types which one can select to _ll in an elasticity object (isotropic, orthotropic, etc).

**elasticity <ELASTICITY>

The keyword **elasticity used here is in fact specific to the behaviour model. While we frequently see the same keyword indicating classes between behaviours, this is not necessarily so. The function of each sub-command will be described in the discussion of the behaviour model itself. What defines the syntax which follows this line is the ELASTICITY notation, indicating an elasticity matrix should be input. Again, the use should then go to the ELASTICITY section of the handbook, and investigate the possible models for this option.

Many behaviour models also include the possibility of multiple instances of certain keywords. These possibilities will be described in the section of the containing class (behaviour is a “material piece" class, but there are many others which can contain sub-pieces themselves).

The standard notation for multiple instances of a class is to include three dots following the data entry line:

*kinematic <KINEMATIC>

This means that the material at this location can take any number of *kinematic entries, in any order, and with no restriction on type. FEM software actually do not include in their libraries, the elasto-visco-platic one, since its complexity and high technology content, together with the limited computational capacity of most of common personal computers, did not permit its implementation.

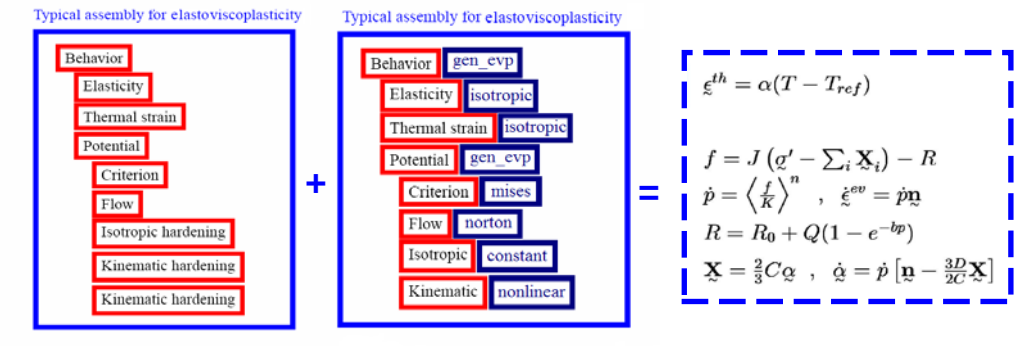

Figure 5.4- Z-Mat Objects + Classes = Constitutive laws

This is the reason why to implement such a model, is necessary to use external software like Z-mat.

5.5.7.3 Material Files

The material and global-scope coefficients to be used are defined in a separate file henceforth described as the material file. The material file is a standard ASCII text file of form similar to the main input file. Most instances where a material filename needs to be specified allows an optional integer value for the instance of behaviour in that file, the default instance being the first. So, when a material file is opened, the program will search for the n^{th} occurrence of the keyword ***behaviour, skipping all other data contained before. Frequently for example and verification problems, the material file is given in the same physical file as the referring input file for compactness and file management purposes.

Regardless of how or where the material file is located, the material file is a separate entity from the other input commands, with an independent command hierarchy starting at the ***-level.

6 Elasto-Visco-Plastic Models

6.1 Constitutive theories based on microscopic and/or crystallographic phenomenological descriptions

Many different concepts are proposed in the literature for representing the thermo-mechanical behaviour of material bodies: e.g. Jou et al. (1996), Maugin and Muschik (1994), Meixner and Reik (1959), Muller and Ruggeri (1998), Truesdell and Noll (1965), and Ziegler (1977).

The development of the constitutive equations follows a thermo-mechanical framework, which was established by Coleman and Gurtin (1967), Coleman and Noll (1963), and Truesdell and Noll (1965). In this theory, the second law of thermodynamics is represented by the local form of the Clausius–Duhem inequality and implies a constraint, which must be satisfied by the constitutive relations for every admissible thermodynamic process (cf. the discussions in Jou et al. (1996) and Maugin and Muschik (1994)). In contrast to this concept, Germain et al. (1983) introduces a pseudopotential of dissipation and Green and Naghdi (1978) as well as Ziegler (1977) suggest a constitutive relation for the rate of dissipation (cf. the remarks in Maugin and Muschik (1994)). In these frameworks, the evolution equations of internal variables are often determined by using the postulate of maximum dissipation (cf. Deseri and Mares, 2000; Miehe, 1998; Rajagopal and Srinivasa, 1998b), which can be traced back in its thermo-mechanical formulation to Ziegler (1963) and Ziegler (1977). In plasticity theory, a related concept was formulated by von Mises (1928) and Hill (1950).

In addition to the modelling of the mechanical behaviour, the representation of the thermo-mechanical coupling phenomena is of special interest (Bodner and Lindenfeld, 1995; Chaboche, 1993b; Hakansson et al., 2005; Haupt et al., 1997; Helm, 1998; Jansohn, 1997; Kamlah and Haupt, 1998; Mollica et al., 2001; Tsakmakis, 1998): it is well known that metals show thermoelastic coupling phenomena. Moreover, a part of the work required to produce plastic deformations is stored as internal energy in the microstructure of the material. Since the basic results of Taylor and Quinney (1934), this phenomenon has been investigated in detail: cf. Bever et al. (1973), Chrysochoos et al. (1989), Helm (1998), Oliferuk et al. (1985), and Rosakis et al. (2000). In the first studies (cf. Taylor and Quinney, 1934), a small amount of approximately 11% of the introduced cold work is stored in the microstructure. In contrast to this, subsequent studies (e.g. Bever et al., 1973;

Chrysochoos et al., 1989; Helm, 1998; Oliferuk et al., 1985) led to the result that the stored energy depends on the deformation history and that more than 11%, up to approximately 70%, of the cold work is stored in the microstructure of the material.

For solving initial-boundary value problems, the stress state must be calculated by integrating a system of ordinary differential equations. In the framework of numerical methods like the finite element method, the system of differential equations is numerically solved by an appropriate integration scheme. In the framework of implicit finite element methods, the most popular strategy to integrate plastic or visco-plastic models is the backward Euler scheme (see e.g. Hartmann et al., 1997; Simo and Miehe, 1992; Simo and Hughes, 1998) as well as the exponential algorithm (see e.g. Miehe and Stein, 1992; Simo, 1993), which was originally proposed in finite visco-plasticity by Weber and Anand (1990).

The exponential algorithm has the advantage that the incompressibility of the inelastic deformations is always fulfilled (cf. Remark 2). In contrast to this, the backward Euler method does not preserve the plastic incompressibility at finite step sizes. Consequently, the backward Euler scheme leads to incommensurate errors if large step sizes are applied (see e.g. the numerical studies in Tsakmakis and Willuweit (2003)). In Simo et al. (1985), Simo and Miehe (1992) and also in Lu¨hrs et al. (1997) the error is eliminated due to an additional assumption, which leads to a cubic equation for a scalar-valued variable.

Ponter and Leckie's theory is based on a Bailey-Orowan theory of creep (Bailey [1926] and Orowan [1947]). The concept of internal state variables, as it applies to polycrystalline metals, and the thermodynamic constraints placed on the theoretical formulation are discussed in the next section. Moreover an Omega-form theory of visco-plasticity is derived for kinematic hardening materials to introduce non linear strain hardening into the theory. The dynamic recovery approach is preferred over the hardening function approach for realistic modelling of material behaviour.

A novel approach for incorporating isotropic hardening into the theory is presented too, wherein the limit stress for the kinematic saturation of state is considered to be the independent state variable. Each material element i s considered to be isotropic and to carry no stress in its initial virgin condition. But while each material element deforms homogeneously, it may lose some or all of its

material symmetries. Small strains, displacements, and rotations are considered to compose the deformation of each material element.

The changing internal structure of a material element is characterized by the pair (σ, S), where σ is the state of stress and S is the state of a finite number of internal state variables: that is, $S = \{ s_1 , s_2, \ldots , S_n \}$. The stress accounts for the elastic (or reversible) changes in internal structure, while the internal state variables account for the inelastic (or irreversible) changes in internal structure. These inelastic changes influence the future response of the material element.

The theory developed in this section considers two main internal state variables. They are $S = (\xi, \eta)$, where ξ is a deviatoric tensor of second rank and η is a scalar, such that in the virgin state:

$$\xi (0) = 0 \quad \text{and} \quad \eta (0) = \eta_0 > 0 \qquad (0.52)$$

That is

$$S_0 = (0, \eta_0). \qquad (0.53)$$

The deviatoric tensor accounts for kinematic hardening effects, whereas the scalar accounts for isotropic hardening effects.

Thermodynamics with internal variables offers a good framework to introduce constitutive equations. It offers both a guideline and some constraints for the choice of thermodynamically consistent evolution equations. A special form uses the notion of a standard generalized material, where the complete thermo-elastic-inelastic behaviour is defined from the knowledge of two potentials; the thermodynamic potential to describe the present state and the dissipative potential for the irreversible evolutions, is proposed.

Introducing mechanical constitutive models into a thermodynamic framework allows the partition of the plastic work into the energy stored by the material and the one dissipated away as heat. The constitutive equations are derived from the first and second laws of thermodynamics, the expression of Helmholtz free energy, the additive decomposition of the total strain rate into elastic and visco-plastic, the Clasius-Duhem inequality, the maximum dissipation principle, generalized

normality, and the thermo-mechanical heat equation. The visco-plastic yield criterion adopted in this work is of a *von Mises* type, but it needs to be modified to account for high-strain rates and temperature dependency. This is done by replacing the yield strength, the hardening function, and the viscous stress by the physically based flow stress model that will be developed in the first part of this work. The irreversible thermodynamic process can be characterized by a time incremental approach allowing for the equilibrium thermodynamic characterization. The irreversible thermodynamic is compensated for by introducing internal state variables such that they are implicitly non-equilibrated by a set of fictitious thermodynamic conjugate forces.

6.2 Constitutive time-dependent Theories

The inelastic response of materials is perhaps inevitably rate dependent. When material rate dependence is accounted for, there is no loss for ellipticity in quasi static problems and wave speed remains real, as long as stress levels remain small compared to elastic stiffness. Even though the phenomenology of localization can be the same for both rate dependent and rate-independent material behaviour, pathological mesh dependence does not occur in numerical solutions for rate-dependent solids because boundary value problems remain well posed. The rate independent solid does emerge as the appropriate limit.

One approach to remedying this situation is to explicitly introduce a length scale into the material characterization by using a nonlocal constitutive relation. In this dissertation, we will show that material rate dependence, no matter how small, leads to well posed boundary value problems with unique solutions. This can be viewed in terms of material rate dependence implicitly introducing a length scale into the boundary value problem formulation. Of course, in any particular circumstance, the question remains as to whether or not this is the relevant length scale.

Since modern structures exhibit a strong rate dependency especially at elevated temperatures, the constitutive relations who have been developed to describe the behaviour of different types of metals must be able to reproduce these facts. Processes related with high velocities therefore must be described by a rate-dependent visco-plasticity whereas the same constitutive relations for vanishing velocities must turn over to a rate-independent plasticity. Prior to establishing

constitutive relations that can fulfil these conditions, a proper physical interpretation of the phenomena observed during inelastic deformation is needed.

This means that the different mechanisms that can explain the dissipation implied by internal changes of the material are to be analyzed. It is known from appropriate microscopic investigations that in a temperature, strain rate spectrum in general different regions can be observed reflecting different mechanisms of inelastic deformation. These are:

- Athermal mechanisms characterized by a yield stress (e.g. fcc metals) or hardening stress (e.g., bcc metals) relatively insensitive to the strain rate;
- Thermally activated dislocation motion. Characterized by a more markedly, temperature and rate sensitivity of the yield and hardening stresses.

The foundation of an Q-form theory of visco-plasticity is the normality structure of a potential function Q. The advantage of this approach is that I the choice of two scalar-valued functions of state (i.e., E and Q).

6.3 Visco-plastic Theories Based on Intrinsic Time Function

Generally, the additive decomposition of the total strain rate into elastic and plastic components is generally assumed in plasticity/visco-plasticity constitutive modelling for small elastic strains. Various Visco-plastic material models have been proposed. Some of them are physically based and others are phenomenological. A widely used Visco-plastic formulation is the Perzyna model (Perzyna, 1963; 1966; 1986, 1988, 1998).

The main feature of Perzyna model is the dynamic yield surface which is used in describing the Visco-plastic strain. This dynamic yield surface can be larger than zero, and is known as the “overstress”. In other words, the overstress is defined as the difference between the dynamic stress and its static counterpart and it is the common notion of visco-plasticity, which implies that an inelastic process can only take place if, and only if, the overstress is positive.

On the other hand, visco-plasticity can be modelled by incorporation of the time dependency in a yield function, which, together with the consistency parameter, obeys the classical Kuhn-Tucker relations. In Wang et al. (1997) and Wang (1997), a so-called Consistency model has been proposed, in which the time-derivative of a rate-dependent yield surface governs the irreversible viscous deformation behaviour. Furthermore, Mahnken et al. (1998) and Johansson et al. (1999) have considered a rate-dependent yield formulation in combination with coupling to damage. Very recently, Ristinmaa and Ottosen (2000) have given a thorough discussion on the main features and implications of modelling rate-dependency within a yield surface concept.

6.4 Chaboche elasto-visco-plastic model

This material model is a generalized implementation of elastic, elastic-plastic or visco-plastic, and multi potential constitutive equations. The model is constructed entirely using object “bricks”. For the moment, the model will be constructed using an elasticity object, a number of “potentials" and interactions between the potentials. Potentials represent inelastic dissipations which describe the evolution of independent inelastic deformation mechanisms.

Hardening mechanisms are modelled with objects within the individual potentials (type of hardening depending on the type of potential) and are thus not yet specified. This behaviour is essentially a manager of sub-model objects, and will be discussed in general terms about the permissible variables.

The model's internal variables are determined by the sub-objects, which have been selected by the user. The general storage form includes variables, which are “global" to the material laws, and therefore form relations with the imposed (observable) variables or apply to all the potentials. Each potential may additionally contain “parameter" variables, which do not have associated forces, and “hardening" variables, which do have associated forces. The distinction concerns the form of interaction, which is possible.

6.4.1 Costitutive Laws

In this model, total strain ε_{to} can be divided into the following terms:

$$\varepsilon_{to} = \varepsilon_{el} + \varepsilon_{th} + \varepsilon_{pl} \quad (0.54)$$

In which:

ε_{el} = elastic strain
ε_{th} = thermal strain
ε_{pl} = plastic or inelastic strain

In the same way, total strain rate can be divided into the following terms:

$$\dot{\varepsilon}_{to} = \dot{\varepsilon}_{el} + \dot{\varepsilon}_{th} + \dot{\varepsilon}_{pl} \quad (0.55)$$

Where overwritten symbols represent time derivatives of the terms.

In the proposed elasto-visco-plastic Chaboche model, plastic strain rate, $\dot{\varepsilon}_{p}$, is expressed as:

$$\dot{\varepsilon}_{pl} = \dot{\lambda}\mathbf{n} \quad (0.56)$$

with:

$$\dot{\lambda} = \left\langle \frac{f}{K} \right\rangle^{n} \quad \textbf{Norton Law} \quad (0.57)$$

and:

$$\mathbf{n} = \frac{3}{2}\frac{\sigma' - \mathbf{X}'}{J_2(\sigma - \mathbf{X})} \quad (0.58)$$

Where f is the effective tension:

$$f = J_2(\sigma - \mathbf{X}) - R \quad \textbf{\textit{Von Mises} criterion} \quad (0.59)$$

In the overwritten equations, the apexes quantities indicate the deviatoric component of tension:

$$\sigma'_{ij} = \sigma_{ij} - \frac{1}{3}\sigma_{kk}\delta_{ij} \quad (0.60)$$

According to the following definitions:

- Stress first invariant (or linear invariant):

$$\sigma_{kk} = \sigma_{11} + \sigma_{22} + \sigma_{33} \quad (0.61)$$

- Kronecker's delta or unit tensor:

$$\delta_{ij} = \begin{cases} 1, & i = j, \\ 0, & i \neq j, \end{cases} \quad (0.62)$$

- Stress second invariant (or Von Mises Equivalent Stress)

$$J_2(\sigma - \mathbf{X}) = \sqrt{\frac{3}{2}(\sigma_{ij} - X_{ij}) \cdot (\sigma_{ij} - X_{ij})} \quad (0.63)$$

The stress tensor X represents *kinematic hardening*, and corresponds to the stress variation in the elastic dominion. **X** is called *back stress* too.

In Chaboche elasto-visco-plastic model kinematic hardening rule is non linear and is expressed through the **Armstrong-Frederick non-linear law**:

$$\mathbf{X} = \frac{2}{3}C\alpha \quad (0.64)$$

$$\square = \lambda\left[\mathbf{n} - \frac{3}{2}\frac{D}{C}\mathbf{X}\right] \quad (0.65)$$

This is the way that the stress tensor X (back stress) has been correlated to the strain tensor $\boldsymbol{\alpha}$ (back strain).

The scalar stress R represents isotropic hardening, and corresponds to a variation of the indicated radius into the elasticity domain.

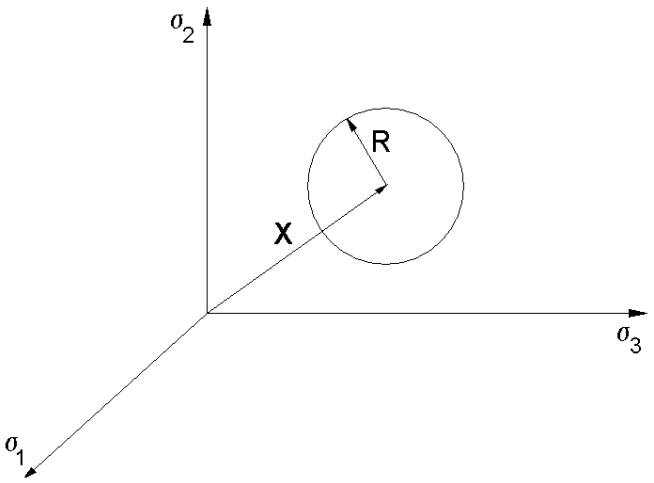

Figure 6.1- Isotropic deformation field sketch

In the elasto-visco-plastic model proposed by Chaboche, we find isotropic hardening defined as a constant:

$$R = R_0 \qquad (0.66)$$

In order to obtain a visco-plastic formulation that can be considered valid within a wide strain rate range, using an unified complete model, the elasto-visco-plastic Chaboche model introduces a multipotential plasticity/visco-plasticity formulation. For this reason, plastic deformation is divided into two different terms:

$$\varepsilon_{pl} = \varepsilon_{evr} + \varepsilon_{evl} \qquad (0.67)$$

With:

ε_{ev} visco-plastic deformation for high strain rates

ε_{ev} visco-plastic deformation for slow strain rates

Both strain potentials have got visco-plastic features, their strain functions depends directly from time. The first potential has got a yielding point and an hardening rule. The second one, instead, give us a creep evolution mechanism including neither hardening nor yielding.

In this way, the first potential will give:

$$\dot{\boldsymbol{\varepsilon}}_{evr} = \dot{\lambda}_r \mathbf{n}_r \tag{0.68}$$

With:

$$\dot{\lambda}_r = \left\langle \frac{f_r}{K_r} \right\rangle^{n_r} \tag{0.69}$$

$$\mathbf{n}_r = \frac{3}{2} \frac{\boldsymbol{\sigma} - \mathbf{X}'}{J_2(\boldsymbol{\sigma} - \mathbf{X})} \tag{0.70}$$

$$f_r = J_2(\boldsymbol{\sigma} - \mathbf{X}) - R_0 \tag{0.71}$$

In this way we will have:

$$\dot{\boldsymbol{\varepsilon}}_{evr} = \left\langle \frac{J_2(\boldsymbol{\sigma} - \mathbf{X}) - R_0}{\mathbf{K}_r} \right\rangle^{n_r} \frac{3}{2} \frac{\boldsymbol{\sigma} - \mathbf{X}'}{J_2(\boldsymbol{\sigma} - \mathbf{X})} \tag{0.72}$$

The first potential (usable for high strain rates) will result dependent from these parameters:

n_r, K_r, that define Norton's Law
C, D, that define kinematic Hardening
R_0 (yielding point), that defines isotropic hardening

The second potential will give:

$$\dot{\varepsilon}_{evl} = \dot{\lambda}_l \mathbf{n_l} \tag{0.73}$$

With:

$$\dot{\lambda}_l = \left\langle \frac{f_l}{K_l} \right\rangle^{n_l} \tag{0.74}$$

$$\mathbf{n_l} = \frac{3}{2} \frac{\sigma}{J_2(\sigma)} \tag{0.75}$$

$$f_l = J_2(\quad) \tag{0.76}$$

In this way, user will obtain:

$$\dot{\omega}_{evl} = \left\langle \frac{J_2(\sigma)}{K_l} \right\rangle^{n_l} \frac{3}{2} \frac{\sigma}{J_2(\sigma)} \tag{0.77}$$

The second potential (vailid for slow strain rates) will be defined by the two following parameters:

n_l, K_l, that define the well known Norton's Law

6.5 Z-Mat Chaboche Model implementation

A particular form of the Chaboche model will be used, including thermal strain, non-linear isotropic hardening, linear and non-linear kinematic hardening, and some coefficients that vary with temperature. The behaviour model is only a framework for building up particular hardening/criterion/flow/etc combinations. The basic form of the model is stated in the previous paragraph. The model supports any number of kinematic hardening variables, and all coefficients in the model may be variable.

To start the material file, the ***behaviour keyword must be used to indicate a generic behaviour object is to be created. All such objects will have a "class" keyword (here, behaviour), followed by a particular type of that class. For this

model, the type is gen_evp for generalized elasto-visco-plastic. It should be noted that the asterisks in the Z-mat file indicate not only keywords, but a hierarchy of sub-commands. Thus all keywords of **-level are sub-commands of the behaviour, and the next ***-level command (here ***return) terminates the behaviour read. For this model, the elasticity matrix, thermal strain, and potential keywords are used.

The potential object is the most interesting one here, as it defiles all the plasticity characteristics. The potential model chosen is again named gen_evp (but could be one of many others), and the characters following are an optional name for the potential. Output variables and coupling use this user-determined name.

A particular form of the model will be used, including thermal strain, non-linear isotropic hardening, linear and non-linear kinematic hardening, and some coefficients, which vary with temperature.

The following is an example of a elasto-visco-plastic material created joining each applicable class with corresponding subclasses and tuning opportunely their instances and values.

```
***behavior gen_evp auto_step
**elasticity isotropic
    young    temperature
 215000.0      20.
 ……..……..
 poisson  0.3

**thermal_strain isotropic
 alpha      temperature
  0.12500000E-04  0.
.....
**potential gen_evp evr
*criterion mises
*flow norton
     K        temperature
 114.956        20.
     n        temperature
 12.496         20.
 *kinematic nonlinear
     D       temperature
  596.336       20.
    C       temperature
 187123.4       20.
 *isotropic constant
    R0       temperature
 232.226         20.
……..……..
**potential gen_evp evl
*criterion mises
*flow norton
    K     temperature
 3093.09    20.
n       temperature
 21.       20.
 *isotropic constant
  R0    0.

***return
```

Table 6.2- Z-Mat elasto-visco-plastic material scheme

The behaviour model is only a framework for building up particular hardening/criterion/flow/etc combinations. The basic form of the model is stated simply below.

The material file structure for the gen elasto-visco-plastic model consists of an elasticity object, an optional thermal strain object, an optional arbitrary number of potentials (without restriction on types), and a number of optional interaction objects:

***behavior gen_evp [modifier]
  **elasticity <ELASTICITY>
[**damage <DAMAGE>]

[**localization <LOCALIZATION>]
[**global_function <GLOBAL_FUNCTION>]
[**thermal_strain <THERMAL_STRAIN>]
[**conductivity <CONDUCTIVITY>]
[**potential <POTENTIAL> [name]]
...
[**interaction <INTERACTION>]
…

Table 6.3- Z-Mat elasto-visco-plastic material scheme

The compatibility of objects with the other objects, and with the integration method will be investigated during the running of the problem. Because of the dynamic nature of these models however, it is often difficult to make any verification as to the physical meaning of a particular model combination. It is therefore strongly advised to observe the material behaviour on a single element. This allows experimentation of the integration method and selection of the output variables without performing costly full-scale calculations.

Multi-potential models are primarily used for cases of time independent plasticity in combination with visco-plastic deformation, or to assemble multiple crystalline deformation systems.

By default, there is no thermal strain, no inelastic deformation or any interactions. The optional names (name) given after each potential type are used as a means to specify individual potentials (for interactions), and in construction of the output variable names.

Normally, it is advised to use *ep* for a plastic potential's name, and *ev* for a visco-plastic one.

7 Material characterization – Inconel 7xx

7.1 Description

Inconel 718 is a precipitation-hardenable nickel-chromium austenitic super-alloy containing significant amounts of iron, niobium, and molybdenum along with lesser amounts of aluminium and titanium. It combines corrosion resistance and high strength with optimum weldability, including resistance to post weld cracking. The alloy has excellent creep-rupture strength at temperatures up to 700 °C (1300 °F). Used in gas turbines, rocket motors, spacecraft, nuclear reactors, pumps, and tooling.

7.2 Material Features

Inconel alloys are oxidation and corrosion resistant materials well suited for service in extreme environments. When heated, Inconel forms a thick, stable, passivating oxide layer protecting the surface from further attack. Inconel retains strength over a wide temperature range, attractive for high temperature applications where aluminium and steel would succumb to creep as a result of thermally induced crystal vacancies (see Arrhenius equation). Inconel's high temperature strength is developed by solid solution strengthening or precipitation strengthening, depending on the alloy. In age hardening or precipitation strengthening varieties, small amounts of niobium combine with nickel to form the intermetallic compound Ni_3Nb or gamma prime (γ'). Gamma prime forms small cubic crystals that inhibit slip and creep effectively at elevated temperatures.

7.3 Material Characterization

Material Characterization represents many different disciplines depending upon the background of the user. These concepts range from that of the scientist, who thinks of it in atomic terms, to that of the process engineer, who thinks of it in terms of properties, procedures, and quality assurance, to that of the mechanical engineer, who thinks of it in terms of stress distributions and heat transfer. The definition selected for the ASM-International Materials Characterization Handbook is as follows: "Characterization describes those features of composition and structure (including defects) of a material that are significant for a particular preparation, study of properties, or use, and suffice for reproduction of the material." This definition limits the characterization methods to those that provide

information about composition, structure, and defects and excludes those methods that yield information primarily related to materials properties, such as thermal, electrical, and mechanical properties.

7.4 Material Testing

The study has in particular dealt with the research of correlation between results of mechanical tests and fatigue, creep, yield stress and rupture sensitivity. At the same time, metallographic and fractographic investigations have been performed, giving further indications and allowing various parameters deduced from mechanical tests to be critically evaluated. An experimental confirmation has been obtained on a minimum number of three series of samples submitted to suitable heat treatments in order to obtain specific microstructures.

7.5 Test matrix

In the following page is reported a table with the complete test matrix, designed in order to provide a sufficient statistical base to calculate minimum (-3sigma) and average material curves. The type of tests were foreseen in order to be able to obtain all the necessary experimental data to grab the 7 material coefficient required by the Chaboche elato-visco-plastic material model.

Tensile tests at various temperatures have been used to determine base material mechanical properties such as Young's Modulus, yield strength, Poisson's ratio, etc. LCF and HCF tests have been performed in order to record material behaviour under various load application rates at imposed and controlled cycle types. Some tests have been performed in order to determine material hardening behaviour. Some other ones have the objective to evaluate material stabilization laws.

High temperature creep tests have been performed in order to evaluate creep behaviour of the superalloy. With more details on this subject, stress relaxation time has been extracted from test data. Creep strain too has been one of the most important obtained data. High temperature tests, have been used to obtain oxidation curves too.

TYPE OF TEST	PARAMETERS		N° OF TESTS		Output
	Temperature [°C]	Test Main Parameters	Repetitions	Total	
TENSILE	ISO-148-204-260-315-371-427-482-538 593-649-704-760-815-871-926-954-982	Strain rate: δε/δt= 10-2/s e 10-5/s	4	144	E, R0
CREEP	760-815-871-926-954-982	Stress Controlled - 5 Levels from 1000 to 12000 h	3	90	PLM - n - K - IsoT
	593-649-704	Stress Controlled - 3 Levels USL ε = 2%	3	27	
LCF	371-482-593-760-815-871	Rε=-1 Strain Rate 10-2/s e 10-5/s Rε=0 Strain Rate 10-2/s e 10-5/s 6 levels of Δε	2	288	C, D, b, Q
	871-926	Rε=-1 Strain Rate 10-2/s 10-5/s 6 levels of Δε — 15' hold time	2	48	
	371-427-815-871	3 Δε levels in blocks with δeI/δt cycles of 10-2/s 10-5/s	2	24	
HCF	260-315-371-427	Rσ=-1 3 levels from 270 to 380 MPa Rσ=0 3 levels from 270 to 380 MPa	4	96	Rf @ 10M cycles

Table 7.1- Test matrix

7.5.1 Tensile Test

Tests are performed as per the ASTM E8, ASTM A370, ASTM B557, IS/ BS Standards. A tensile test measures the resistance of a material to a static or slowly applied force. A machined specimen is placed in the testing machine and load is applied. A strain gage or extensometer is used to measure elongation. The stress obtained at the highest applied force is the Tensile Strength. The Yield Strength is the stress at which a prescribed amount of plastic deformation (commonly 0.2%) is produced. Elongation describes the extent to which the specimen stretched before fracture. Information concerning the strength, stiffness, and ductility of a material can be obtained from a tensile test. Variations of the tensile testing include; Room Temperature, Low Temperature, Elevated Temperature (ASTM E21), Shear, Temperature and Humidity, Combined Tension and Compression, Through Thickness, True Strain, Notched Tensile, and r (ASTM E646) & n (ASTM E517) values.

The following figure shows, for example, the experimental results obtained on a tensile test.

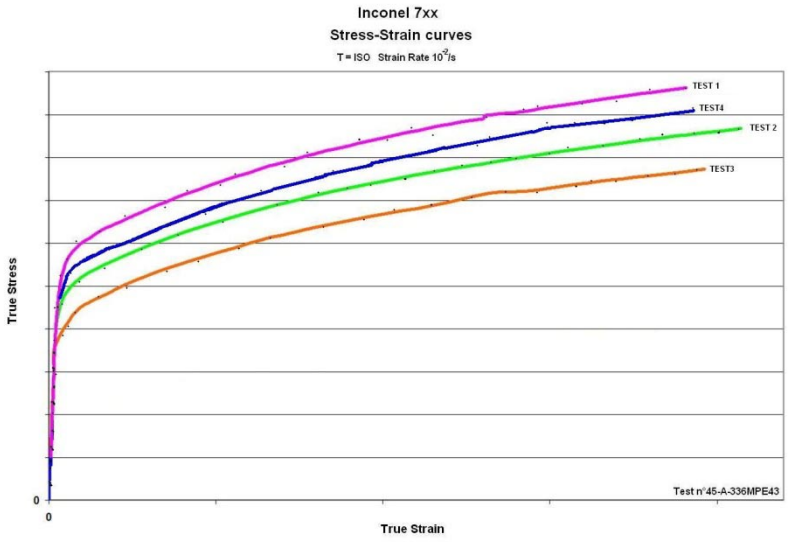

Figure 7.2- Tensile test experimental data

Tensile Test results provide the following data:

- Tensile strength at yield.
- Tensile strength at break.
- Tensile modulus.
- Tensile Strain.
- Tensile elongation and percent-elongation at yield.
- Tensile elongation and percent-elongation at break.

7.5.2 Fatigue Test

Fatigue tests are made according to ASTM E466-E606 and E647 specifications, with the object of determining the relationship between the stress range and the number of times it can be applied before causing failure. Testing machines are used for applying cyclically varying stresses and cover tension, compression, torsion and bending or a combination of these stresses.

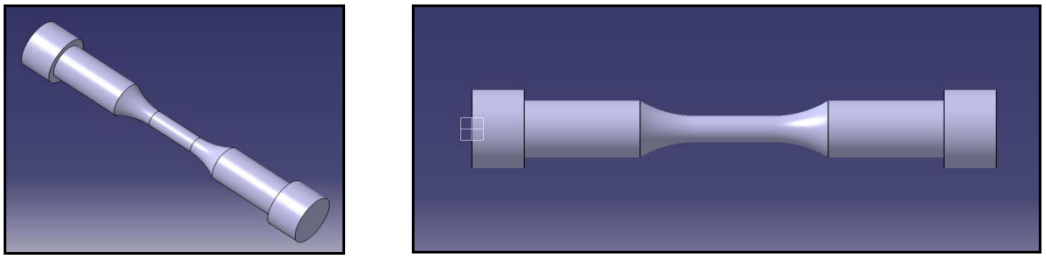

Figure 7.3- Fatigue test specimens

Performing a load or position controlled fatigue test requires a servo controlled test machine. Fatigue testing machines historically have been servo hydraulic or servo control of a hydraulic actuator.

The following pictures shows, for example, the experimental results obtained on a fatigue test. In the first picture, the showed experimental cycles are the first one, and the one that has been considered the stabilized one.

In the second picture, instead, there is the post-processing of the Ansys simulation for that test. These simulations were executed in order to tune material model coefficient s into the Z.Mat + ansys FEM analysis.

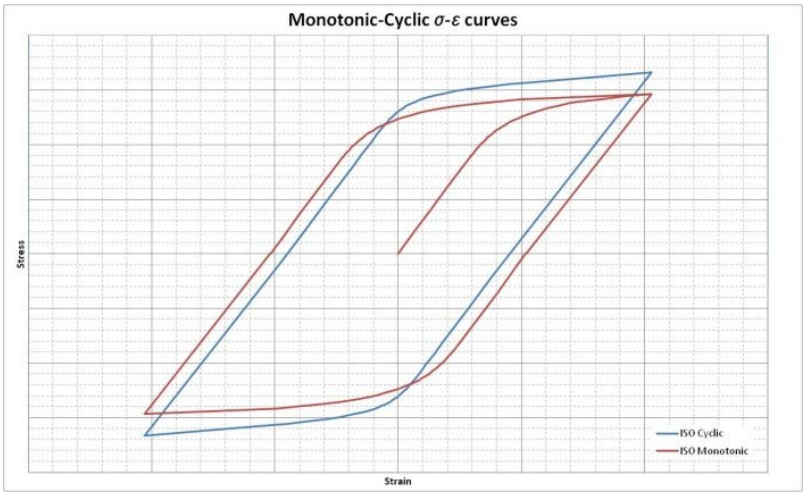

Figure 7.4- Fatigue test post-processing

Thanks to these kinds of experimental data has been possible to estimate stabilization time and hardening type and law.

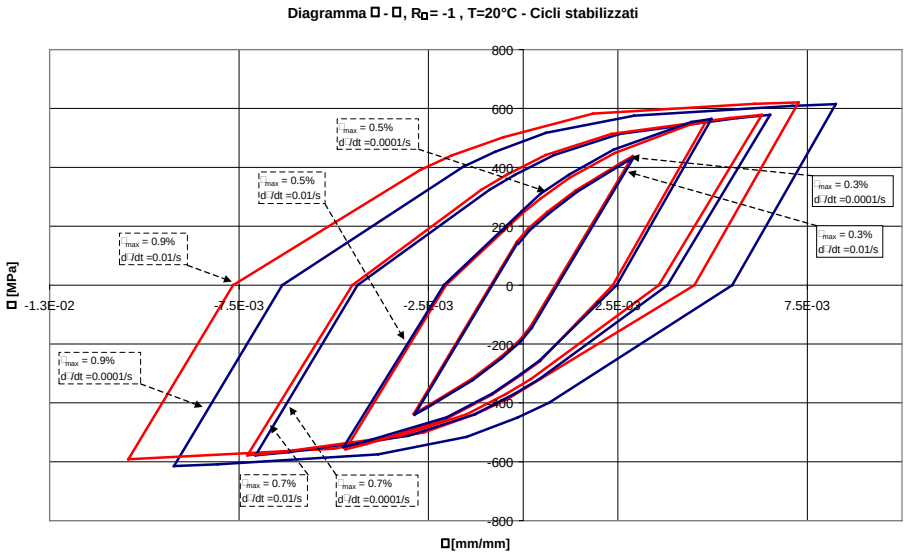

Figure 7.5- Fatigue test post-processing

The following graph shows schematically the test matrix for the fatigue tests. In the same graph are reported either LCF than HCF tests.

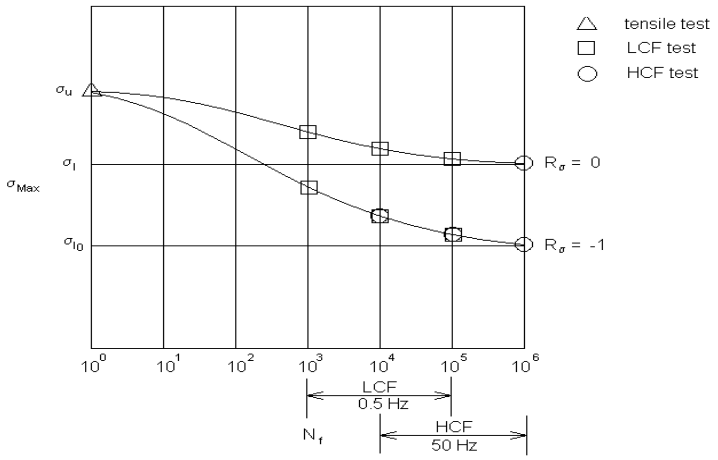

Figure 7.6- Fatigue test matrix

7.5.3 Creep Test

This test determines the deformation behaviour under long-term static tensile stress. Each of the specimens is subject to a different load remaining constant for some time while the deformation is measured simultaneously. The test may be carried out within a temperature range from +23 ºC to +150 ºC. The results can be used to estimate the deformation behaviour of components that are exposed to long-term tensile stresses.

The creep test is always performed with a load level maintained constant and by measuring the resulting strain versus time. These tests are quite often achieved for the determination of creep limits in to be able to perform structural dimensioning or guarantee that the structure does not undergo any creep strain during operation.

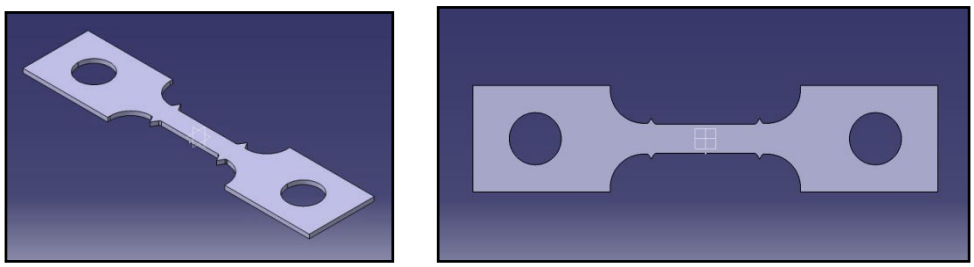

Figure 7.7- Fatigue test specimens

Due to the axial strain instrumentation with extensometer, it is also possible to perform relaxation test during which strain is maintained constant. By doing so, the stress is decreasing with time. This gives information concerning the behaviour of structural components and the evolution of stresses in case of imposed strain. There are two creep relaxation machines in GRC plant in Munich Germany.

Figure 7.8- Creep Test Machine

The main characteristics of these electromechanical machines are:

- Electro-mechanic jack with a maximum stroke of ± 50 mm,
- Load cells: 50 kN and 5 kN
- Displacement rate: 0,5 mm/s down to 1 μm/h
- Temperature range: +50°C to +800°C
- Axial and diametrical extensometers with ceramic rods
- Atmosphere: Air or Argon flow
- Control and Software: Rubicon system, DMG Creep- Relaxation software
- Specimen Types: Flat or cylindrical tensile specimen, cladding tube.

Extensometers for tensile or creep tests are used. They have successfully undergone a series of tests and modifications. That is a new aspect in comparison

with the old laboratory (LHA) where tensile tests were performed without extensometer, only with stroke displacement and compliance correction. This will improve our measurements.

These mechanical extensometers are able to measure the axial or diametrical strain on samples during tests performed as well at high temperatures (up to 1000°C), as well at low temperatures with liquid nitrogen (-160°C). They are used for uniaxial tensile, creep and relaxation. Operating these extensometers with telemanipulators has required many adaptations from the producer (Maytec GmbH) and from the laboratory technicians.

In particular, the precise and stable positioning of the ceramic rods on the specimen was very important. It was possible only by the use of micrometric plateau supports for the extensometers. Another important challenge was to be able to replace the ceramic rods without damaging the very tiny mechanical system linked to the LVDT sensor. For this purpose, an aluminium specific tool was designed and machined. The tensile-creep modulus, the isochronous stress-strain curve, the creep-to-rupture curve and the relaxation behaviour can be determined from the creep curves.

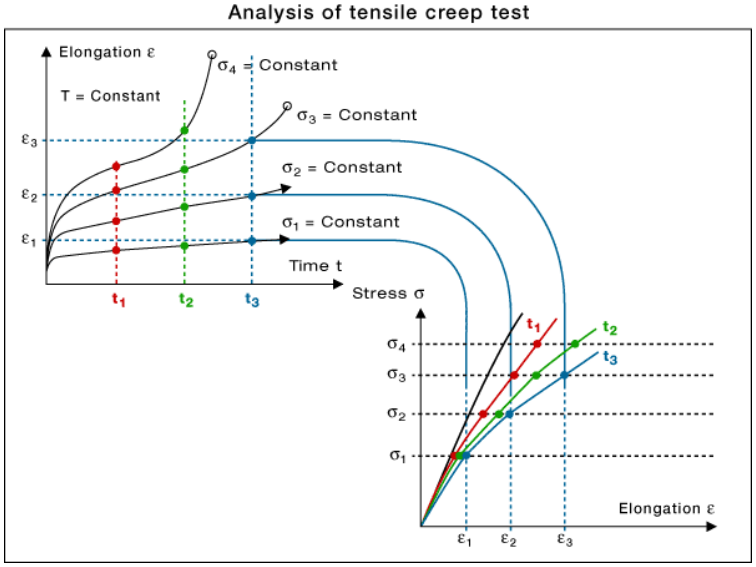

Figure 7.9- Determination of Creep Coefficients

7.6 Material Coefficients extraction

In order to be able to determine the material coefficients coming from the experimental data, an iterative procedure has been designed. The initial parameters, given by tentative, are fitted to the real curves trough the described processes of simulation and optimization.

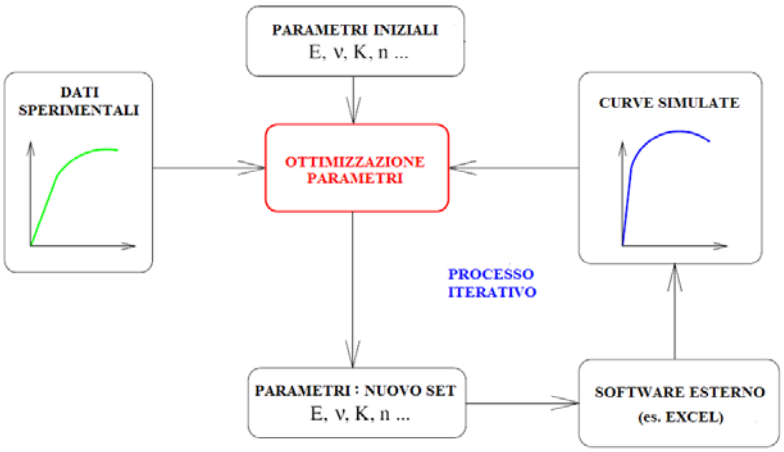

Figure 7.10- Creep Test Machine

This iterative process was set up for every experimental test in order to determine the proper coefficient for each investigated property.

8 Creation and Validation of a Procedure for FEM Structural Analysis using an elasto-visco-platic material model.

8.1 Material models construction and implementation using Z-Mat

In a Finite Element code, constitutive equations are used at each integration point to simulate material behaviour. Z-mat adds capability by providing advanced constitutive equations based on the rigorous thermodynamic state variable formulation.

The primary numerical task for material simulation code for FEA calculations is to provide the value of the stress tensor and the state variables at the end of a loading increment, knowing the values at the beginning of the increment and a trial strain increment. More precisely, we can define an "object" BEHAVIOR as the collection of:

- Primal prescribed variable (e.g. strain) and dual (associated) variable (e.g. stress).
- Set of state dependent variables V.
- Set of auxiliary variables, A, not necessary for the computation, but used in the post-processing.
- External parameters, P, prescribed by the user and acting like an external load (e.g. temperature in a mechanical uncoupled calculation).
- Material parameters, M, to be identified for each material.

The constitutive equations are normally expressed as a first order ordinary differential system (ODE), the derivative of the state variables being defined as functions of the prescribed primal variable, of A, P and M. The integration of this system can be made by explicit and implicit methods. Both techniques are included in Z-mat as follows:

- Runge-Kutta method with automatic time stepping.
- Modified midpoint (q-method), solved with a Newton algorithm.

The explicit integration is easier to implement, and therefore is used for fast prototyping. Implicit integration however demands the definition of the local Jacobian matrix defining the behaviour, which is a more complex affair, but the method is more robust for large time steps, as it provides (for free!) the information needed to compute the global consistent tangent matrix, and therefore permit quadratic global convergence.

Z-mat treats all model formulations in the most general sense, employing object-oriented design to achieve a high level of flexibility. With this approach, the models are described in terms of material building “bricks,” such as yield criterion, isotropic or kinematic hardening evolution, or visco-plastic flow. A model is much more powerful with this approach because all the different “brick” types can be combined by the user to effectively make new models at run-time. In fact, even the coefficients are generalized (abstracted), allowing constant values, tabular values, or c-type syntax functions.

There are two ways of using Z-mat

- User-mode
- Developer-mode

As many constitutive equations are already implemented in Z-mat, most users can simply make use of those in their calculations. A small change in the Ansys input file is necessary to access the Z-mat library, and an external material definition file must also be created.

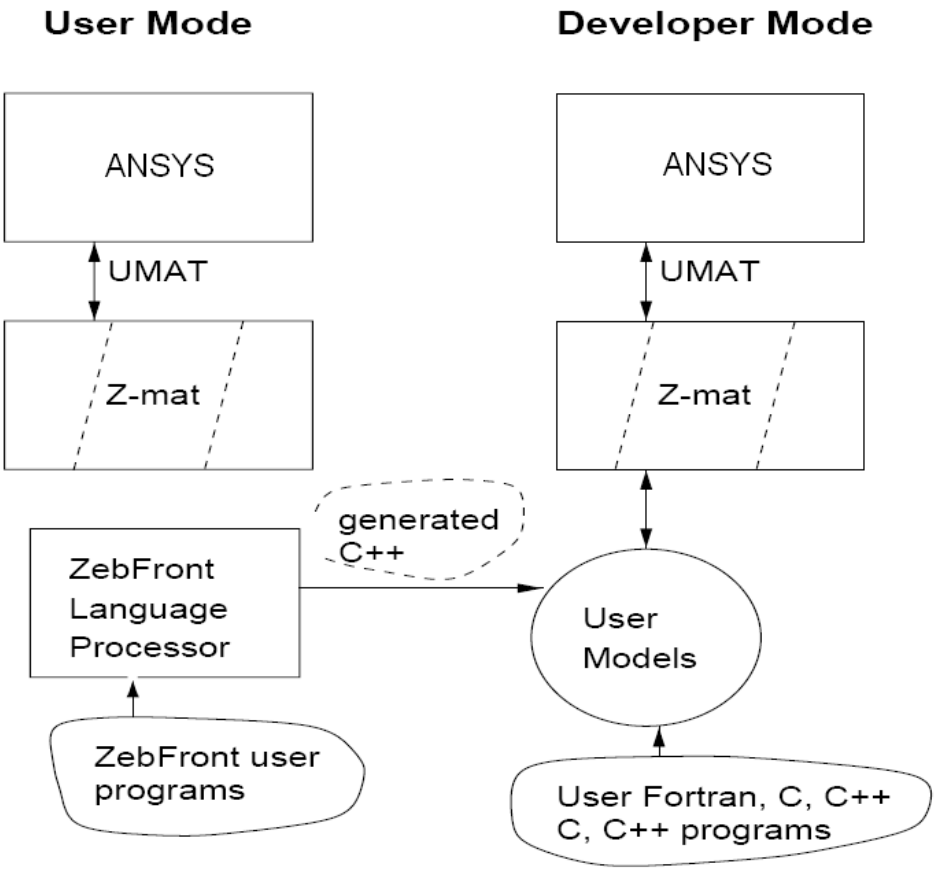

Figure 8.1- Determination of Creep Coefficients

The input file modifications must give the material name, which will become the name of an external material definition file to control Z-mat. The number of state variables is also required. Z-mat does not use any information regarding coefficients or material parameters from the Ansys input. Any number of Z-mat materials is accepted in the same run.

8.1.1 User Mode

Using the material laws contained in the Z-mat library involves changing the material definition in the *Ansys.inp* file, and creating a Z-mat material definition file. These Z-mat input files may be stored in a common location, allowing a site to easily manage their different material inputs.

The modifications of the *Ansys.inp* file are essentially constant between different analyses, except for the number of integrated state variables (using the DEPVAR keyword). For a given Z-mat material file, the utility program Zpreload will output all the lines which are needed. Note that Z-mat does not use the Ansys input material coefficients, but this line is still needed by Ansys to use the USERMAT routine.

The Z-mat material file customizes the way materials are entered into Ansys. Local convergence and automatic time step parameters can be adjusted, material rotations specified, and variables initialized. The material definitions itself is marked by the keyword ***behaviour, followed by a keyword for the type of behaviour, and its options. All material “building bricks” are constructed in this way, and each such “object” creation may be added to with user programs.

8.1.2 Developer Mode

Extended use of Z-mat can be made by adding other levels in the library. In fact, the large number of predefined constitutive models represents only a part of the code — the developer also has access to:

- Basic objects, which can be used in his own constitutive equations, offering the power of already tested bricks of behaviour: for instance using the "elasticity" object allows the user, without any effort, to have a direct access to any kind of elasticity in the code without any flag in the local code: the type of elasticity is automatically determined by the code from the data file, and the corresponding behaviour is then dynamically applied to the material.

- Integration methods; the developer has then the choice of using the integrators only, or use basic objects in the integrators.

The developing user can program any number of additions, including multiple additions of the same “type.” For example, multiple new material behaviours can be added, along with additional isotropic hardening “bricks.”

These later models can be used by the new user behaviour models, and by all the standard Z-mat library models. The input interface for user “bricks” is also exactly the same as for the standard models supplied with Z-mat, so user

extensions are seamlessly integrated into the library (in contrast to the user definition of USERMAT in the Ansys file).

Additions may be programmed in C++, or use the “material programming” language of ZebFront. ZebFront adds special commands for declaring material model data and functions (such as scalar, vector, or tensorial state variables, and coefficients), and automatically generates material file read functions and function prototypes. The end result is a material model, which can be close to a 1:1 listing of the model equations.

These equations can be written in full tensor or matrix form as well, eliminating many program loops. A typical ZebFront model includes a “class” declaration, where the model data structures are defined, a post step calculation, and either or both explicit or implicit integration implementations (the model equations). The class can be “derived” from more than one base type, which determines the functionality of the class. Often material models are derived from both BASIC_NL_BEHAVIOR and BASIC_SIMULATOR to provide FEA behaviour and simulation with the same code.

To assist with the developer mode, the Z-mat library comes with a set of development tools to generate make-files from multiple source files, link shared libraries on many platforms, and manage multiple architectures. Debugging tools are provided as well, to assist in debugging code running in Ansys.

8.1.3 Material models: determination of the coefficients.

The ANSYS interface in Z-mat is very robust, due to the complete and flexible USERMAT routine in ANSYS, as well as the full support of user routines in ANSYS post-processing.

To use Z-Mat, a user material needs to be defined in the ANSYS input file, and the problem launched with the Z-mat script. There is significance to the name of the material given with the *MATERIAL,NAME= option because it gives in fact the name of an external formatted ASCII file for configuring everything to do with the Z-mat material.

The material file then is loaded from the file named. Note that material coefficients are only defined in the Z-mat file. Coefficients can be defined by the somewhat more flexible format in Z-mat including tabular, functional and other formats, and can depend on temperature or any of the 9 user defined field variables. Also, some models such as the porous plasticity model above allow the coefficients to depend on integrated variables as well .

8.1.3.1 Simulation

As part of the Z-set/Z-mat package there is a model simulation mode, which can be applied to the following:

- Drive any differential model as supplied by the user.
- Used to simulate material behaviour for a volume element based on one of the standard behaviours or User behaviour (see the developers handbook for a description of the later).

To allow rapid prototyping of models, user modes are available in either a pure model definition, or (with small additions) to user behaviours defined in this manner.

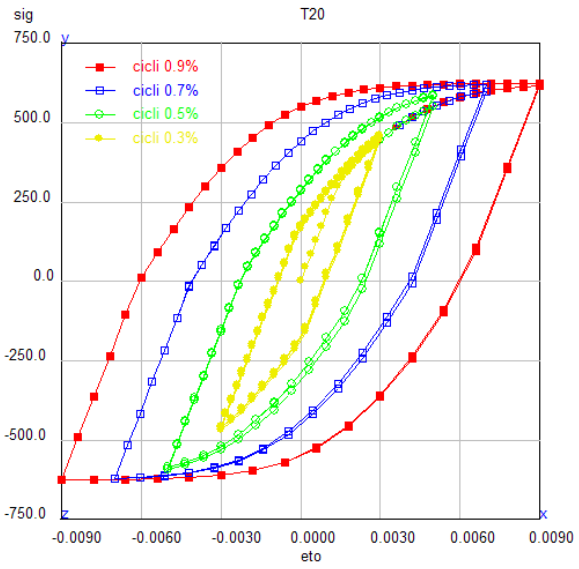

Figure 8.2- Simulated cycles at strain-control different values (R_ε = -1)

For mechanical material behaviours, some special functionality is provided. This includes generalized mixed-mode loading, and the visualization of yield surfaces. Note that curve output of a finite element calculation may be obtained using the **curve command, and then fed into the simulator for loading to obtain more detailed output or yield surface visualization. Extensive experimental test results can also be loaded directly to simulate real histories of a test, and comparisons made for model calibration and optimization.

There are many options for choosing “simulation solvers." Most of all, it is possible to run finite strain models as driven by the deformation gradient and nominal engineering stress directly. In addition, there are simulation “wrapper" type solvers which can be used in association with different finite element solvers in order to use the convenient simulation interface with material models non-native to Z-set/Z-mat, or simulation with a structural meshed specimen in place of a single pure stress-strain state.

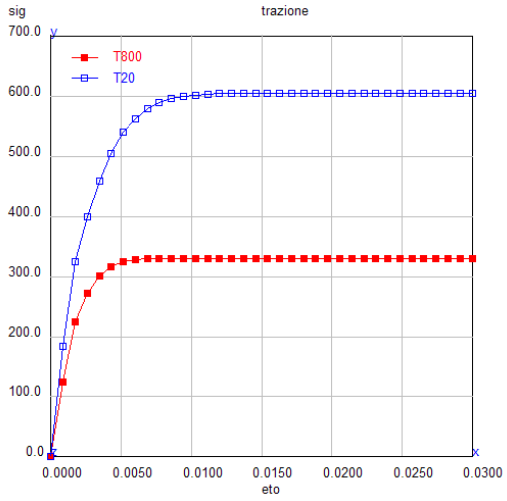

Figure 8.3- Simulated traction tests at different temperatures.

The Simulations command allows building interactively input files for the Z-Sim module (see the Z-Mat user manual for a complete reference on this program). The simulation results can then be used to define comparisons with experimental results to drive the optimization module.

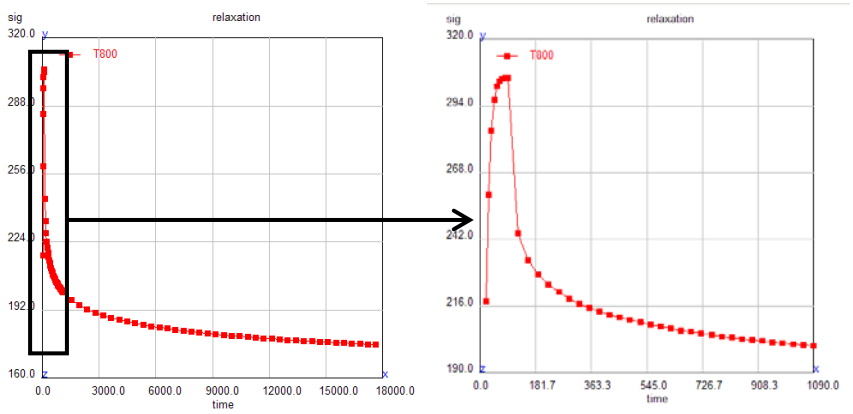

Figure 8.4- Simulated traction tests at different temperatures.

8.1.3.2 Optimization

Optimization is a generalized module, which may be used to identify material coefficients, optimize geometry, etc. The optimizer will modify tokenized parameters in a different user specified ASCII files in order to minimize the combined error of a variety of tests. Each test will generally consist of one or more shell scripts or sub-processes used for “simulation" of the test, and a certain method of comparison with experimental, reference data, or optimal condition. No explicit assumption is made to the nature of simulation method so these simulations may be made using the Z-set programs internally, or by another means. The real strength of this method is one can obtain the best comprehensive approximation to many data sets, even if they are theoretically over-constrained.

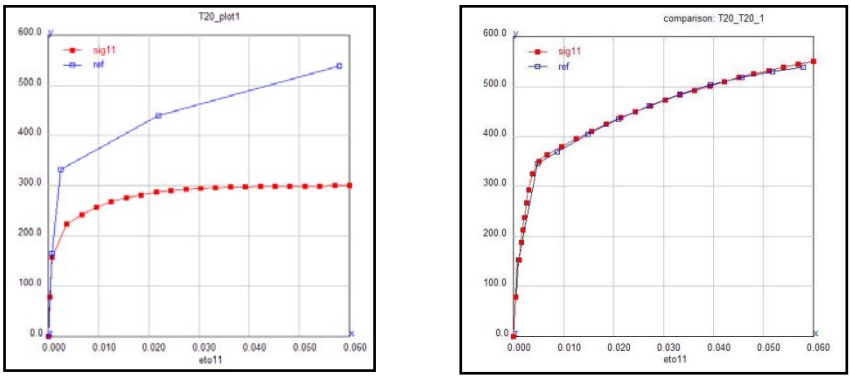

Figure 8.5- Optimized traction tests at fixed temperature.

The optimizer problem and its solution are defined in an input text file, similar to that for the other main program types. The optimizer uses a template file for definition of the parameters to be modified. The Optimizations command allows building interactively input files for the Z-Opt module (see the Z-Mat user manual for a complete reference on this program).

8.1.4 Elastic Model Construction and Validation

The linear material properties used by the element type are listed under "Material Properties" in the input table for each element type and are input using the MP command. A brief description (including the label used in the MP command) of all linear material properties is given at the end of this section.

These properties (which may be functions of temperature) are called linear properties because typical non-thermal analyses with these properties require only a single iteration. Conversely, if properties needed for a thermal analysis (e.g., KXX) are temperature-dependent, the problem is nonlinear. Properties such as stress-strain data (described in Nonlinear Stress-Strain Materials) are called nonlinear properties because an analysis with these properties requires an iterative solution.

Linear material properties that are required for an element, but which are not defined, use the default values as described below (except that EX and KXX must be input with a nonzero value where applicable). Any additional material properties are ignored. The X, Y, and Z refer to the element coordinate system. In general, if a material is isotropic, only the “X” and possibly the “XY” term is input.

Structural material properties must be input as an isotropic, orthotropic, or anisotropic material.

If the material is **isotropic**: Young's modulus (EX) must be input. Poisson's ratio (PRXY or NUXY) defaults to 0.3. If a zero value is desired, user must input PRXY or NUXY with a zero or blank value.

The shear modulus (GXY) defaults to EX / (2(1+NUXY)). If GXY is input, it must match EX / (2 (1+NUXY)). Hence, the only reason for inputting GXY is to

ensure consistency with the other two properties. Also, Poisson's ratio should not be equal to or greater than 0.5.

If the material is **orthotropic**: EX, EY, EZ, (PRXY, PRYZ, PRXZ, or NUXY, NUYZ, NUXZ), GXY, GYZ, and GXZ must all be input if the element type uses the material property. There are no defaults. Note that, for example, if only EX and EY are input (with different values) to a plane stress element, an error will result indicating that the material is orthotropic and that GXY and NUXY are also needed.

Poisson's ratio may be input in either major (PRXY, PRYZ, PRXZ) or minor (NUXY, NUYZ, NUXZ) form, but not both for a particular material. The major form is converted to the minor form during the solve operation [SOLVE]. Solution output is in terms of the minor form, regardless of how the data was input. If zero values are desired, input the labels with a zero (or blank) value.

For axisymmetric analyses, the X, Y, and Z labels refer to the radial (R), axial (Z), and hoop (θ) directions, respectively. Orthotropic properties given in the R, Z, θ system should be input as follows: EX = ER, EY = EZ, and EZ = E θ. An additional transformation is required for Poisson's ratios. If the given R, Z, θ properties are column-normalized, NUXY = NURZ, NUYZ = NUZ θ = (ET/EZ) *NU θZ, and NUXZ = NUR θ. If the given R, Z, θ properties are row-normalized, NUXY = (EZ/ER)*NURZ, NUYZ = (E θ/EZ)*NUZ θ = NU θZ, and NUXZ = (E θ/ER)*NUR θ.

For all other orthotropic materials (including ALPX, ALPY, and ALPZ), the X, Y, and Z part of the label (e.g. KXX, KYY, and KZZ) refers to the direction (in the element coordinate system) in which that particular property acts. The Y and Z directions of the properties default to the X direction (e.g., KYY and KZZ default to KXX) to reduce the amount of input required.

Material dependent damping (DAMP) is an additional method of including structural damping for dynamic analyses and is useful when different parts of the model have different damping values. If DAMP is included, the DAMP value is added to the value defined with BETAD as appropriate. DAMP is not assumed to be temperature dependent and is always evaluated at T = 0.0. Special purpose elements, such as COMBIN7, LINK11, CONTAC12, MATRIX27, FLUID29, and

VISCO88, generally do not require damping. However, if material property DAMP is specified for these elements, the value will be used to create the damping matrix at solution time.

Constant material damping coefficient (DMPR) is a material-dependent damping coefficient that is constant with respect to the excitation frequency in harmonic analysis and is useful when different parts of the model have different damping values (see Damping Matrices in the ANSYS, Inc. Theory Reference). DMPR is not temperature dependent and is always evaluated at T = 0.0. See Damping in the ANSYS Structural Analysis Guide for more information about DMPR.

The uniform temperature does not default to REFT (but does default to TREF on the TREF command).

The effects of thermal expansion can be accounted for in three different (and mutually exclusive) ways:

- Secant coefficient of thermal expansion (ALPX, ALPY, ALPZ)
- Instantaneous coefficient of thermal expansion (CTEX, CTEY, CTEZ)
- Thermal strain (THSX, THSY, THSZ)

When you use ALPX to enter values for the secant coefficient of thermal expansion (α_{se}), the programs interprets those values as secant or mean values, taken with respect to some common datum or definition temperature. For instance, suppose you measured thermal strains in a test laboratory, starting at 23°C, and took readings at 200°, 400°, 600°, 800°, and 1000°. When you plot this strain-temperature data, you could input this directly using THSX.

The slopes of the secants to the strain-temperature curve would be the mean (or secant) values of the coefficient of thermal expansion, defined with respect to the common temperature of 23° (To). You can also input the instantaneous coefficient of thermal expansion (α_{in}, using CTEX). The slopes of the tangents to this curve represent the instantaneous values. Hence, the figure below shows how the alternate ways of inputting coefficients of thermal expansion relate to each other.

8.1.5 Elasto-Plastic Model Construction and Validation

The available options for describing plasticity behaviour are described in this section. Here is reported a table containing all the allowable plasticity behaviours.

Bilinear Kinematic Hardening	Multilinear Kinematic Hardening	Nonlinear Kinematic Hardening
Bilinear Isotropic Hardening	Anisotropic	Hill Anisotropy
Drucker-Prager	Extended Drucker -Prager	Cast Iron
Multilinear Isotropic Hardening	Nonlinear Isotropic Hardening	

Table 8.6- Elasto plastic material models summary

Other options can be easily incorporated into the program by using User Programmable Features (see the Guide to ANSYS User Programmable Features).

8.1.5.1 Bilinear Kinematics Hardening.

The Bilinear Kinematics Hardening (BKIN) option assumes the total stress range is equal to twice the yield stress, so that the Bauschinger effect is included.

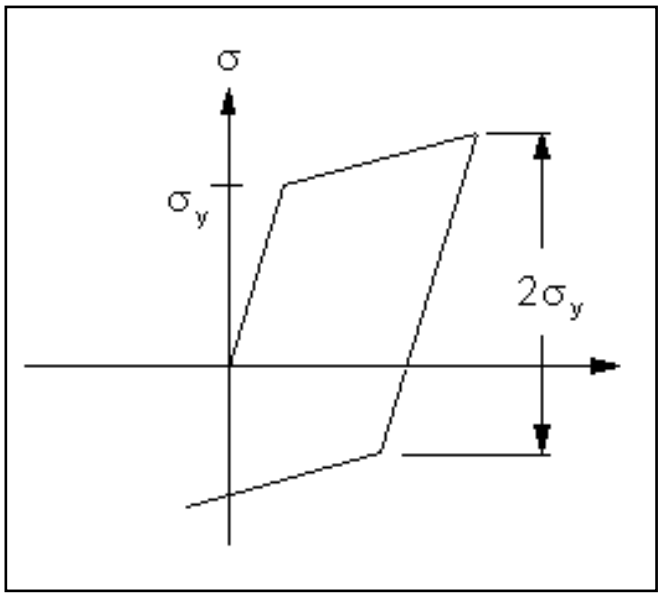

Figure 8.7- Bauschinger Effect

This option is recommended for general small-strain use for materials that obey *von Mises* yield criteria (which includes most metals). It is not recommended for large-strain applications. You can combine the BKIN option with creep and Hill anisotropy options to simulate more complex material behaviours. See Material Model Combinations in the ANSYS Elements Reference for the combination possibilities. Also, see Material Model Combinations in this chapter for sample input listings of material combinations.

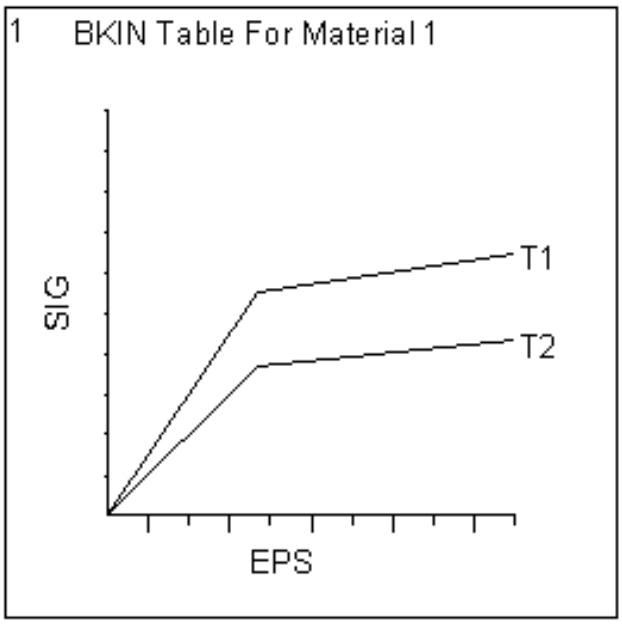

Figure 8.8- Bilinear Kinematics Hardening

This is a typical display [TBPLOT] of bilinear kinematic hardening properties.

8.1.5.2 Multilinear Kinematics Hardening.

The Multilinear Kinematics Hardening (KINH and MKIN) options use the Besseling model, also called the sub-layer or overlay model, so that the Bauschinger effect is included. KINH is preferred for use over MKIN because it uses Rice's model where the total plastic strains remain constant by scaling the sub-layers. KINH allows you to define more stress-strain curves (40 vs. 5), and more points per curve (20 vs. 5).

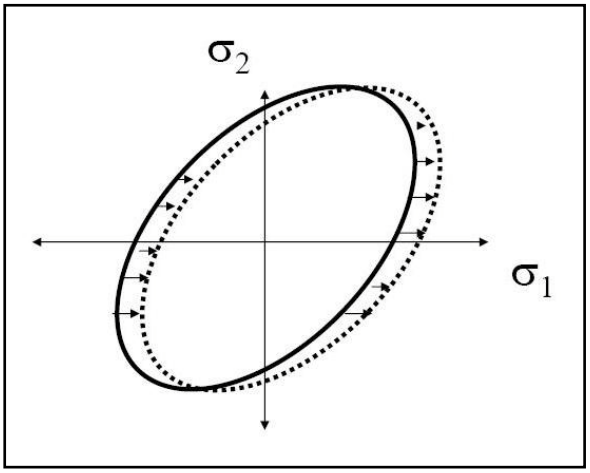

Figure 8.9- Multilinear Kinematic Hardening

Also, when KINH is used with LINK180, SHELL181, PLANE182, PLANE183, SOLID185, SOLID186, SOLID187, SOLSH190, BEAM188, BEAM189, SHELL208, and SHELL209, you can use TBOPT = 4 (or PLASTIC) to define the stress vs. plastic strain curve. For either option, if you define more than one stress-strain curve for temperature dependent properties, then each curve should contain the same number of points. The assumption is that the corresponding points on the different stress-strain curves represent the temperature dependent yield behaviour of a particular sub-layer.

These options are not recommended for large-strain analyses. You can combine either of these options with the Hill anisotropy option to simulate more complex material behaviours.

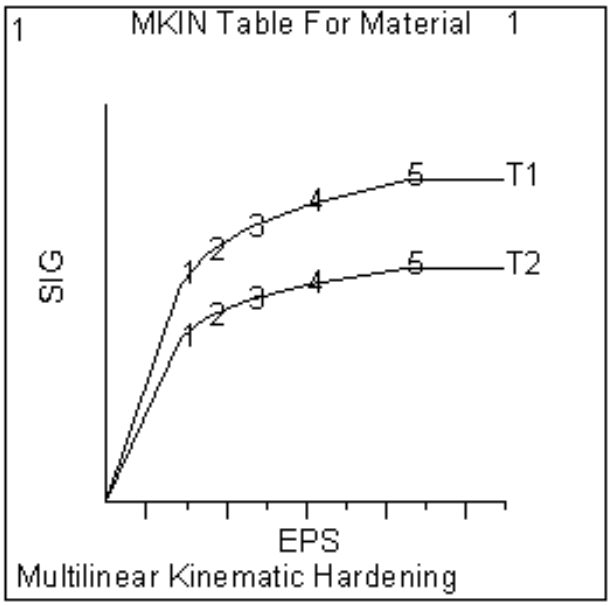

Figure 8.10- Multilinear Kinematic Hardening -Curves

This is a typical representation of the typical stress-strain curves for the MKIN option.

8.1.5.3 Bilinear Isotropic Hardening

The Bilinear Isotropic Hardening (BISO) option uses the *von Mises* yield criteria coupled with an isotropic work hardening assumption. This option is often preferred for large strain analyses. You can combine BISO with Chaboche, creep, visco-plastic, and Hill anisotropy options to simulate more complex material behaviours.

8.1.5.4 Multilinear Isotropic Hardening

The Multilinear Isotropic Hardening (MISO) option is like the bilinear isotropic hardening option, except that a multilinear curve is used instead of a bilinear curve. This option is not recommended for cyclic or highly non-proportional load histories in small-strain analyses. It is, however, recommended for large strain analyses. The MISO option can contain up to 20 different temperature curves, with up to 100 different stress-strain points allowed per curve.

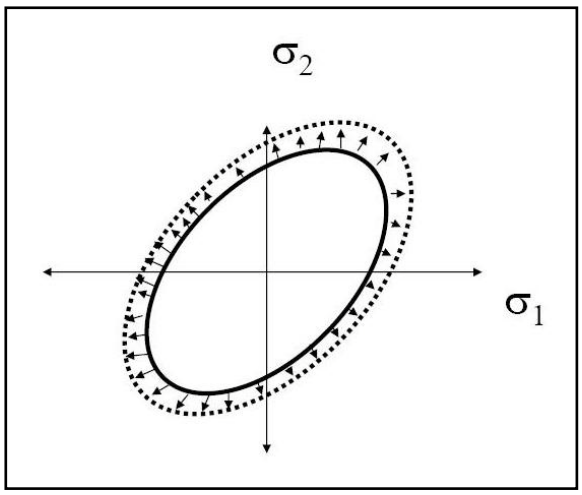

Figure 8.11- Multilinear Isotropic Hardening

Strain points can differ from curve to curve. You can combine this option with nonlinear kinematics hardening (CHABOCHE) for simulating cyclic hardening or softening. You can also combine the MISO option with creep, visco-plastic, and Hill anisotropy options to simulate more complex material behaviours. The stress-strain-temperature curves from the MKIN example would be input for a multilinear isotropic hardening material as follows:

8.1.5.5 Nonlinear Kinematic Hardening.

The Nonlinear Kinematic Hardening option uses the Chaboche model, which is a multi-component nonlinear kinematic hardening model that allows you to superpose several kinematics models. See the ANSYS, Inc. Theory Reference for details. Like the BKIN and MKIN options, you can use the CHABOCHE option to simulate monotonic hardening and the Bauschinger effect.

This option also allows you to simulate the ratcheting and shakedown effect of materials. By combining the CHABOCHE option with isotropic hardening model options BISO, MISO, and NLISO, you have the further capability of simulating cyclic hardening or softening. You can also combine this option with the Hill anisotropy option to simulate more complex material behaviours.

The model has 1 + 2 x n constants, where n is the number of kinematic models, and is defined by NPTS in the TB command. See the ANSYS, Inc. Theory Reference for details. You define the material constants using the TBTEMP and TBDATA commands. This model is suitable for large strain analysis.

Here's a summary of the properties and features of each of them:

Name	TB Lab	Yield Criterion	Flow Rule	Hardening Rule	Material Response
Classic Bilinear Kinematic Hardening	BKIN	**von Mises**	**associative** Prandtl – Reuss equations	Kinematic Hardening	Bilinear
Multilinear Kinematic Hardening	MKIN	**von Mises**	**associative**	Kinematic Hardening	Multilinear
Bilinear Isotropic Hardening	BISO	**von Mises**	**associative**	Isotropic Hardening	Bilinear
Mutilinear Isotropic Hardening	MISO	**von Mises**	**associative**	Isotropic Hardening	Multilinear
Anisotropic	ANISO	**modified von Mises**	**associative**	Work Hardening	Bilinear – each direction and tension different
Drucker - Prager	DF	**von Mises** with dependence on hidrostatic stress	**associative or not**	none	Elastic-Pefectly Plastic

Table 8.12- Elasto plastic material models summary

8.1.6 Elasto-Visco-Plastic Model Procedure Construction and Validation

The following procedure has been adopted to calculate the stress-strain state of a structural component, through the implementation of an elasto-visco-plastic model with non linear interaction between creep and fatigue, in Ansys finite element software.

Moreover, the same procedure can be utilized to determinate fatigue and creep damage using General Electric dedicated software, SUSAN, keeping advantage of the overwritten interaction. Last but not least, using dedicated software, PROPLife, the same procedure can help user to better estimate life of a component.

Elasto-Visco-Plastic analysis can be performed adopting Zansys module implemented in Z-Mat software. It is sufficient to generate a subroutine that links Ansys to Z-Mat. More in detail will be sufficient to put in a folder

- The file (i.e. *Jobname.inp*) containing FE model, loads boundary conditions and solution parameters.

- The file containing all the necessary material parameters (classes, modules and coefficients).

It is important to notice that the material filename must be always defined as 10x.txt where x is a number varying from 1 to 9. If there will be different materials constituting the structural component, will be necessary to insert different files for each material.

8.1.7 Jobname.inp file compiling.

The first step to build the file is to provide for the material model: will be necessary to choose between all the Ansys elements that are defined as *user-mat;* in fact, for these kinds of elements will be possible to define an external material model and behaviour.

The file jobname.inp is obtained by issuing the Ansys command CDWRITE after than the model has been completely meshed, all the boundary conditions and forces have been applied, and a dummy material model has been assigned.

In the /PREP7 section, after the ANTYPE command, which selects the type of analysis, must be added the lines recalling the external material model. Using the TB Ansys command whit the USER and STATE options:

```
TB, USER, 1, 0, 0
TB, STATE, , 40
```

These lines recall the material file defined as *101.txt*

At the end of all these activities, the /SOLU Ansys command must be issued. In this step must be defined the type of analysis and its options, loads will be applied, together with load-step options.

Through the EQSLV is chosen the type of analysis. The preferred one must be the PCG (Pre-conditioned Conjugate Gradient iterative equation solver), because is the one that best fits non-linear analyses.

By issuing the command NROPT, FULL, , OFF can be activated the Newton-Raphson “complete” solution method. In this last one, the stiffness material matrix is calculated each equilibrium iteration. Is always preferable to associate to this command the *adaptive descent off* option. In this way the PCG goes through the usage of a “tangent stiffness matrix” in each equilibrium iteration.

Issuing the command NROPT,FULL,,OFF “complete” Newton-Raphson method will be selected, in this way, the stiffness matrix of the element is calculated at each equilibrium iteration. At this command, has been associated the option *adaptive descent off* that uses “tangent stiffness matrix” every equilibriun iteraction.

The following step is to proceed to loads applications ad load-step lenght definition. Of course, loadsteps and substep definition can be set to variable dimension in each cycle.

The allowable options to perform a non linear analysis are the following:

- TIME is a parameter that grows monotonically, never equal to zero. With this command ANSYS identifies each load step and substeps.

- NSUBST defines number of substeps in which each load step is divided. This option allows to establish initial value and minimum and maximum step amplitude.

- AUTOTS is a command that allow software to decide how many time steps are foreseen in each load step. At the end of each time step, the amplitude of the following one is predicted based on the number of equilibrium iterations spent in the previous loadstep. (The more is the number of equilibrium iterations, the less is the amplitude of the time step)

Using the command AUTOTS, ON an automatic restart technique is activated if convergence within the specified loadstep parameters is not reached. Infatti, il programma ritorna alla fine dell’ultimo time step nel quale era stata raggiunta la convergenza, dimezza il successivo time step e automaticamente ricomincia l’analisi. Questo processo viene ripetuto fino a quando non si raggiunge la convergenza o l’ampiezza minima del time step. (Si noti che l’ampiezza minima

del time step corrisponde al massimo numero di substeps specificati con il comando NSUBST)

Il programma continuerà ad effettuare equazioni di equilibrio, fino a quando i criteri di convergenza stabiliti dall'utente attraverso il comando CNVTOL non saranno soddisfatti (oppure fino a quando non viene raggiunto il massimo numero di iterazioni di equilibrio stabilito attraverso il comando NEQIT)

The output control is executed through the OUTRES command. With this command is possible to establish the frequency of the solution steps that have to be saved in the output file rst. The solutions calculations start executing SOLVE command. To close the solution it is necessary to issue the FINISH command.

8.1.8 New generated models versus Ansys models

This part of the document includes the description of the material models validation. To validate each model, the same analysis has been performed in Ansys with its implemented material model, than using Z-Mat once the material card has been reverted into the Z-Mat coefficients.

8.1.8.1 Comparative analyses and results verification.

In this part are inserted the result with elastic model and elasto-plastic one (MKIN). Stress and Strain contour plots have been compared. Each comparison has been performed applying same loads and boundary conditions have been applied. Result files give exactly the same output.

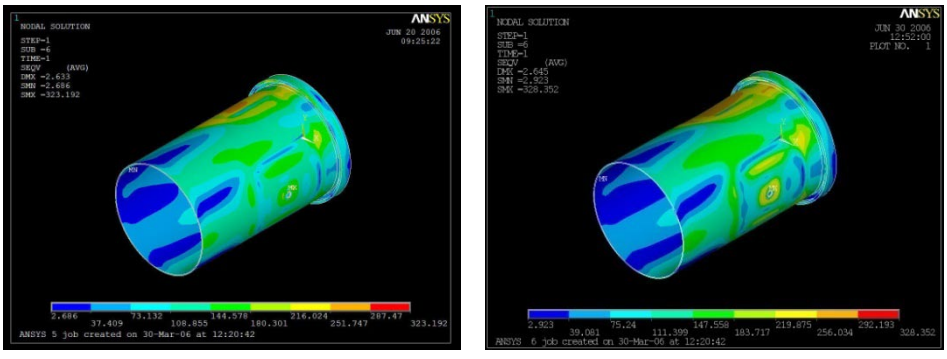

Figure 8.13- Ansys vs Ansys+Z-Mat – Stress Contour Plots Comparison

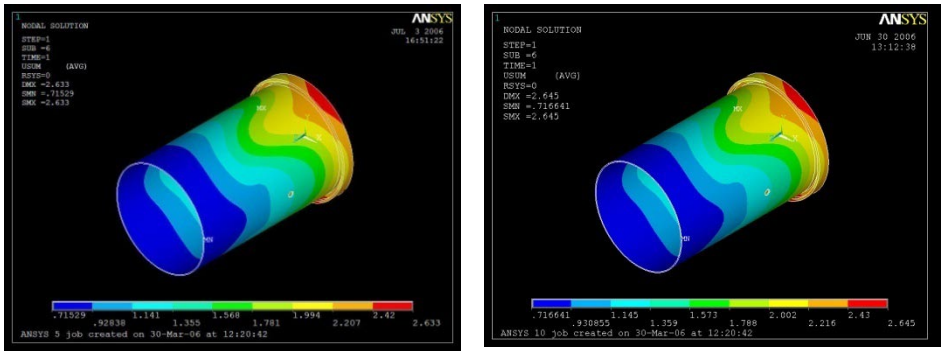

Figure 8.14- Ansys vs Ansys+Z-Mat – Displacement Contour Plots Comparison

The comparisons written above have been performed for:

- Elastic material model
- Elasto-plastic with isotropic hardening rule
- Elasto-plastic with kinematics hardening rule

Each of them gave exactly the same results. For these reasons the elastic model and the elasto-plastic one, have been considered totally reliable.

8.1.8.2 Fatigue estimation

Fatigue life estimation has been performed calculating fatigue life reproducing fatigue tests on Inconel test tools. Each calculation has been performed through a “Rainflow” counting type algorithm.

The rainflow-counting algorithm (also known as the "rain-flow counting method") is used in the analysis of fatigue data in order to reduce a spectrum of varying stress into a set of simple stress reversals. Its importance is that it allows the application of Miner's rule in order to assess the fatigue life of a structure subject to complex loading. The algorithm was developed by Tatsuo Endo and M. Matsuiski in 19681. Though there are a number of cycle-counting algorithms for such applications, the rainflow method is, as of 2004, the most popular.

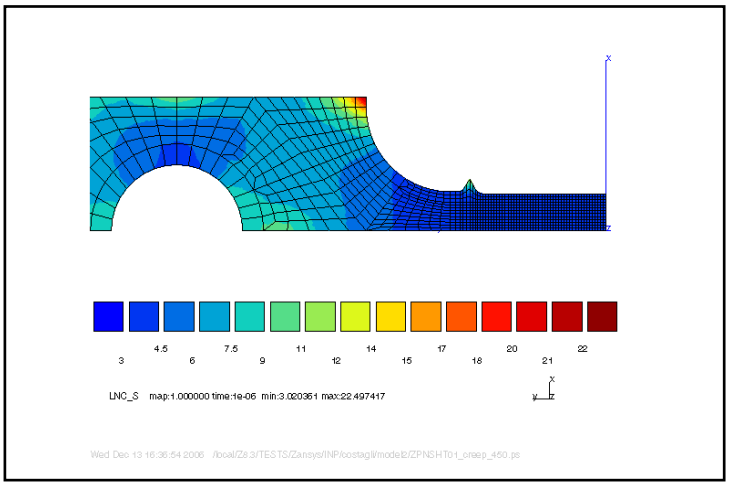

Figure 8.15- Fatigue test simulation

8.1.9 Implementation of the coefficients in Susan and PROPLife

8.1.9.1 SUSAN

SUSAN is a tool created in GE to evaluate creep in structures. The reasons that lead to the research of such a software were that the creep model implemented in ANSYS was heavily inaccurate when performing estimation using interpolated temperatures. This problem, recognized from the same ANSYS developers, will be fixed in the next revisions of the software.

For this reason, SUSAN was developed to fix this problem. These are two through the most significant graphs explaining the interpolation mistake due to integration (of a linearly interpolated parameter, while should have been logarithmic).

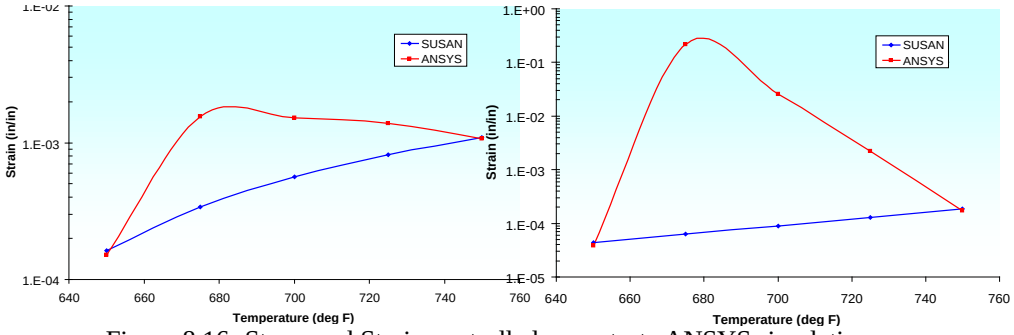

Figure 8.16- Stress and Strain controlled creep tests ANSYS simulations

The following graphs show the region in which this mismatches occur. On the left part of the graph is reported the logarithmic law that should be implemented, on the right part of the graph itself there is the creep region in which this mismatch is involved.

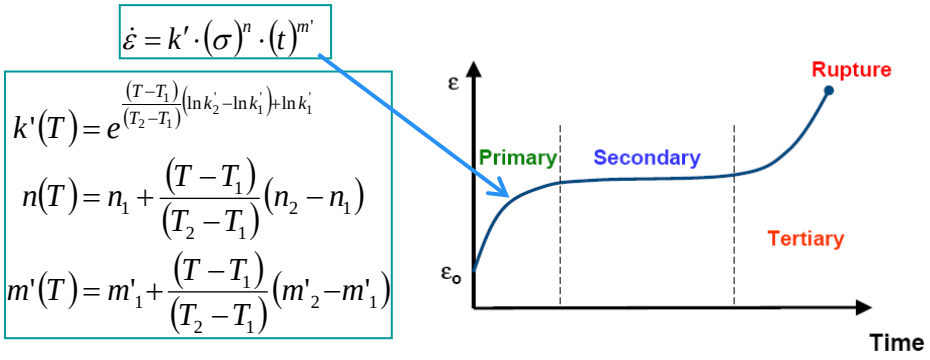

Figure 8.17- Creep laws and creep behaviour

8.1.9.2 PROPLife

PROPLife, developed from GE AE and part of the SIESTA software, is a fracture mechanics and fatigue life estimation software. Actually is able to perform analyses and calculations on the following topics:

- Fracture Toughness of Steels
- Temper Embitterment of Steels
- Fatigue Life Estimation
- Enhanced Analysis of Subsurface Cracks
- Automated Material Property Database

PROPLife uses as input loads, geometry, material properties and boundary conditions of the FE model. Using load cycle information is able to provide, as output the umbers of cycle to failure for the component according to the Ramberg-Osgood temperature dependent formulation.

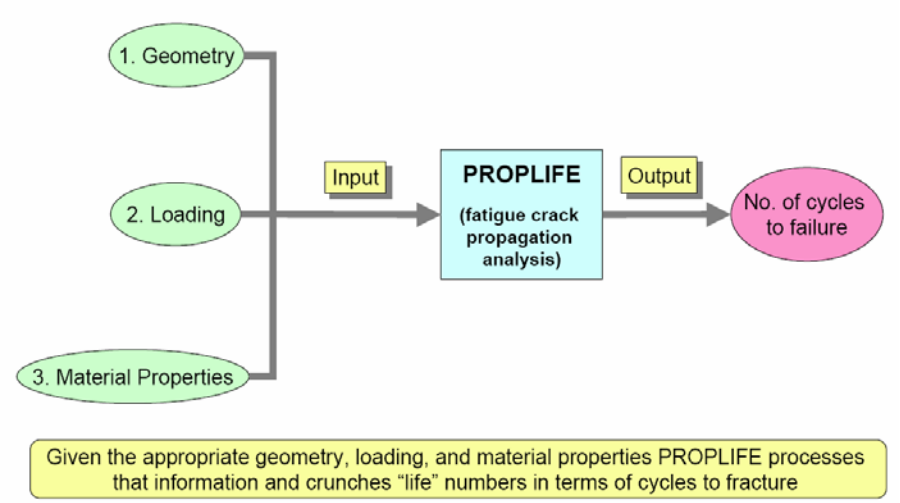

Figure 8.18- PROPLife block diagram

His major features are:

- Stress gradients: up to 100 gradients/mission and 1000 gradients/analysis
- Neuber correction based on max. Plastic strain point in the mission rather than the max. Stress point.
- New procedure for calculating minor cycles crack growth.
- Temperature interpolation procedure for material properties (current production PROPLIFE uses the closest temperature instead of performing interpolation).
- The "Hold Time" analysis option is automatically turned on – user has to turn it off if not running a hold time analysis.

The following is a brief scheme of the points of the program in which the material model coefficients influence the life calculations.

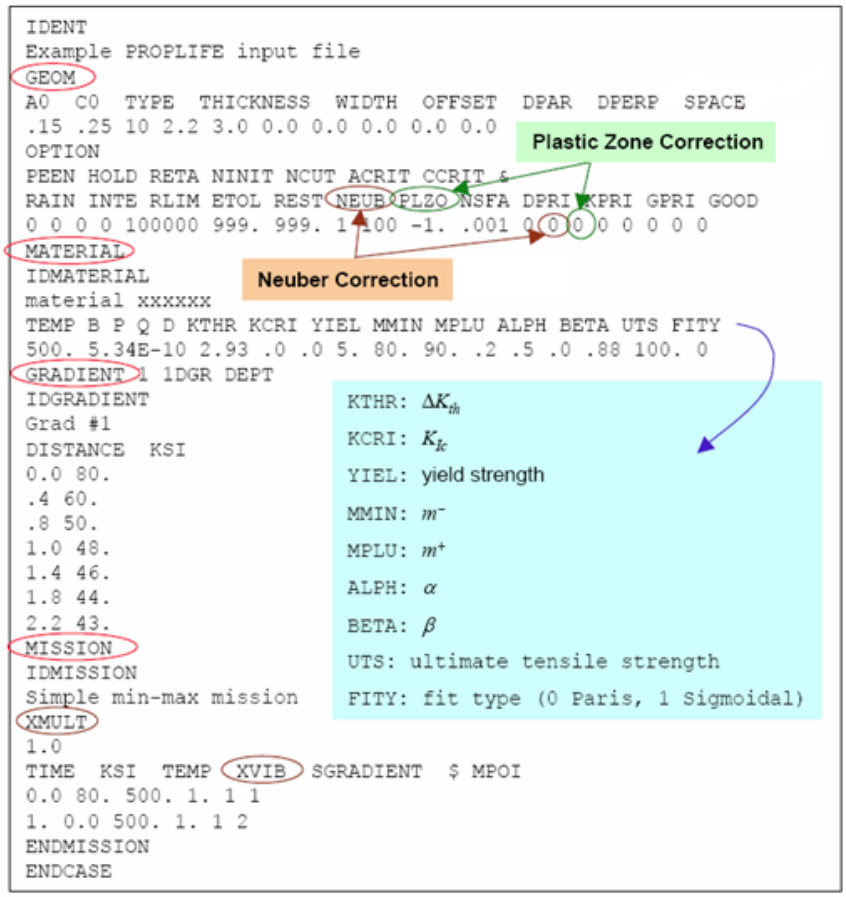

Figure 8.19- PROPLife block diagram

8.1.10 Comparison of tool results

The results coming from the different tools SUSAN and PROPlife, modified with the elasto-visco-plastic coefficients have been compared with the same software left unmodified. In this way it has been possible to evaluate differences between them. The comparison matrix, comprehensive of the stress calculations comparison analyses, is here represented:

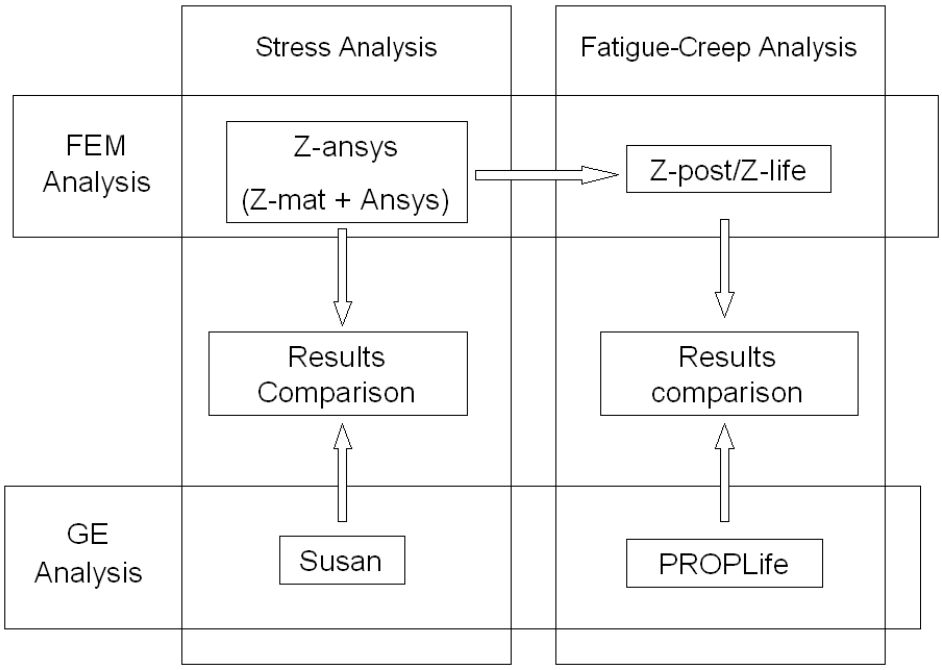

Figure 8.20- Comparison matrix

From this comparison chart is evident the intent to verify the correctness of the procedure and, at the same time provide the main differences between the existing way to proceed and the new results provided by the model.

9 Industrial application of the procedure.

The main intent of this work was to design, create and validate a procedure for gas turbine structural analysis able to cover one of the known limitations of the actual procedures: in life calculations, fatigue and creep are treated using formulations that are not able to take in account of their interaction. The damage calculation was performed simply adding the two effects using the effects superimposing principle.

The resulting calculation is actually considered too marginal. New models are requested in order to be able to refine life prediction.

Is well known, in fact, that under certain conditions, creep and fatigue damage interact one each other, due to crystallographic modification. The procedure itself has been applied to a typical condition, to test the effect of the introduction of this new model.

9.1 Introduction

The PGT25+G4 is a 34MW gas turbine consisting of an enhanced LM2500+ G4 Gas Generator coupled with a 2-stage High Speed Power Turbine Module with increased flow capacity.

Figure 9.1- PGT25*G4 Layout

High efficiency and reliability together with fuel flexibility and low emissions are just some of the many features that make this product the ideal choice for both mechanical drive and power generation in pipeline and E&P applications both onshore and offshore. Upgrade kits for the installed base of PGT25+ units are available to increase output power by 10%.

9.2 Product description - Gas Generator

The gas generator of the PGT25+G4 is that of the PGT25+ upgraded for increased flow capacity of the high pressure (HP) compressor and turbine. The pressure ratio increases from 23.6 for the PGT25+ to 24.2 for the PGT25+G4. Design changes have been limited to minor blade and stationary vane airfoil adjustments that provide the required mass flow increase. The HPT modifications include minor blade cooling improvements and proven material upgrades from recent aircraft engine technologies that provide improved higher temperature capability. These enhancements translate into customer savings. The effective area of the compressor discharge pressure seal was adjusted in order to maintain the optimum rotor thrust balance.

Figure 9.2- LM 2500+ Gas Generator Layout

Structurally, all frames (e.g., front, compressor rear, turbine mid and turbine rear frames) remain unchanged. Likewise, the HP compressor front and aft cases, sump hardware, and the number of main shaft bearings remain unchanged. These all share the successful experience of the PGT25+.

On DLE applications the combustor is upgraded by providing B ring wingless heat shields, cut back A and C ring heat shields and bolt-in heat shields that allow field replacement, and hence shorten the overall combustor maintenance cycle.

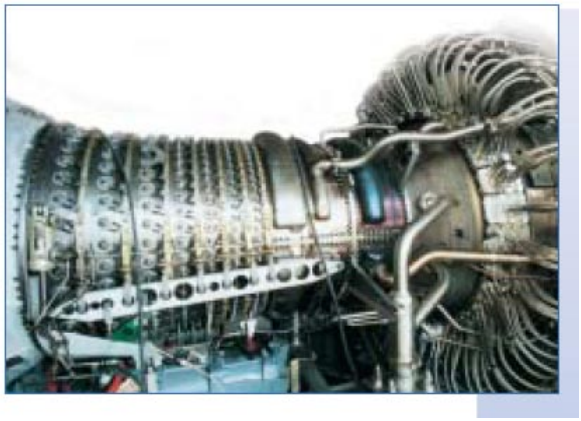

Figure 9.3- LM2500+ Gas Generator

9.3 Product Description – Power Turbine

The power turbine for the PGT25+G4 was developed based on GE's extensive experience with heavy duty gas turbines. The aerodynamic blades design provides high efficiency at both the design point and at reduced speed.

The 6100-rpm design permits direct coupling with the driven equipment, simplifying the system and enhancing the overall efficiency and availability of the plant. The cartridge philosophy significantly reduces the maintenance intervals, cutting costs and increasing availability. Optimized cooling flows in conjunction with the latest generation of seals, increases component life and maintains the efficiency of this gas turbine at its peak. The upgrades have been designed for ease of application.

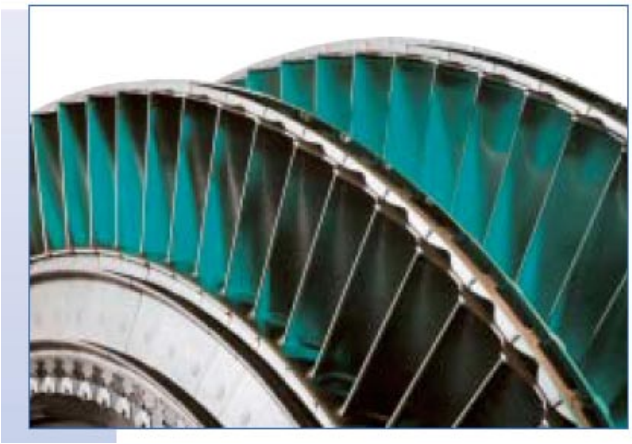

Figure 9.4- Power Turbine

9.4 Scope of work

Main scope of this part of the research is to apply the overwritten procedure on the stator cone of the power turbine. This kind of component is the one that withstand all stator casing of the power turbine. For this reason it is a component that, during machine operation, is subjected to high stress, low cycle fatigue, high temperatures.

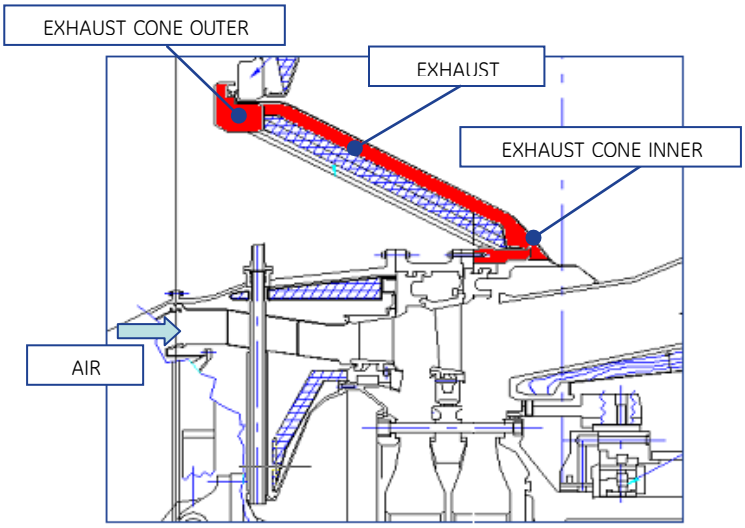

Figure 9.5- Stator Cone Cross section

These were the reason why GE Oil&Gas uses structural analysis software to estimate stress behaviour and LCF and creep tools to calculate life.

Field experiences, testing and measurements on stator cones at major maintenance inspections (50000 hours of duty), showed that though permanently deformed because of plasticity due to fatigue and creep, the overall cone's conditions were not as expected. The major inspection, in fact, was the calculated milestone to designate the end of life for the component in subject, whilst cones effective conditions did not revealed this critical situation.

9.5 Field data collection

These evidences have been collected in a series of field data reports. Trough all of them, the ones reporting machines exerted at almost the same conditions were collected together:

- Mechanical drive
- More than 2000 start-up and shutdown cycles
- More than 48000 hours of service
- More than 95% reliability

For all these occurrences (15), have been extracted cone's structural tests, shape measurements and, material reports.

Figure 9.6- Stator Cone Field Measurements

Cone’s temperature measurements through FLIR infrared camera have been performed in order to data match the thermal maps.

9.5.1 Thermography measurements

Thermographic cameras detect radiation in the infrared range of the electromagnetic spectrum (roughly 900–14,000 nanometres or 0.9–14 µm) and produce images of that radiation. Since infrared radiation is emitted by all objects based on their temperatures, according to the black body radiation law, thermography makes it possible to "see" one's environment with or without visible illumination. The amount of radiation emitted by an object increases with temperature; therefore thermography allows one to see variations in temperature.

A thermographic camera, sometimes called a FLIR (Forward Looking Infrared), or an infrared camera less specifically, is a device that forms an image using infrared radiation, similar to a common camera that forms an image using visible light. Instead of the 450–750 nanometre range of the visible light camera, infrared cameras operate in wavelengths as long as 14,000 nm (14 µm).

Thermographic measurements have been taken for sake of cone’s thermal map construction and verification.

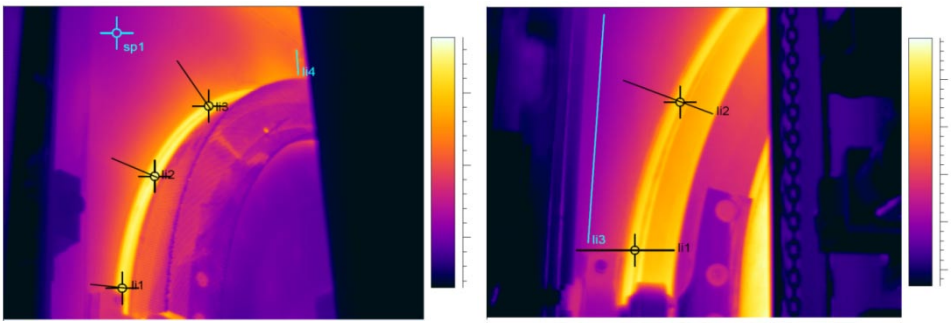

Figure 9.7- Stator cone thermographic maps

9.5.2 Geometrical shape measurements

Field data measurements are here briefly described. Using a scanning laser vibrometer, measurements of exerted cones have been taken in order to estimate residual deformation.

Particular care was taken for flanges planarity and circularity together with cone's ovalization.

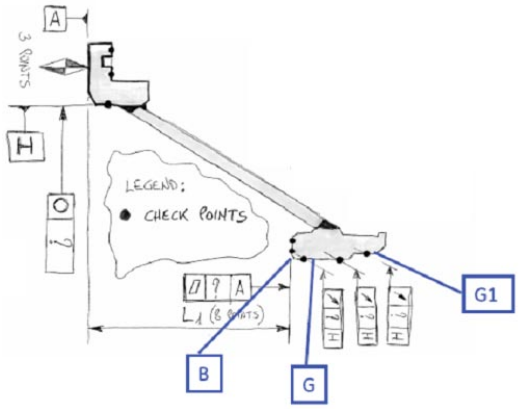

Figure 9.8- Stator Cone Measuremnt Points

The report of the previous described measurements campaign was reproduced in radar plots in order to evaluate deviations from design requirements. In the following pictures are reported as example ovalization measurements and out of plane rear flange measurements.

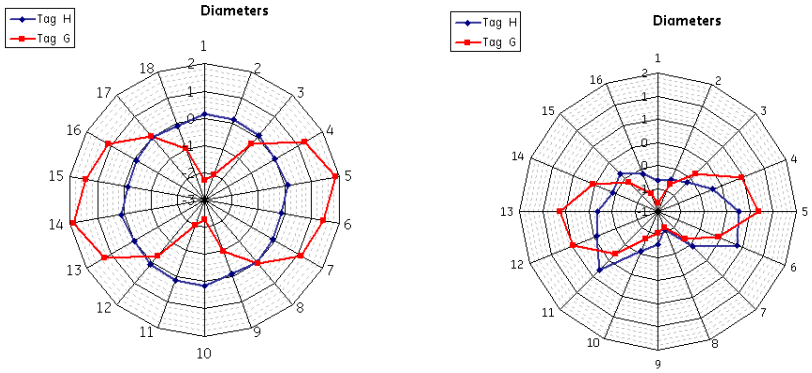

Figure 9.9- Stator Cone Ovalization

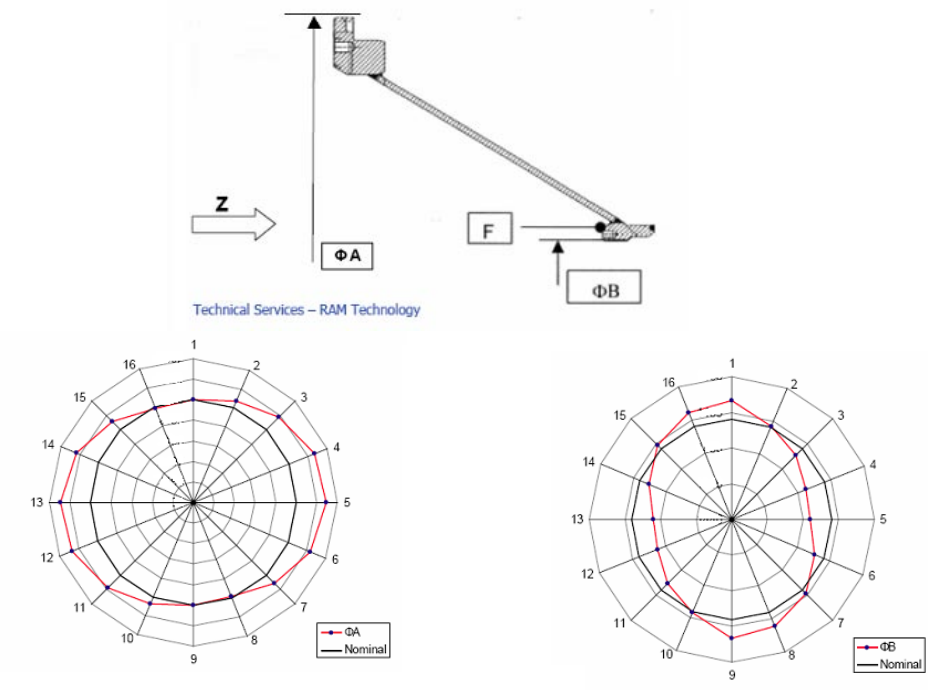

Figure 9.10- Stator Cone Rear Flange Out of Plane

Together with the field data measurements, a micro-crystallographic analysis has been performed in order to evaluate real conditions of the exerted cone. This information was necessary to establish if cone's calculated life is in line with real condition of the exerted cone.

According to the analysis results, fatigue and creep cone's conditions are not in line with calculation predictions.

The following pictures are extracted from metallographic reports from DNV, using TEM techniques.

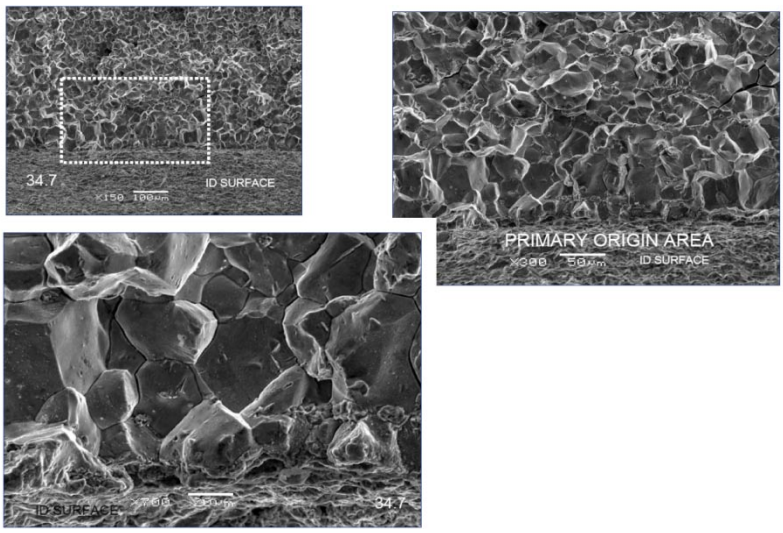

Figure 9.11- Crystallographic analysis - Fatigue

The morphology of all analyzed zones reveals that there are some zones in which we can find inter granular fatigue. (Low cycle fatigue)

Some other zones reveals, instead, first stage creep.

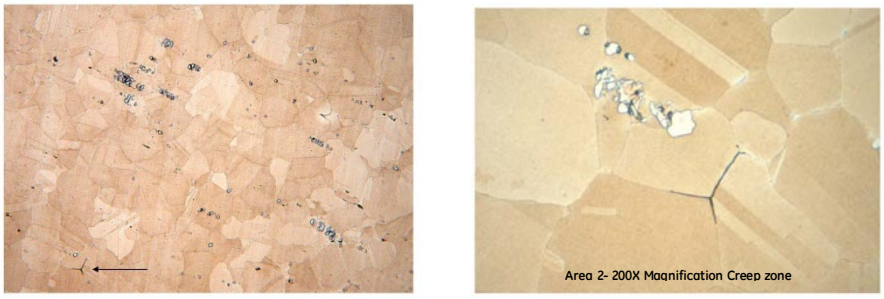

Figure 9.12- Crystallographic analysis - Creep

The resulting report reveals that though the structure has got limited zones in which inter granular fatigue took place and other high temperature zones with creep nucleation, its condition are not in line with an expected steel structure at the end of its duty life.

9.5.3 Mission definition

A mission has been defined based on field data too. Each GE Oil&Gas Turbine is remotely monitored in order to keep under control all the vital parameters of the Gas Turbine. Pressures and temperatures have been recorded in different conditions. Normal start-up and shutdown, hot restart and emergency trip have been considered. In a more detailed way:

- Cold Start-up + SS + Shut-down (ESD)
- Cold Start-up + SS + Trip (TRIP)
- Hot Restart 5000 sec (HRS-1.2)
- Hot Restart 10000 sec (HRS-1.3)

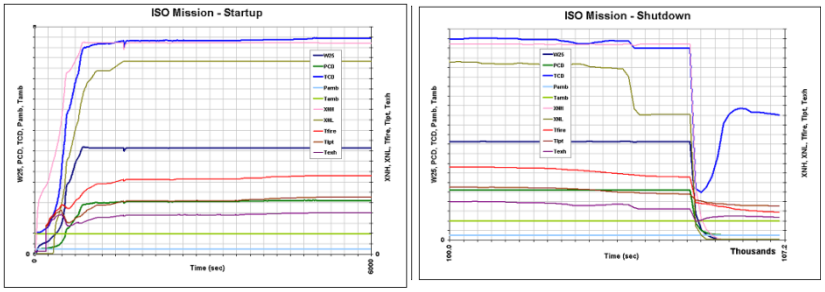

Figure 9.13- Start up and shut down missions

After probabilistic considerations a typical mission has been built. On these data a transient and steady state profiles have been set-up for the analyses.

9.5.4 FEM modelling

A complex 3D model has been developed to simulate system behaviour; a dummy model of the gas generator has been modelled and linked to the power turbine through a detailed model of the transition piece.

The following picture shows a isometric layout of the fem model. In all the following pictures, dimensions, plot and details have been omitted because they are intellectual property and GE proprietary information.

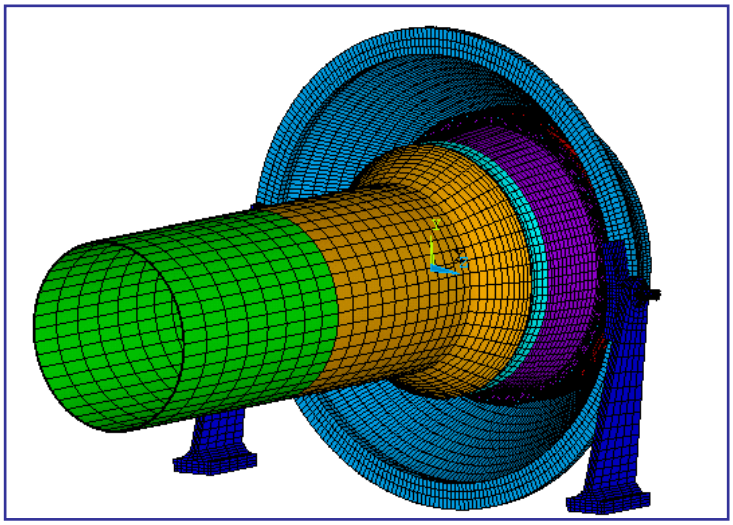

Figure 9.14- FE model Layout

Stator components: 1st stage casing, 2nd stage casing and support cone have been modelled in detail, with all their bolt and nut connections through beams and contact-target elements. Support legs have been modelled and connected to the stator components using friction and contact elements. Shrouds (1st and 2nd stage) have been connected through contacts and gap elements.

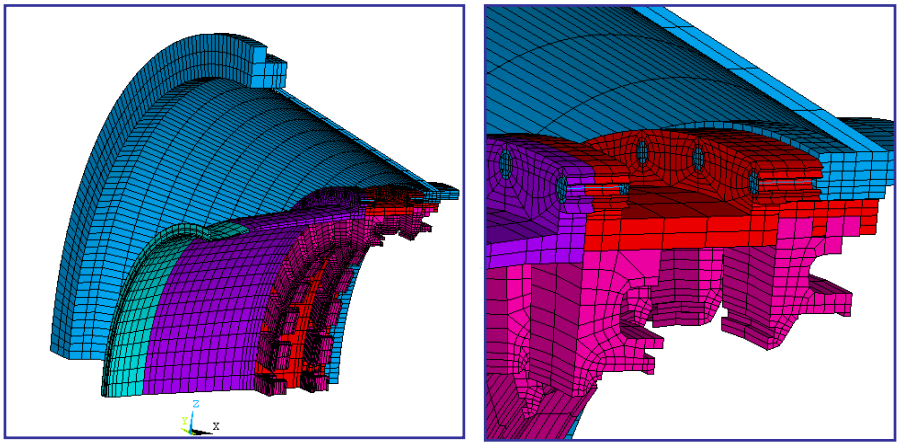

Figure 9.15- FE model Details Stator components and bolted flanges

In the same way, have been modelled nozzles and diaphragm.

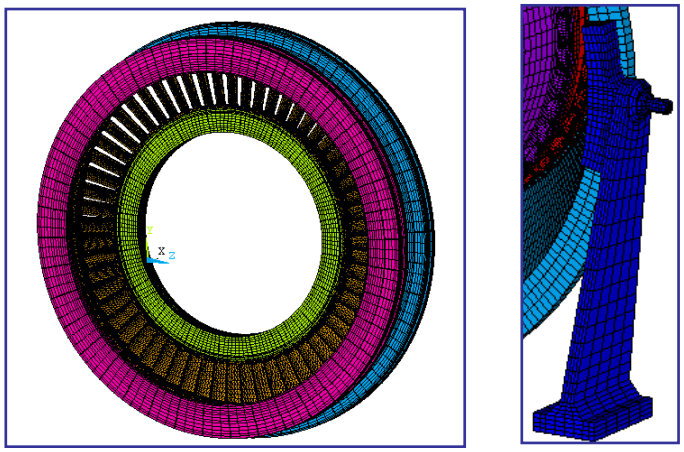

Figure 9.16- FE model Nozzles and legs

In the following bullets, a brief description of the FE model details:

NODES: 261248 ELEMENTS: 396832

- Gas Generator elements: SHELL and PIPE at imposed stiffness.
- Bolt simulated with SOLID and contact elements
- Flange contacts and other connections: CONTACT e TARGET
- Rigid sliding parts CONTAC12

9.5.4.1 Boundary Conditions

Boundary conditions have been applied to the meshed model in order to reproduce system layout, constraint equations have been properly applied together with supports on gas generator and fixed points on legs base. Thermal map extracted and data matched with field data have been applied to the metal skin. GE Oil&Gas CFD team has provided thermal exchange coefficients, aerodynamic forces on nozzles and shrouds have been provided by GE Oil&Gas AERO team, pressures in the flow-path from GE Oil&Gas Secondary Flows team.

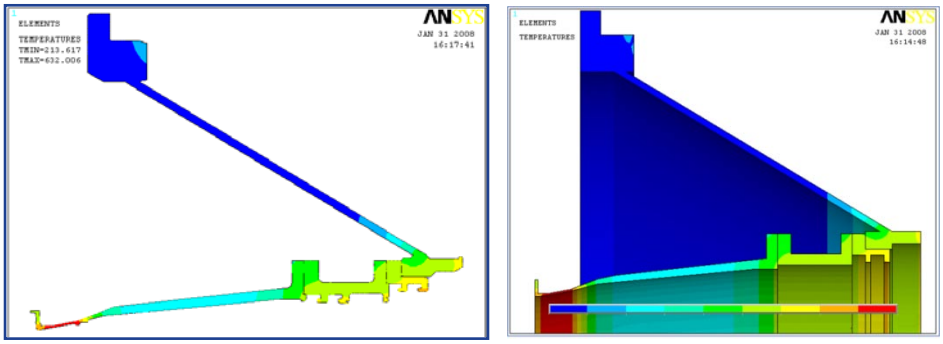

Figure 9.17- Stator cone Ansys thermals

9.5.4.2 Loads

Loads on the system have been applied thanks to data obtained from the Installation Design Manual of the gas generator. From this manual, gas generator thrust and pressures have been extracted. From the test data (from which we obtained turbine shell loads), rotor and casing part radiation and forces.

Gravity load has been applied too.

9.5.5 Data-match and verification

All the inserted data have been applied on the FEM model. A thermal analysis has been performed in order to compare field data results with the ones obtained from Pthermal (thermal maps inside each component) and Ansys Thermal result file (analysis for conduction, convection and radiation of the whole system).

A first, qualitative analysis of the results has been carried out in order to evaluate results data. Cone out of roundness and flange's planarity have been evaluated.

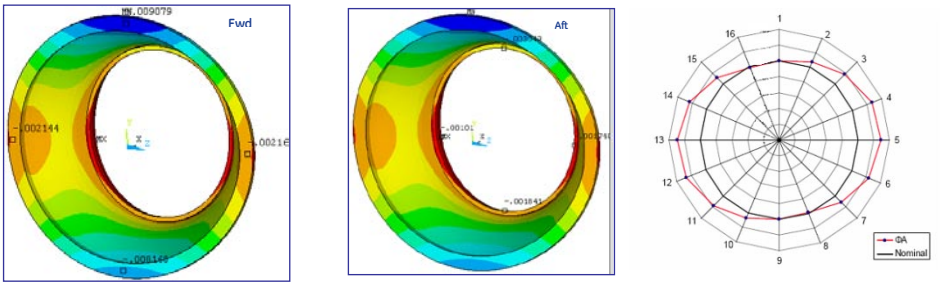

Figure 9.18- Predicted and field residual deformation - Axial

The FE model seems to well reproduce the exerted conditions.

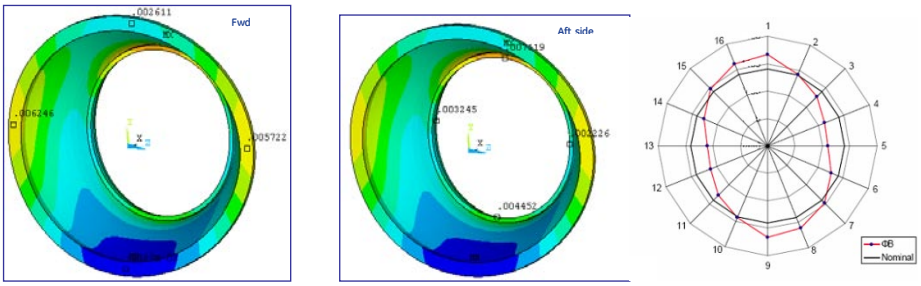

Figure 9.19- Predicted and field residual deformation - Radial

9.6 Results evaluation

This part of the work shows and evaluates the quality of results and the differences between the standard solution results and the elasto-visco-plastic one.

Each result has been valuated reading into the .rst file generated by the non-linear solution. The definition of each curve depends from the load steps and the sub step frequency of savings.

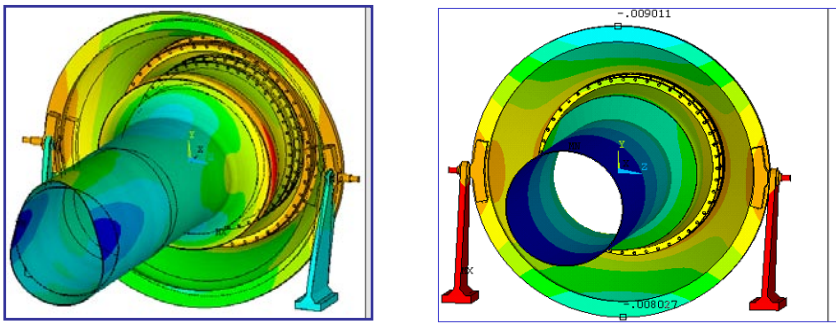

Figure 9.20- Stator cone Axial and Radial displacements

9.6.1 Stress cycles Stabilization and Relaxation

The mission data in this part have been identified with letters. The second part of the result checking was the evaluation of the new capacities of the material model. Investigating on the phenomenon that the new introduced material is able to describe.

The mission steady state points at start-up and shut down have been identified with A and B letters. The first investigated things where material stabilization cycle in a critical point, and stress relaxation.

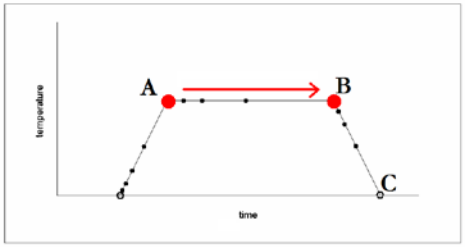

Figure 9.21- Misson schematization

To investigate on the first point, stress and strain histories have been taken from POST26 data (time-history post processing). Then resulting data have been plotted on a sigma-epsilon diagram in order to evaluate stabilization.

The results, showed in the picture down, seem to represent cycle stabilization at the 10th cycle. In this case too, results are almost in accordance with expected data.

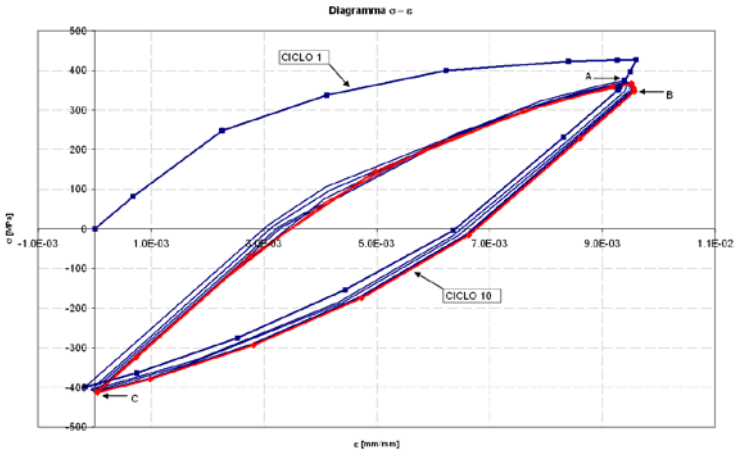

Figure 9.22- Punctual stress stabilization

The following graph shows the same stabilization points in a time-stress plot.

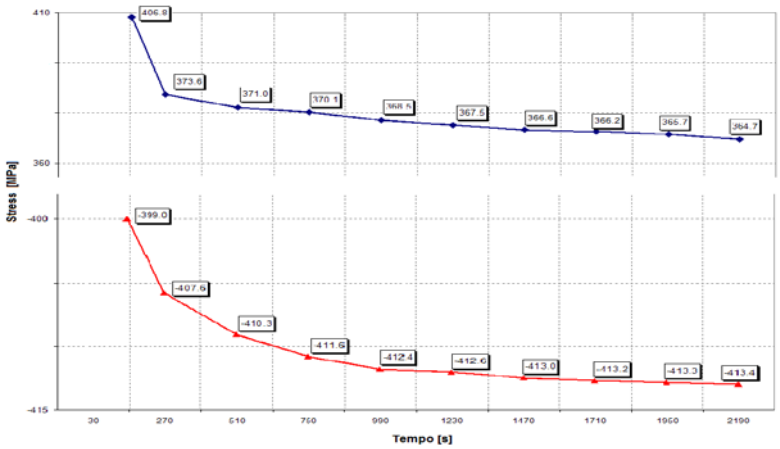

Figure 9.23- Cyclic stress stabilization

The last plot shows, instead, the stress delta between a cycle and the next one, until the 10th.

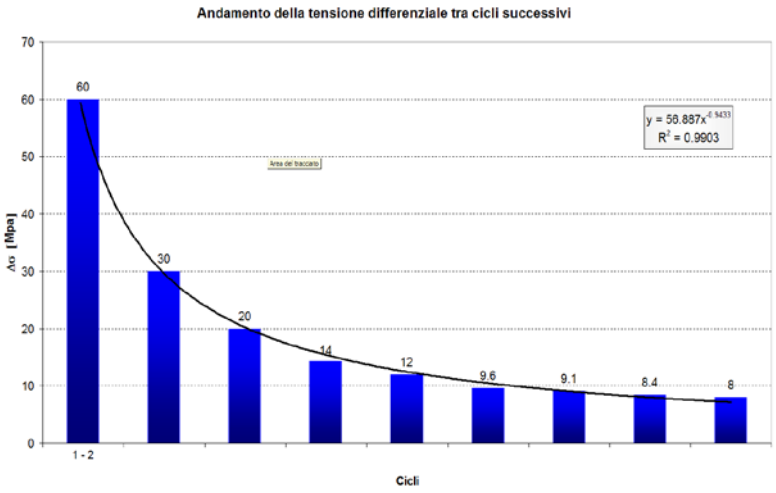

Figure 9.24- Stress Delta between cycles

The following plots show the results of the stress relaxation that the components has during its steady state condition.

The two stress contour plots show the same structure, in the same cycle at the end of the start up sequence and before the shut down procedure. In this specific case 48 hours of duty cycle were considered.

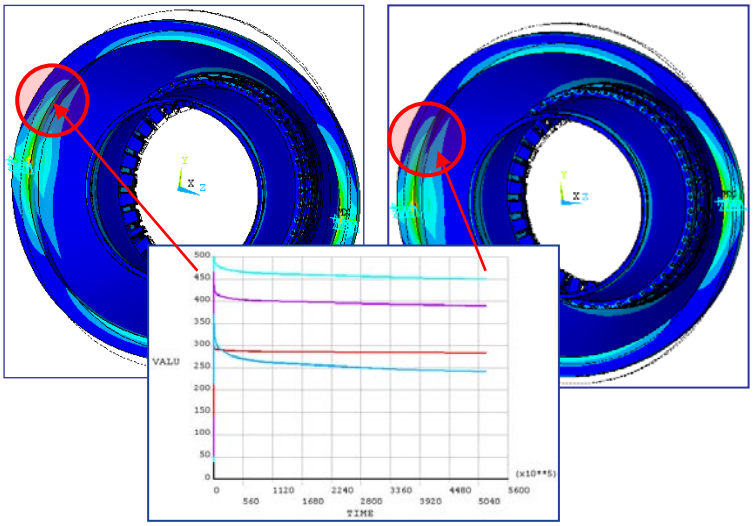

Figure 9.25- Stress Relaxation within a cycle

Previous material models were not able to show stress relaxation.

Elasto-plastic models always show the same stress if loads and boundary conditions remains the same. This is not the case of this time dependent material model.

9.7 Creep and Fatigue-Life Calculations

Once applied the modified coefficient to SUSAN and PROPLife, obtained the result file from the ANSYS calculation, creep damage and life calculations have been performed.

In the following page are showed some of the results obtained.

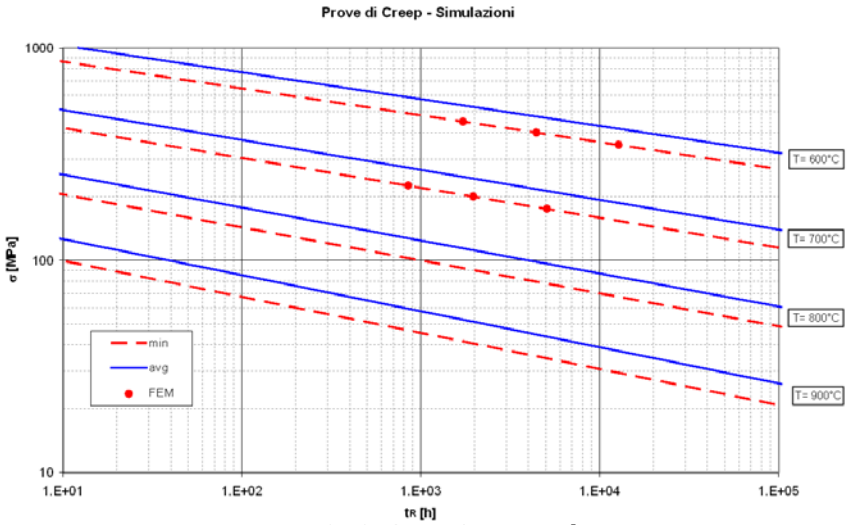

Figure 9.26- Creep Strain results

Creep life and fatigue life have been determined in order to compare life of the component with the previous calculations. The results have been arranged in Wholer curves in order to estimate life of the component in the case of non-linear interaction between creep and fatigue.

In the graph below, at different temperatures and in logarithmic scale, are shown the points in which, the FEM calculated life has been obtained.

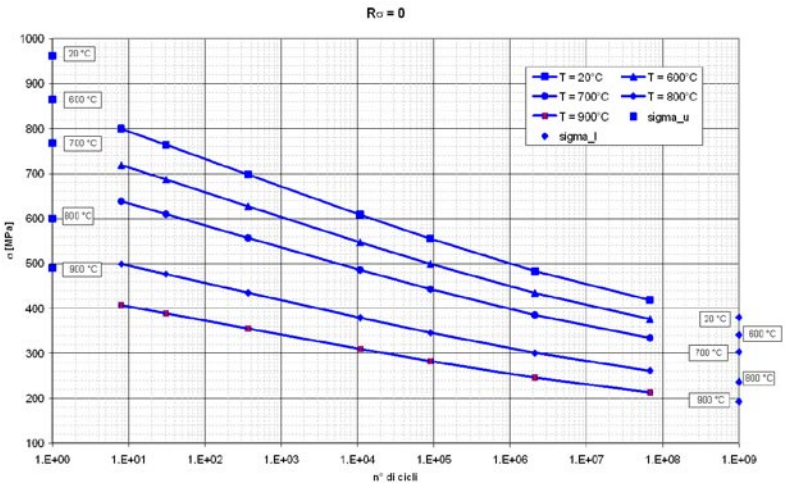

Figure 9.27- Wholer Curves

Joining all these results in only one chart, life of the component has been recalculated according to the new constitutive laws.

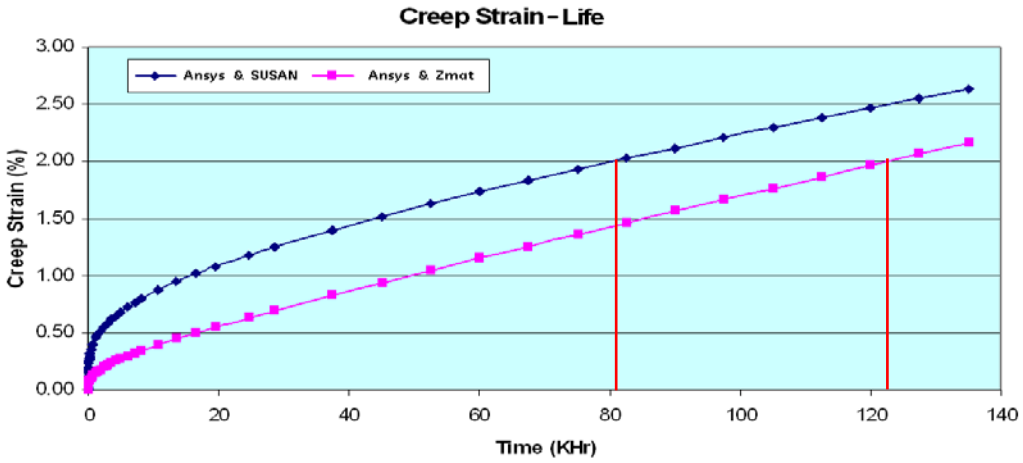

Figure 9.28- Life calculations

From this graph we can conclude that life of this component, if calculated through a non-linear interaction mechanism between fatigue and creep, will be augmented of almost 33%.

10 Correlated Activities

In this last part of the present work, are briefly illustrated all the correlated activities relating this procedures. They've been divided into activities that are on their way to completion, and the other ones that are to be taken.

10.1 Ongoing activities

In this paragraph are illustrated activities that are actually taking place in order to complete. The procedure itself, even if has been validated, since has the intention to be entered in the process as a New Product Introduction in the GE Oil&Gas procedural analysis system, has to pass further steps in order to complete the process. One of these steps are the CPU Time analysis evaluation and Failure Modes and Effects Analysis.

10.1.1 CPU Time estimation

An estimation of the CPU Time is made in order to evaluate machine time increment due to the contemporary memory occupation of the software running in parallel. In the following table can be shown a brief resume of the over mentioned time.

TIME [s]		File dimensions
MEAN VALUES	CPU TIME	FILE *.rst
First cycle	57000 s = 16 hours	440 [1]
Other Cycles	38000 s = 10	370 [2]
Total (10 cycles)	106 hours	-----

Table 10.1- CPU Time

10.1.2 FMEA Analysis

At the end of the Tollgate process, a Failure Modes and Effect Analysis (FMEA) have to be performed in order to evaluate risks and take all the necessary actions to reduce them. A brainstorming activity has already been performed, critical points have been found and each risk has been set.

At the end of the validation process each of the crucial risk has been mitigated, some minor issues left points have been completed too. No residual risk, through the ones individuated, has been left unresolved.

10.1.3 Life extension program

A program to recalculate life of gas turbine components has been set up.

Based on the results of such activity, an evaluation to use this software to simulate and recalculate life of a component is taking place.

Due to Company policies no further information can be actually provided.

10.2 Planned activities

Automatic procedure for gathering elasto-visco-plastic coefficients within SUSAN and PROPLife has been planned. This activity will take place in GRC (General Electric Research Centre).

Another activity will have as main scope the usage of this procedure to simulate rotor components repairing processes (wheels, blades, etc.)

Conclusions

The problem of developing a continuum micromechanical-based theory which could be used as an engineering tool both in analysis and in computer-aided design of materials, is a topical and still unsolved material science problem. Attempts to construct such a theory are faced with the difficulties in describing the microscopic structure of materials in terms of continuum mechanics. When load is applied, the elastic and inelastic deformation of materials occurs in most cases not homogeneously, but reveals fluctuations on various space scales. This heterogeneity plays a key role in determining the mechanical properties of materials. This work is collocated in the framework of a consolidated experience acquired from the DIAS and AELAB at Department of Aerospace Engineering of University of Naples joined to the ones coming from AVIO Aerospace Propulsion S.p.A. Research and Development Department and General Electric Oil&Gas Machine Design – Gas Turbine Engineering. The present work wants to give a contribution to the capacity to predict life of a structural component. More in detail, conscious that the simple superimposing of creep and fatigue damage is too conservative for actual industrial needs, this work wants to help optimization and design of gas turbine components. For this reason, a procedure to study and implement creep and fatigue damage non-linear interaction has been designed and validated. As expected, being able to implement such a material model, allowed user to be able to describe through finite element modelling, material specific behaviours such as stress relaxation and cycle stabilization. Moreover, being able to insert the new calculated material coefficients into a fatigue and creep damage calculation tools, life prediction of a component has been significantly increased.

References and Bibliography

1. Benallal, A., Le Gallo, P., Marquis, D., 1989. An experimental investigation of cyclic hardening of 316 stainless steel and of 2024 aluminium alloy under multiaxial loadings. Nuclear Engineering and Design 114, 345–353.

2. Bertram, A., 1998. An alternative approach to finite plasticity based on material isomorphisms. International Journal of Plasticity 52, 353–374.

3. Bertram, A., 2003. Finite thermoplasticity based on isomorphisms. International Journal of Plasticity 19, 2027–2050.

4. Bever, M., Holt, D., Titchener, A., 1973. The Stored Energy of Cold Work. Progress in Materials Science, vol. 17. Pergamon, Oxford.

5. Bodner, S.R., Lindenfeld, A., 1995. Constitutive modelling of the stored energy of cold work under cyclic loading. European Journal of Mechanics A – Solids 14, 333–348.

6. Bruhns, O., Lehmann, T., Pape, A., 1992. On the description of transient cyclic hardening behaviour of mild steel CK15. International Journal of Plasticity 8, 331–359.

7. Bucher, A., Go¨rke, U.-J., Kreißig, R., 2004. A material model for finite elasto-plastic deformations considering a substructure. International Journal of Plasticity 20, 619–642.

8. Casey, J., Naghdi, P., 1980. A remark on the use of the decomposition F = FeFp in plasticity. Journal of Applied Mechanics 47, 672–675.

9. Chaboche, J.L., 1977. Visco-plastic constitutive equations for the description of cyclic and anisotropic behaviour of metals. Bulletin de L'Academie Polonaise des Sciences 25, 33–41.

10. Chaboche, J.-L., 1993a. Cyclic visco-plastic constitutive equations, Part I: A thermodynamically consistent formulation. Journal of Applied Mechanics 60, 813–821.

11. Chaboche, J.-L., 1993b. Cyclic visco-plastic constitutive equations, Part I: A thermodynamically consistent formulation, Part II: Stored energy – comparison between models and experiments. Journal of Applied Mechanics 60, 813–828.

12. Chaboche, J., 1996. Unified cyclic visco-plastic constitutive equations: development, capabilities, and thermodynamic framework. In: Krausz, A., Krausz, K. (Eds.), Unified Constitutive Laws of Plastic Deformation. Academic Press, New York, pp. 1–68.

13. Chaboche, J., Lemaitre, J., 1990. Mechanics of Solid Materials. Cambridge Press, Cambridge, New York.

14. Chrysochoos, A., Maisonneuve, O., Martin, G., Caumon, H., Chezeaux, J., 1989. Plastic and dissipated work and stored energy. Nuclear Engineering and Design 114, 323–333.

15. Coleman, B., Gurtin, M., 1967. Thermodynamics with internal state variables. Journal of Chemical Physics 47, 597–613.

16. Coleman, B., Noll, W., 1963. The thermodynamics of elastic materials with heat conduction and viscosity. Archive for Rational Mechanics and Analysis 13, 167–178.

17. Coleman, B., Owen, D., 1975. On thermodynamics and elastic–plastic materials. Archive for Rational Mechanics and Analysis 59, 25–51.

18. Deseri, L., Mares, R., 2000. A class of viscoelastoplastic constitutive models based on the maximum dissipation principle. Mechanics of Materials 32, 389–403.

19. Dettmer, W., Reese, S., 2004. On the theoretical and numerical modelling of Armstrong–Frederick kinematic hardening in the finite strain regime. Computer Methods in Applied Mechanics and Engineering 193, 87–116.

20. Eckart, C., 1948. The thermodynamics of irreversible processes IV: the theory of elasticity and anelasticity. Physical Review 73, 373–382.

21. Flory, P., 1961. Thermodynamic relations for high elastic materials. Transactions of the Faraday Society 57, 829–838.

22. Germain, P., Nguyen, Q.S., Suquet, P., 1983. Continuum thermodynamics. Transaction of the ASME 50, 1010–1020.

23. Glaser, S., 1991. Berechnung gekoppelter thermomechanischer Prozesse. Ph.D. Thesis, Institut fu¨ r Statik und Dynamik, Bericht Nr. 91/3, Universita¨t Stuttgart.

24. Green, A.E., Naghdi, P.M., 1965. A general theory of an elastic–plastic continuum. Archive for Rational Mechanics and Analysis 18, 251–281.

25. Green, A.E., Naghdi, P.M., 1971. Some remarks on elastic–plastic deformation at finite strain. International Journal of Engineering Science, 1219–1229.

26. Green, A.E., Naghdi, P.M., 1978. The second law of thermodynamics and cyclic processes. Journal of Applied Mechanics 45, 487–492.

27. Gurtin, M., Anand, L., 2005. The decomposition F = FeFp, material symmetry, and plastic irrotationality for solids that are isotropic-visco-plastic or amorphous. International Journal of Plasticity 21, 1686–1719.

28. Hairer, E., 2001. Geometric integration of ordinary differential equations on manifolds. BIT Numerical Mathematics 41 (5), 996–1007.

29. Hairer, E., Lubich, C., Wanner, G., 2002. Geometric Numerical Integration. Springer, Berlin.

30. Ha˚kansson, P., Wallin, M., Ristinmaa, M., 2005. Comparison of isotropic hardening and kinematic hardening in thermoplasticity. International Journal of Plasticity 21, 1435–1460.

31. Hartmann, S., Lu¨ hrs, G., Haupt, P., 1997. An efficient stress algorithm with application in visco-plasticity and plasticity. International Journal for Numerical Methods in Engineering 40, 991–1013.

32. Haupt, P., 2002. Continuum Mechanics and Theory of Materials. Springer, Berlin.

33. Haupt, P., Kamlah, M., 1995. Representation of cyclic hardening and softening properties using continuous variables. International Journal of Plasticity 11, 267–291.

34. Haupt, P., Lion, A., 1995. Experimental identification and mathematical modelling of visco-plastic material behavior. Continuum Mechanics and Thermodynamics 7, 73–96.

35. Haupt, P., Tsakmakis, C., 1989. On the application of dual variables in continuum mechanics. Continuum Mechanics and Thermodynamics 1, 165–196.

36. Haupt, P., Helm, D., Tsakmakis, C., 1997. Stored energy and dissipation in thermovisco-plasticity. ZAMM 77, S119–S120.

37. Helm, D., 1998. Experimentelle Untersuchung und pha¨nomenologische Modellierung thermomechanischer Kopplungseffekte in der Metallplastizita¨t. In: Hartmann, S., Tsakmakis, C. (Eds.), Aspekte der Kontinuumsmechanik.

38. Festschrift zum 60. Geburtstag von Professor Peter Haupt. Berichte des Instituts fu¨r Mechanik, Institut fu¨r Mechanik der Universita¨t Kassel, pp. 81–105.

39. Helm, D., 2001. Formgeda¨chtnislegierungen: Experimentelle Untersuchung, pha¨nomenologische Modellierung und numerische

Simulation der thermomechanischen Materialeigenschaften. Ph.D. Thesis, Institut fu¨r Mechanik, Universita¨t Gesamthochschule Kassel, Kassel.

40. Hibbitt, Karlsson & Sorensen, Inc., 2002a. ABAQUS Theory Manual. Version 6.3, Hibbitt, Karlsson & Sorensen, Inc.

41. Hibbitt, Karlsson & Sorensen, Inc., 2002b. ABAQUS/Explicit User's Manual. Version 6.3, Hibbitt, Karlsson & Sorensen, Inc.

42. Hill, R., 1950. The Mathematical Theory of Plasticity. Oxford University Press, Oxford.

43. Hohenemser, K., Prager, W., 1932. U¨ ber die Ansa¨tze der Mechanik isotroper Kontinua. ZAMM 12, 216–226.

44. Jansohn, W., 1997. Formulierung und Integration von Stoffgesetzen zur Beschreibung großer Deformationen in der Thermoplastizita¨t und -viskoplastizita¨ t. Ph.D. thesis, Institut fu¨ r Materialforschung, Forschungszentrum Karlsruhe.

45. Jou, D., Casas-Va´zquez, J., Lebon, G., 1996. Extended Irreversible Thermodynamics. Springer, Berlin/Heidelberg/New York.

46. Kamlah, M., Haupt, P., 1998. On the macroscopic description of stored energy and self-heating during plastic deformations. International Journal of Plasticity 13, 893–911.

47. Kamlah, M., Tsakmakis, C., 1999. Use of isotropic thermoelasticity laws in finite deformation visco-plasticity models. Continuum Mechanics and Thermodynamics 36, 73–88.

48. Khan, A.S., Jackson, K.M., 1999. On the evolution of isotropic hardening with finite plastic deformation. Part I: compression/tension loading of OFHC copper cylinders. International Journal of Plasticity 15, 1265–1275.

49. Krempl, E., 1979. An experimental study of room-temperature rate-sensitivity, creep and relaxation of AISI Type 304 stainless steel. Journal of Mechanics and Physics of Solids 27, 363–375.

50. Krempl, E., 1987. Models of visco-plasticity. Some comments on equilibrium (back) stress and drag stress. Acta Mechanica 69, 25–42.

51. Krempl, E., Khan, F., 2003. Rate (time)-dependent deformation behavior: an overview of some properties of metals and solid polymers. International Journal of Plasticity 19, 1069–1095.

52. Kro¨ner, E., 1958. Kontinuumstheorie der Versetzungen und Eigenspannungen. Springer, Berlin.

53. Kro¨ner, E., 1960. Allgemeine Kontinuumstheorie der Versetzungen und Eigenspannungen. Archive for Rational Mechanics and Analysis 4, 273–334.

54. Lee, E., 1969. Elastic–plastic deformation at finite strains. Journal of Applied Mechanics 36, 59–67.

55. Lee, E., Liu, D., 1967. Finite-strain elastic–plastic theory with application to plane-wave analysis. Journal of Applied Physics 38, 19–27.

56. Lehmann, T., 1983. On a Generalized Constitutive Law in ThermoplasticityPlasticity Today. Elsevier, Amsterdam.

57. Lehmann, T., Blix, U., 1985. On the coupled thermo-mechanical process in the necking problem. International Journal of Plasticity 1, 175–188.

58. Lion, A., 1994. Materialeigenschaften der Viskoplastizita¨ t, Experimente, Modellbildung und Parameteridentifikation. Ph.D. Thesis, Institut fu¨ r Mechanik, Bericht Nr. 1/1994, Universita¨ t Gesamthochschule Kassel.

59. Lion, A., 2000. Constitutive modelling in finite thermovisco-plasticity: a physical approach based on nonlinear rheological models. International Journal of Plasticity 16, 469–494.

60. Liu, I.-S., 2002. Continuum Mechanics. Springer, Berlin.

61. Lubliner, J., 1985. A model of rubber viscoelasticity. Mechanics Research Communications 12, 93–99.

62. Lubliner, J., 1990. Plasticity Theory. Macmillan Publishing Company, New York, London.

63. Lu¨ hrs, G., Hartmann, S., Haupt, P., 1997. On the numerical treatment of finite deformations in elastovisco-plasticity. Computer Methods in Applied Mechanics and Engineering 144, 1–21.

64. Mandel, J., 1972. Plasticite´ Classique et Visco-plasticite´. CISM Courses, vol. 97. Springer, Berlin.

65. Maugin, G., Muschik, W., 1994. Thermodynamics with internal variables Part I. General concepts. Part II. Applications. Journal of Non-Equilibrium Thermodynamics 19, 250–289.

66. Meixner, J., Reik, H., 1959. Thermodynamik der irreversiblen Prozesse. In: Flu¨gge, S. (Ed.), Handbuch der Physik, Band III/2. Springer, Berlin.

67. Miehe, C., 1988. Zur numerischen Behandlung thermomechanischer Prozesse. Ph.D. Thesis, Fachbereich Bauingenieur- und Vermessungswesen der Universita¨t Hannover.

68. Miehe, C., 1998. A constitutive frame of elastoplasticity at large strains based on the notion of a plastic metric. International Journal of Solids Structures 35, 3859–3897.

69. Miehe, C., Stein, E., 1992. A canonical model of multiplicative elasto-plasticity: formulation and aspects of the numerical implementation. European Journal of Mechanics A – Solids 11, 25–43.

70. Mollica, F., Rajagopal, K.R., Srinivasa, A.R., 2001. The inelastic behavior of metals subject to loading reversal. International Journal of Plasticity 17, 1119–1146.

71. Mu¨ller, I., Ruggeri, 1998. Rational Extended Thermodynamics. Springer, Berlin/Heidelberg/New York.

72. Oliferuk, W., Gadaj, S., Grabski, W., 1985. Energy storage during tensile deformation of Armco iron and austenitic steel. Materials Science and Engineering 70, 131–141.

73. Perzyna, P., 1963. The constitutive equations for rate sensitive plastic materials. Quarterly of Applied Mathematics 20, 321–332.

74. Pinsky, P., Ortiz, M., Taylor, R., 1983. Operator split methods in the numerical solution of the finite deformation elastoplastic dynamic problem. Computer and Structures 17, 345–359.

75. Rajagopal, K.R., Srinivasa, A.R., 1998a. Mechanics of the inelastic behavior of materials – Part 1: Theoretical underpinnings. International Journal of Plasticity 14, 945–967.

76. Rajagopal, K.R., Srinivasa, A.R., 1998b. Mechanics of the inelastic behavior of materials – Part 2: Inelastic response. International Journal of Plasticity 14, 969–995.

77. Rosakis, P., Rosakis, A.J., Ravichandran, G., Hodowany, J., 2000. A thermodynamic internal variable model for the partition of plastic work into heat and stored energy in metals. Journal of the Mechanics and Physics of Solids 48, 581–607.

78. Scheidler, M., Wright, T., 2001. A continuum framework for finite visco-plasticity. International Journal of Plasticity 17, 1033–1085.

79. Simo, J., 1988. A framework for finite strain elastoplasticity based on maximum plastic dissipation and the multiplicative decomposition: Part I:

Continuum formulation. Computer Methods in Applied Mechanics and Engineering 66, 199–219.

80. Simo, J., 1993. Recent developments in the numerical analysis of plasticity. In: Stein, E. (Ed.), Progress in Computational Analysis of Inelastic Structures, CISM Report No. 321, Udine, Springer Verlag, Wien, New York, pp. 115–173.

81. Simo, J., Hughes, T., 1998. Computational Inelasticity. Springer.

82. Simo, J., Miehe, C., 1992. Associative coupled thermoplasticity at finite strains formulation, numerical analysis and implementation. Computer Methods in Applied Mechanics and Engineering 98, 41–104.

83. Simo, J., Pister, K., 1984. Remarks on rate constitutive equations for finite deformation problems. Computer Methods in Applied Mechanics and Engineering 46, 201–215.

84. Simo, J., Taylor, R., Pister, K., 1985. Variational and projection methods for the volume constraint in finite deformation elasto-plasticity. Computer Methods in Applied Mechanics and Engineering 51, 177–208.

85. Taylor, G., Quinney, M., 1934. The latent energy remaining in a metal after cold working. Proceedings of the Royal Society of London A 143, 307.

86. Truesdell, C., 1984. Rational Thermodynamics, second ed. Springer, New York, Berlin.

87. Truesdell, C., Noll, W., 1965. The Non-Linear Field Theories of Mechanics. In: Flugge, S. (Ed.), Handbuch der Physik, Band III/3. Springer, Berlin.

88. Tsakmakis, C., 1996. Kinematic hardening rules in finite plasticity Part I: a constitutive approach. Continuum Mechanics and Thermodynamics 8, 215–231.

89. Tsakmakis, C., 1998. Energiehaushalt des elastisch-plastischen Ko¨ rpers. Unpublished paper presented in the symposium: Aspekte der Kontinuumsmechanik und Materialtheorie. Kassel, 14 April.

90. Tsakmakis, C., 2004. Description of plastic anisotropy effects at large deformations. Part I: restrictions imposed by the second law and the postulate of Il'iushin. International Journal of Plasticity 20, 167–198.

91. Tsakmakis, C., Willuweit, A., 2003. Use of the elastic predictor–plastic corrector method for integrating finite deformation plasticity laws. In: Hutter, K., Baaser, H. (Eds.), Deformation and Failure in Metallic Materials. Springer, Berlin, Heidelberg, New York, pp. 79–108.

92. von Mises, R., 1913. Mechanik der festen Ko¨rper im plastisch-deformablen Zustand. Go¨ ttinger Nachrichten mathematisch-physikalischer Klasse, 582–592.

93. von Mises, R., 1928. Mechanik der plastischen Forma¨nderungen von Kristallen. ZAMM 8, 161–185.

94. Wallin, M., Ristinmaa, M., 2005. Deformation gradient based kinematic hardening model. International Journal of Plasticity 21, 2025–2050.

95. Weber, G., Anand, L., 1990. Finite deformation constitutive equations and a time integration procedure for isotropic, hyperelastic-visco-plastic solids. Computer Methods in Applied Mechanics and Engineering 79, 173–202.

96. Wriggers, P., Miehe, C., Kleiber, M., Simo, J., 1992. On the coupled thermomechanical treatment of necking problems via finite element methods. International Journal for Numerical Methods in Engineering 33, 869–883.

97. Ziegler, H., 1963. Some extremum principles in irreversible thermodynamics with applications to continuum mechanics. In: Sneddon, I.N., Koiter, W. (Eds.), Progress in Solid Mechanics, vol. IV. North-Holland, Amsterdam, pp. 93–193.

98. Ziegler, H., 1977. An Introduction to Thermomechanics. North-Holland, Amsterdam.

99. Metals Handbook 9th edition, “Mechanical Testing”, vol.8, ASM, 1985.

100. Sims C.T., Hagel W.C. “The Superalloys”, Wiles, New York, 1972.

101. Aerospace Materials Specification AMS – 5662E.

102. Sjoberg G., Ingesten N.G. “Grain Boundary □-Phase Morphologies, Carbides and Notch Rupture Sensitivity of Cast Alloy 718”, in: Superalloys 718, 625 and Various Derivatives. Loria A. et al., The Minerals, Metals and Materials Society, 1991.

103. Srinivas S., Satyanarayana D.V.V., Gopikrishna D., Pandey M.C. “Investigation on notch embrittlement of a Ni-base superalloy”, Scripta Metallurgica et Materialia, 32,1145-1148, 1995.

104. Brooks J.W., Bridges P.J. “Metallurgical Stability of Inconel Alloy *718”*, in: Superalloys 1988, The Metallurgical Society, 1988.

105. E.M. Arruda and M.C. Boyce, \Evolution of Plastic Anisotropy in Amorphous Polymers During Finite Straining," Int. J. Plasticity 9 697-720 (1993).

106. T.F. Back. “A survey of evolution strategies." In R.K. Belew and L.B.Booker, editors, Proc. of the 4th International Conference on Genetic Algorithms, volume I, pages 2{9, USA, Morgan Kauffmann (1991).

107. Belytschko, W.K. Liu, B. Moran, Nonlinear Finite Elements for Continua and Structures, John Wiley & Sons (2000).

108. J. Bonet and R.D.Wood Nonlinear Continuum Mechanics for Finite Element Analysis Cambridge University Press Cambridge, United Kingdom(1997).

109. M.C. Boyce, D.M. Parks, and A.S. Argon, \Plastic Flow in Oriented Glassy Polymers," Int. J. Plasticity 5 593-615 (1989).

110. M.C. Boyce, E.M. Arruda, “An Experimental and Analytical Investigation of the Large Strain Compressive and Tensile Response of Glassy Polymers," in Mechanics of Plastics and Plastic Composites, e.d. V.K. Stokes, AMD-Vol. 104 ASME, New York, NY (1989).

111. E. Contesti and G. Cailletaud, “Description of Creep-Plasticity Interaction with Non-United Constitutive Equations: Application to Austenitic Stainless Steel," Nuclear Engineering Design 116, 265-280 (1989).

112. G. Cailletaud, “A Micromechanical Approach to Inelastic Behaviour of Metals," Int. J. Plasticity, 8, 55-73 (1992).

113. Cailletaud, P. Pilvin, “Utilisation de modeles polycristallins pour le calcul parallel elements finis" Revue europeenne des elements finis, 515-542, 1994

114. G. Cailletaud and K. Saff, "Study of Plastic/Visco-plastic Models with various Inelastic Mechanisms," Int. J. Plasticity, 10 (1995).

115. D. Croizet, L. M_eric, M. Boussuge G. Cailletaud, “General Formulation of a Plasticity / Visco-plasticity Algorithm in Finite Element," Num. Meth. Eng `92. ed. C. Hirsch et al, Bruxelles, 741-747 (1992).

116. P. Delobelle, P. Robinet, P. Geyer, and P. Boufoux, “A Model to Describe the Anisotropic Visco-plastic Behaviour of Zircaloy-4 Tubes," J. Nuclear Materials 238 135-162 (1996).

117. N. A. Fleck, L. T. Kuhn, and R. M. McMeeking, “Yielding of metal powder bonded by isolated contacts. J. Mech. Phys. Solids, 40, 1139-1162, (1992).

118. A.E. Green and P.M. Naghdi, “A General Theory of Elastic-Plastic Continuum,"Arch. Rat. Mech. Anal. 18, 251-281 (1965).

119. Gur Z. Gurdal R.T. Haftka, \Elements of Structural Optimization" Kluwer Academic Publishers, (1992).

120. H.E. Hjelm, “Yield Surface for Grey Cast Iron Under Biaxial Stress," J. Eng. Mater. Tech 116 148-154 (1994).

121. B.L. Josetson, U. Stigh, and H.E. Hjelm, “A Nonlinear Kinematic Hardening Model for Elastoplastic Deformations in Grey Cast Iron," J. Eng. Mater. Tech, 117 145-149 (1995).

122. P. Ladev_eze, “Sur la Theorie de la Plasticite en Grandes Deformations," ENS-Cachan-LMT Internal Report No. 9 (1980).

123. J. Lemaitre and J-L. Chaboche, Mechanics of Solid Materials, Cambridge University press (1985).

124. Levenberg. “A method for the solution of certain non-linear problems in least squares." Quaterly of Applied Mathematics, 2, 164{168 (1944).

125. A. Miller, “An Inelastic Constutive Model for Monotonic, Cyclic, and Creep Deformation: Part I and II. J. Eng. Mater. Tech, 97-113 (1976).

126. J.J. More. “The levenberg-marquardt algorithm: Implementation and theory." In G.A. Watson, editor, Numerical Analysis Proceedings, Lecture Notes in Mathematics, pages 105-116, Springer Verlag, Berlin, Germany (1977).

127. C. Nagtegaal, “On the Implementation of Inelastic Constitutive Equations with Special Reference to Large Deformation Problems," Comp. Meth. Applied Mech. Eng., 33, 469-484 (1982).

128. J.A. Nelder and R. Mead, A simple method for function minimization. Computer Journal, 7, 308{313 (1965).

129. P. Pilvin, “The Contribution of Micromechanical Approaches to the Modelling of Inelastic Behavior of Polycrystals," Fourth International

Conference on Biaxial/Multiaxial Fatigue, May 31-June 3, Paris, France (1994).

130. P. Pilvin, Sidolo2.3, Manuel utilisateur, Centre des Materiaux, Ecole de Mines de Paris, France (1996).

131. J.C. Simo and T.J.R. Hughes, Computational Inelasticity Springer-Verlag, New York (1998).

132. K. Schittkowski, QLD : A FORTRAN Code for Quadratic Programming, User's Guide, Mathematisches Institut, Universitat Bayreuth, Germany, (1986).

133. J.L. Zhou C. Lawrence and A.L. Tits, User's Guide for CFSQP Version 2.5 Inst. for System Research TR-94-16r1, Univ. of Maryland, College Park, MD 20742, (1997).

134. Ahmad, S., Irons, B. M. and Zienkiewicz, O. C., "Analysis of Thick and Thin Shell Structures by Curved Finite Elements", International Journal for Numerical Methods in Engineering, Vol. 2, No. 3, pp. 419-451 (1970).

135. Bathe, K. J., Finite Element Procedures, Prentice-Hall, Englewood Cliffs (1996).

136. Biot, M. A., Mechanics of Incremental Deformation, John Wiley and Sons, New York (1965).

137. Chen, L. H., "Piping Flexibility Analysis by Stiffness Matrix", ASME, Journal of Applied Mechanics (December, 1959).

138. Cook, R. D., Concepts and Applications of Finite Element Analysis, Second Edition, John Wiley and Sons, New York (1981).

139. Cook, R. D., "Two Hybrid Elements for Analysis of Thick, Thin and Sandwich Plates", International Journal for Numerical Methods in Engineering, Vol. 5, No. 2, pp. 277-288 (1972).

140. Cuniff, D. F., and O'Hara, G. J., "Normal Mode Theory for Three-Directional Motion", NRL Report 6170, U. S. Naval Research Laboratory, Washington D. C. (1965).

141. Denn, M. M., Optimization by Variational Methods, McGraw-Hill, New York (1969).

142. Henshell, K. D. and Ong, J. H., "Automatic Masters for Eigenvalue Economization", Earthquake Engineering and Structural Dynamics, Vol. 3, pp. 375-383 (1975).

143. Imgrund, M. C., ANSYS® Verification Manual, Swanson Analysis Systems, Inc. (1992).

144. Flugge, W., Stresses in Shells, Springer Verlag, Berlin (1967).

145. Fritz, R. J., "The Effect of Liquids on the Dynamic Motions of Immersed Solids", ASME Journal of Engineering for Industry (February, 1972)

146. Galambos, T. V., Structural Members and Frames, Prentice-Hall, Englewood Cliffs (1968).

147. Guyan, R. J., "Reduction of Stiffness and Mass Matrices", AIAA Journal, Vol. 3, No. 2 (February, 1965).

148. Hall, A. S., and Woodhead, R. W., Frame Analysis, John Wiley and Sons, New York (1961).

149. Rajakumar, C. and Rogers, C. R., "The Lanczos Algorithm Applied to Unsymmetric Generalized Eigenvalue Problem", International Journal for Numerical Methods in Engineering, Vol. 32, pp. 1009-1026 (1992).

150. Irons, B. M., "A Frontal Solution Program for Finite Element Analysis", International Journal for Numerical Methods in Engineering, Vol. 2, No. 1, January, 1970, pp. 5-23 (Discussion May, 1970, p. 149).

151. Wilkinson, J. H., The Algebraic Eigenvalue Problem, Clarendon Press, Oxford, pp. 515-569 (1988).

152. Kohnke, P. C., and Swanson, J. A., "Thermo-Electric Finite Elements", Proceedings, International Conference on Numerical Methods in Electrical and Magnetic Field Problems, June 1-4, 1976, Santa Margherita Liqure (Italy).

153. Kohnke, P. C., "Large Deflection Analysis of Frame Structures by Fictitious Forces", International Journal of Numerical Methods in Engineering, Vol. 12, No. 8, pp. 1278-1294 (1978).

154. Kollbrunner, C. F., and Basler, K., Torsion in Structures, Springer-Verlag, Berlin, (1969).

155. Konopinski, E. J., Classical Descriptions of Motion, Freeman and Company, San Francisco (1969).

156. Kreyszig, E., Advanced Engineering Mathematics, John Wiley and Sons, Inc., New York (1962).

157. Lekhnitskii, S. G., Theory of Elasticity of an Anisotropic Elastic Body, Holden-Day, San Francisco (1963).

158. Melosh, R. J., and Bamford, R. M., "Efficient Solution of Load-Deflection Equations", ASCE Journal of the Structural Division, Vol. 95, No. ST4, Proc. Paper 6510, Apr., 1969, pp. 661-676 (Discussions Dec., 1969, Jan., Feb., May, 1970, Closure, Feb., 1971).

159. Kanok-Nukulchai, "A Simple and Efficient Finite Element for General Shell Analysis", International Journal for Numerical Methods in Engineering, Vol. 14, pp. 179-200 (1979).

160. Oden, J. T., Mechanics of Elastic Structures, McGraw-Hill, New York (1968).

161. Przemieniecki, J. S., Theory of Matrix Structural Analysis, McGraw-Hill, New York (1968).

162. Schnobrich, W. C., and Suidan, M., "Finite Element Analysis of Reinforced Concrete", ASCE Journal of the Structural Division, ST10, pp. 2109-2122 (October, 1973).

163. Seide, P., "Large Deflection of Rectangular Membranes Under Uniform Pressure", International Journal of Non-Linear Mechanics, Vol. 12, pp. 397-406.

164. Skjelbreia, L., and Hendrickson, J. A., "Fifth Order Gravity Wave Theory", Proceedings, Seventh Conference on Coastal Engineering, Ch. 10, pp. 184-196 (1961).

165. Timoshenko. S., and Woinowskey-Kreiger, S., Theory of Plates and Shells, McGraw-Hill, New York (1959).

166. Tracey, D. M., "Finite Elements for Three Dimensional Elastic Crack Analysis", Nuclear Engineering and Design, 26 (1973).

167. Vanmarcke, E. H., "Structural Response to Earthquakes", Seismic Risk and Engineering Decisions, Elsvier Scientific Publishing Co., Amsterdam-Oxford, New York, (edited by C. Lomnitz and E. Rosemblueth), pp. 287-337 (1976).

168. Wheeler, J. D., "Method of Calculating Forces Produced by Irregular Waves", Journal of Petroleum Technology, Vol. 22, pp. 359-367 (1970).

169. Willam, K. J., University of Colorado, Boulder, (Private Communication) (1982)

170. Willam, K. J., and Warnke, E. D., "Constitutive Model for the Triaxial Behavior of Concrete", Proceedings, International Association for Bridge and Structural Engineering, Vol. 19, ISMES, Bergamo, Italy, p. 174 (1975).

171. Wilson, E. L., Taylor, R. L., Doherty, W. P., and Ghaboussi, J., "Incompatible Displacement Models", Numerical and Computer Methods

in Structural Mechanics, edited by S. J. Fenves, et al., Academic Press, Inc., N. Y. and London, pp. 43-57 (1973).

172. Zienkiewicz, O. C., The Finite Element Method, McGraw-Hill Company, London, (1977).

173. ASME Boiler and Pressure Vessel Code, Section III, Division 1, Subsection NC, Class 2 Components (1974).

174. "Regulatory Guide", Published by the U. S. Nuclear Regulatory Commission, Regulatory Guide 1.92, Revision 1 (February 1976).

175. Tamma, Kumar K. and Namburu, Raju R., "Recent Advances, Trends and New Perspectives Via Enthalpy-Based Finite Element Formulations for Applications to Solidification Problems", International Journal for Numerical Methods in Engineering, Vol. 30, pp. 803-820 (1990).

176. Shore Protection Manual, Published by the U. S. Army Coastal Engineering Research Center, Vol. I, Third Edition (1977).

177. Beer, F. P., and Johnston, R. E., Vector Mechanics for Engineers, Statics and Dynamics, McGraw-Hill, New York (1962).

178. Hinton, E., Rock, A., and Zienkiewicz, O., "A Note on Mass Lumping and Related Processes in the Finite Element Method", International Journal of Earthquake Engineering and Structural Dynamics, Vol. 4, pp. 245-249 (1976).

179. Krieg, R. D., and Krieg, D. B., "Accuracies of Numerical Solution Methods for the Elastic-Perfectly Plastic Model", Journal of Pressure Vessel Technology, Vol. 99, No. 4, Series J, Transactions of the ASME,November, pp. 510-515 (1977).

180. Thomson, William T., Theory of Vibrations with Applications, Prentice Hall, pp. 343-352 (1971).

181. Roark, R. J., and Young, W. C., Formulas for Stress and Strain, McGraw-Hill, New York (1975).

182. Taylor, R. L., Beresford, P. J., and Wilson, E. L., "A Non-Conforming Element for Stress Analysis", International Journal for Numerical Methods in Engineering, Vol. 10, pp. 1211-1219 (1976).

183. Hill, R., The Mathematical Theory of Plasticity, Oxford University Press, New York (1983).

184. Shih, C. F., and Lee, D., "Further Developments in Anisotropic Plasticity", Journal of Engineering Materials and Technology, Vol. 100, pp. 294-302 (July 1978).

185. Valliappan, S., "Nonlinear Analysis for Anistropic Materials", International Journal for Numerical Methods in Engineering, Vol. 10, pp. 597-606 (1976).

186. Besseling, J. F., "A Theory of Elastic, Plastic, and Creep Deformations of an Initially Isotropic Material Showing Aisotropic Strain-Hardening Creep Recovery and Secondary Creep", Journal of Applied Mechanics, pp. 529-536 (December 1958).

187. Owen, R. J., Prakash, A., and Zienkiewicz, O. C., "Finite Element Analysis of Non-Linear Composite Materials by Use of Overlay Sytems", Computers and Structures, Pergamon Press, Vol. 4, pp. 1251-1267.

188. Holman, J. P., Heat Transfer, Fourth Edition, McGraw-Hill, New York (1976).

189. Batoz, J. L., Bathe, K. J., and Ho, L. W., "A Study of Three-Node Triangular Plate Bending Elements", International Journal of Numerical Methods in Engineering, Vol. 15, pp. 1771-1812 (1980).

190. Razzaque, A., "On the Four Noded Discrete Kirchhoff Shell Elements", Robinson, J. (ed.), Accuracy Reliability Training in FEM Technology, pp. 473-483 (1984).

191. Gresho, P. M., and Lee, R. L., "Do not Suppress the Wiggles - They're Telling You Something", Finite Element Methods for Convection Dominated Flows, ASME Publication AMD, Vol. 34, pp. 37-61 (1979).

192. Dean, R. G., Evaluation and Development of Water Wave Theories for Engineering Application, prepared for U. S. Army Corp of Engineers, Coastal Engineering Research Center, (November 1974).

193. ASME Boiler and Pressure Vessel Code, Section III, Division 1-1974, Subsection NB, Class 1 Components.

194. American National Standard Code for Pressure Piping, Power Piping, ANSI B31.1-1977, Published by the American Society of Mechanical Engineers.

195. Orris, R. M., and Petyt, M., "Finite Element Study of Harmonic Wave Propagation in Periodic Structures", Journal of Sound and Vibration, pp. 223-236 (1974).

196. Gordon, J. L., "OUTCUR: An Automated Evaluation of Two-Dimensional Finite Element Stresses" according to ASME, Paper No. 76-WA/PVP-16, ASME Winter Annual Meeting (December 1976).

197. Powell, M. J. D., "An Efficient Method for Finding the Minimum of a Function of Several Variables Without Calculating Derivatives", Computer Journal, Vol. 7, pp. 155-162 (1964).

198. Wilson, E. L., Der Kiereghian, A., and Bayo, E., "A Replacement for the SRSS Method in Seismic Analysis", Earthquake and Structural Dynamics, University of California, Berkeley, Vol. 9, No. 2, p. 187 (March 1981).

199. Rankin, C. C., and Brogan, F. A., "An Element Independent Corotational Procedure for the Treatment of Large Rotations", Journal of Pressure Vessel Technology, Vol. 108, pp. 165-174 (May 1986).

200. Argyris, J., "An Excursion into Large Rotations", Computer Methods in Applied Mechanics and Engineering, Vol. 32, pp. 85-155 (1982).

201. Tse, S., Morse, I. E., and Hinkle, R. T., Mechanical Vibrations, Allyn and Bacon, Boston (1963).

202. Tandon, S. C., and Chari, M. V. K., "Transient Solution of the Diffusion Equation by the Finite Element Method", Journal of Applied Physics (March 1981).

203. Zienkiewicz, O. C., Lyness, J., and Owen, D. R. J., "Three-Dimensional Magnetic Field Determination Using a Scalar Potential - A Finite Element Solution", IEEE Transactions on Magnetics, Vol. MAG-13, No. 5, pp. 1649-1656 (1977).

204. Coulomb, J. L., and Meunier, G., "Finite Element Implementation of Virtual Work Principle for Magnetic for Electric Force and Torque Calculation, IEEE Transactions on Magnetics, Vol. Mag-2D, No. 5, pp. 1894-1896 (1984).

205. Yuan, S. NW., Foundations of Fluid Mechanics, Prentice-Hall International, Inc., London, pp. 71-102 (1976).

206. Clough, Ray W., and Penzien, Joseph, Dynamics of Structures, McGraw-Hill, New York, p. 559 (1975).

207. Kinsler, E. L. et. al., Fundamentals of Acoustics, John Wiley and Sons, New York pp. 98-123 (1982).

208. Craggs, A., "A Finite Element Model for Acoustically Lined Small Rooms", Journal of Sound and Vibration, Vol. 108, No. 2, pp. 327-337.

209. Zienkiewicz, O. C., and Newton, R. E., "Coupled Vibrations of a Structure Submerged in a Compressible Fluid", Proceedings of the Symposium on Finite Element Techniques, University of Stuttgart, Germany (June 1969).

210. Malvern, Lawrence E., Introduction to the Mechanics of a Continuous Medium, Prentice-Hall, Inc., Englewood Cliffs, NJ (1969).